Characterisation of a Novel Group B Oncolytic Adenovirus, ColoAd1

Ying Di

Wolfson College

University of Oxford

A thesis submitted for the degree of Master by Research, to the Faculty of Clinical Medicine, University of Oxford

Trinity Term 2011

Supervisor: Professor L.W.Seymour

Abstract

Developing high potent oncolytic virus with multimodal antitumour capabilities is crucial for realizing the full potential of oncolytic virotherapy in cancer treatment. ColoAd1 is a novel replicating chimeric group B adenovirus recently bioselected from a large library of recombinant viruse. This thesis aims at evaluating the oncolysis ability of ColoAd1, characterization of its cellular activities and the corresponding responses from host tumour cells, elucidating the killing mechanism as well as exploring its potential applications in the advanced cancer therapy.

Among all oncolytic adenoviruses tested, ColoAd1 elicited the strongest cytotoxicity with a rapid killing kinetics in tumour cells. The virus displayed high infection efficiency, enhanced genome replication (compared to other adenoviruses) and strict selectively in tumour cells.The viral oncolysis also induced a bystander killing effect.

Investigation of the host cells responses during ColoAd1 oncolysis showed the virus mediated cell killing is not classic apoptosis but rather necrosis-like. The dying cells displayed the early cytoplasmic membrane leakage, falling intracellular ATP with a rise in calcium, disruption of the cell cycle and cellular DNA damage, with rapid release of progeny virions from the cell; on the other hand, ColoAd1-killing lacked the characteristic hallmarks of apoptosis. Autophagy may play a role in final execution of oncolysis but is not the main death mechanism. The cellular pathway involved in ColoAd1 oncolysis was further studied by using a panel of specific inhibitors. The results indicated the ColoAd1 mediated cell death is PARP- and RIP1- dependent and necroptosis could be the major death mechanism.

The highly oncolytic potency and special killing mechanism of ColoAd1 may have beneficial implication for advanced cancer therapies, including the possibility of circumventing drug resistance and invoking cancer immunotherapy.

The data in this thesis supported ColoAd1 as a novel potent oncolytic virus candidate. It promises to overcome the major drawbacks of Ad5 and therefore could have enhanced therapeutic efficacy in future clinical trial.

Acknowledgements

I would like to thank my supervisor Professor Len Seymour for giving me the inspiration to work on this project and for the help he has given to set my project goals. I am grateful for the precious advices he has given me on scientific thinking, reading and writing throughout this process, and for the way he has always been so kind, so helpful and so patient. I am also thankful that he gave me the opportunity to be one of his students and work on a very promising and fascinating field of oncolytic virus cancer therapy.

I wish to wholeheartedly thank Mrs Christina Woodward. Without her, there would be no this thesis. I would like thank her for all the help and the support she has given in every step of the course, from my initial application, through the study, till the final thesis submission. She is an angel to me and to all other students in the department.

I would also like to thank my colleagues and friends in the group. Dr Kerry Fisher always gave me the best supervision on the project. In the thesis writing, Dr Hannah Chen and Dr Alison Tedcastle helped me to understand the virology aspect, Gray Kueberuwa helped me on death mechanisms; Allia Alamoudi helped me on virus cancer immunotherapy; Lisa Cooper helped me on cell death pathway; Sarina Agkatsev helped me on drug resistance; Megan McGregor helped me on cell biology. I would thank them for the discussion and English correction. In the labs, Dr Robert Carlisle and Clemens Thoma also kindly gave me much help and many suggestions.

Finally I would like to thank my family, Mimi and Lijiang. They have been company for me at the weekends when I needed to study. Mimi cheers me up when I am in a bad mood. Lijiang always criticizes my work (I have to agree, most of the time he is right) and he also helped me to search the most recent relevant publications in the field.

Table of Content

Abstract..... 1
Acknowledgements..... 2
Table of content..... 3
List of abbreviation..... 6

Chapter1: Introduction..... 8
1.1 Oncolytic virotherapy..... 9
1.2 Oncolytic adenoviruses..... 10
1.2.1 Adenovirus..... 10
1.2.2 Group C adenovirus: Ad5..... 12
1.2.3 Group B adenovirus: Ad11..... 13
1.2.4 Chimeric group B adenovirus: ColoAd1..... 15
1.3 Programmed cell deaths..... 15
1.3.1 Morphological features of the death types..... 15
1.3.2 Biochemical characters of the death types..... 16
1.3.3 Biological consequences of the death types..... 19
1.3.4 The crosstalk of the different death types..... 20
1.4 Oncolytic virus mediated cell death..... 21
1.4.1 The cytotoxicity, viral replication and host cell status..... 22
1.4.2 Oncolytic RNA viruses induce apoptosis..... 23
1.4.3 Oncolytic DNA viruses mediate complicate cell deaths..... 25
1.4.3.1 Vaccinia and HSV..... 26
1.4.3.2 Adenovirus..... 28
1.5 Thesis objective..... 33

Chapter2: Materials and Method..... 35

Chapter3:Characterisation of the virology aspects of ColoAd1..... 49
3.1 Introduction..... 50
3.2 Results..... 51
3.2.1 Titre of the stock viruses..... 51
3.2.2 The potency and kinetics of viral oncolysis..... 53
3.2.2.1 Comparison of the viral potencies by end point MTS assay..... 53
3.2.2.2 Comparison of the killing kinetics of the viruses by xCelligence..... 54
3.2.2.3 Comparison of the killing kinetics of the viruses with chemotherapy drugs and H_2O_2..... 55
3.2.3 Virus infectivity and cellular uptake..... 57
3.2.4 Virus selective replication and cytotoxicity..... 58

3.2.4.1 Comparison of the relative cytotoxicity of the viruses in normal cells versus tumour cells..... 58
3.2.4.2 Comparison of the replication of the viruses in normal cells versus tumour cells..... 59
3.2.4.3 ColoAd1 mediated by stander killing of adjacent infected cells..... 60
3.2.5 Susceptibility to neutralization by blood factors..... 62
3.2.5.1 Resistance of the adenoviruses to serum neutralization..... 62
3.2.5.2 Resistance of the adenoviruses to erythrocytes binding..... 64
3.2.5.3 IgGs in neutralizing serum binding patterns with the viruses proteins..... 65
3.2.5.4 Resistance of the adenoviruses to Interferon neutralization..... 66
3.2.6 Comparison of virus spreading through tumour cell monolayer..... 67
3.3 Discussion..... 68
3.4 Conclusion..... 74

Chapter 4: Investigation of the cellular response during ColoAd1..... 77
4.1 Introduction..... 78
4.1.1 Aim of this chapter..... 79
4.1.2 Investigation of characteristic features of different cell death mechanisms..... 79
4.2 Results and discussion..... 85
4.2.1 Morphological observation of adenoviruses oncolysis..... 85
4.2.1.1 Light microscopy observations of cell deaths..... 85
4.2.1.2 Time lapse microscopy..... 86
4.2.1.3 DAPI nuclear staining..... 87
4.2.1.4 Cellular size and granularity change..... 88
4.2.2 Cytoplasmic membrane alteration and leakage during oncolysis..... 89
4.2.2.1 Fluorescence microscopy observation..... 89
4.2.2.2 Annexin V/PI staining characterization by Flow cytometry analysis..... 90
4.2.3 Key cellular protein expression level regulations during oncolysis..... 96
4.2.4 Intracellular ATP and Ca^{2+} levels maintenance during oncolysis..... 99
4.2.5 Cellular DNA damages during oncolysis..... 102
4.2.5.1 DNA histograms of the viruses infected A549 cells..... 102
4.2.5.2 Cell cycle phase distribution..... 105
4.2.6 Progeny virus extracellular release and spread 108
4.3 Summary..... 110

Chapter 5: Cell death pathway inhibition and oncolysis..... 113
5.1 Introduction..... 114
5.2 Results..... 117
5.2.1 The inhibition impact on the cytotoxicity..... 117
5.2.1.1 PARP inhibition..... 117
5.2.1.2 RIP1 inhibition..... 119
5.2.1.3 Caspase inhibition..... 120
5.2.1.4 Autophagy inhibition..... 122
5.2.1.5 E4orf4 inhibition..... 122
5.2.1.6 Calpain and cathepsin inhibition..... 123
5.2.1.7 Intracellular Ca^{2+} manipulation..... 124

5.2.2 Effects of inhibitors on the kinetics of virus cytotoxicity..... 124
5.2.3 Impact of the inhibitors on replication and genome production of ColoAd1..... 127
5.2.4 Impact of the inhbitors on cellular uptake of ColoAd1..... 127
5.2.5 Effects of Necrostatin-1 on cellular features of ColoAd1 oncolysis..... 129
5.3 Discussion..... 131
5.3.1 The cytotoxic mechanisms of Cisplatin and H_2O_2..... 132
5.3.2 Adenoviruses- mediated oncolysis is not apoptotic cell death..... 133
5.3.3 Autophagy is not the main mechanism for Adenovirus killing..... 133
5.3.4 E4orf4 and ADP are involved in killing by Ad5 but not by group B adenoviruses... 135
5.3.5 Adenoviruses mediated oncolysis involves necrosis and PARP activity..... 136
5.3.6 ColoAd1 oncolysis is necroptosis and RIP1 dependent..... 139
5.3.7 The execution of ColoAd1 oncolysis..... 140
5.3.8 The cellular pathway of ColoAd1 oncolysis..... 142

Chapter 6: Potential applications of ColoAd1 oncolysis..... 144
6.1 Introduction..... 145
6.1.1 Drug resistance and virotherapy..... 145
6.1.2 Cancer immunotherapy and virotherapy..... 147
6.2 Results..... 149
6.2.1 ColoAd1's killing on Capan-1 cells..... 149
6.2.2 ColoAd1's killing on HCT116 cells..... 151
6.2.3 Extracellular HSP70 release of the infected tumour cells..... 153
6.2.4 HMGB1 extracellular release from the infected tumour cells..... 155
6.2.5 Extracellular uric acid level from the infected tumour cells..... 156
6.2.6 ColoAd1 oncolysates induce NFκB activation..... 156
6.3 Discussion..... 158
6.3.1 Circumstance drug resistance by ColoAd1 oncolysis..... 158
6.3.2 Induction of antitumour immunity by ColoAd1 oncolysis..... 161

Reference..... 164
Supplementary materials..... 169

List of Abbreviation

3-ABA: 3-Aminobenzamide
3-MA: 3-methyladenine
5FU: 5-Fluorouracil
Ad: Adenovirus
Ad5: Adenovirus 5, group C adenovirus
Ad11: Adenovirus 11, group B adenovirus
Ad3: Adenovirus 3, group B adenovirus
A549: human lung adenocarcinoma epithelial cell line
ADP: Adenovirus death protein
ATP: Adenosine triphosphate
BXPC3: human, pancreas, adenocarcinoma
Capan-1: human pancreas adenocarcinoma
CAR: Coxsackie adenovirus receptor
CHX: cycloheximide
CMV: cytomegalovirus
CPE: cytopathic effect
CR1: complement receptor 1
CRAd: conditionally replicative adenoviruses
DAPI: 4',6-diamidino-2-phenylindole
DMEM: Dulbecco's modified Eagle medium
ECL: enhanced chemiluminescence
ELISA: enzyme-linked immunosorbent assay
GM-CSF; granulocyte-Macrophage Colony Stimulating Factor
FACS: fluorescence-activated cell sorting
FADD: Fas-associated protein with death domain
FASL: Fas ligand
FCS: fetal calf serum
G_0 : quiescence phase
G_1: gap1 phase
G_2: gap2 phase
M: mitosis phase
S: synthesis phase
H460: lung carcinoma cells
HCT116: human colorectal carcinoma
HepG2: human heptocellular carcinoma cell line
HMEC: human mammary epithelial cell line
HMGB1: high-mobility group protein B1 or amphoterin
HSP: heat shock protein
HSV: human Herpes simplex virus
HRP: horseradish peroxidase
HUVEC: human umbilical endothelial cells
IC50: 50% cell killing or 50% cell viability
IgG: immunoglobulin G
IFN: interferon

O.D.: optical density
LC-MS: liquid chromatography–mass spectrometry
LPS: lipopolysaccharide or endotoxin
MOI : multiplicity of infection
MTS : 3-(4,5-dimethylthiazol-2-yl)-5-(3-carboxymethoxyphenyl)-2-(4-sulfophenyl)-2H-tetrazolium
ORF : open reading frame
p53: tumor protein 53
p21: cyclin-dependent kinase inhibitor 1
PAR: poly(ADP-ribose) chain
PARP: poly (ADP-ribose) polymerase
P13K: phosphoinositide 3-kinases
PBS: Dulbecco's phosphate buffer solution
PFU: infectious particle unit per cell
PI: propidium iodide
POI: post of infection
PPC: particle number per cell
P/S: Penicillin/ Streptomycin
PS: phosphatidylserine
QPCR: quantitative polymerse chain reaction
NFκB: nuclear factor kappa-light-chain-enhancer of activated B cells
NDV: Newcastle disease virus
RBC: red blood cells, or erythrocyte
RIP1: kinases receptor interacting protein 1
RIPA: radioimmunoprecipitation assay buffer
RSV: respiratory syncytial virus
SIN: Sindbis virus
SD: standard deviation
SDS-PAGE: sodium dodecyl sulfate polyacrylamide gel electrophoresis
TCID50: 50% tissue culture infective dose
TEM: transmission electron microscopy
TMB: 3,3′,5,5′-Tetramethylbenzidine
TNF: tumor necrosis factor
TRAIL: TNF-related apoptosis-inducing ligand
VSV: vesicular stomatitis virus
VV: Vaccinia
WI-38: human lung fibroblast
YB-1: human transcription factor
zVAD-fmk: benzyloxycarbonyl-Val-Ala-Asp (OMe) fluoromethylketone

Chapter 1: Introduction

1.1 Oncolytic virotherapy

Oncolytic virotherapy represents a novel biotherapy for treating cancer, which is full of promise and potential. The therapeutic strategy is based on the replicating virus lytic cycle: replication-competent or conditionally-replicating viruses infect and preferentially replicate in tumour cells, mediate lysis (oncolysis) of the host cell, which is followed by the release of progeny virions. The virions will then spread into the neighbouring tumour cells to start a new replication cycle (see Fig1.1).

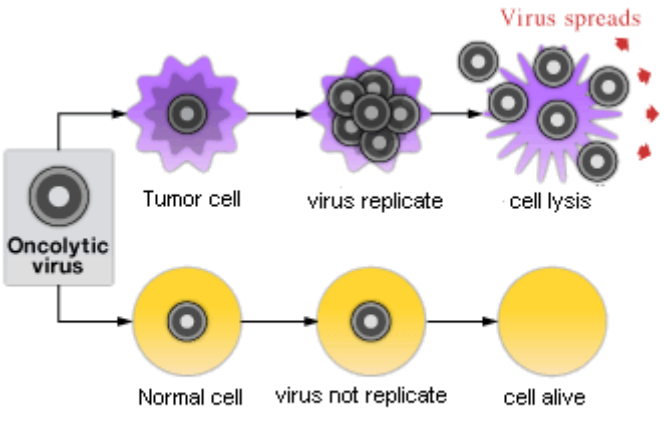


Fig1.1 The concept of oncolytic virotherapy
(modified from http://www.takara-bio.com/medi_e/gene.html)

Compared to the conventional approaches such as chemotherapy and radiotherapy, oncolytic virotherapy is thought to have a number of important advantages:

(1) Potency: very low doses can be used due to amplification in situ, thus minimising off target toxicity;

(2) Specificity: selective targeting to tumour cells while sparing normal cells;

(3) Multimodal actions: oncolysis may also lead to immune activation;

(4) Versatility: a wide range of virus families have been developed since the 1960s for virotherapy, examples include Adenovirus (Ad), Herpes Simplex virus (HSV),

Vaccinia virus (VV) and Sindbis virus (SDV). The advent of genetic engineering makes it feasible to modify or arm the basic virus by incorporating therapeutic transgenes for improved safety and antitumor properties;

(5) Combination therapies: oncolytic virus treatment can be combined with either chemotherapy or radiotherapy in clinical practice; this may provide an effective approach for circumventing drug or radio resistance

However, in reality oncolytic virotherapy has not yet been proved to be as effective as either chemotherapy or radiotherapy in clinical settings (Pesonen, Kangasniemi et al. 2010). Poor blood compatibility of input viruses, coupled with inefficient cytolysis and spreading in the tumour mass could potentially explain the limited therapeutic efficacy observed. Therefore, identifying and developing future generations of oncolytic viruses which have the ability to overcome the current limitations will be critical.

1.2 Oncolytic Adenoviruses

1.2.1 Adenovirus

The DNA virus adenoviruses are the most widely studied and extensively exploited among all oncolytic viruses.

The virion is an icosahedra shaped non-enveloped medium-sized particle that range in diameter from 90-100nm. It is composed of a nucleocapsid which

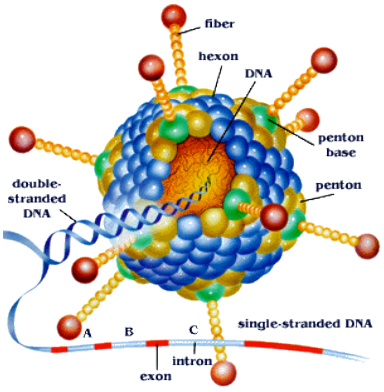


Fig1.2 the structure of Adenovirus
http://med.mui.ac.ir/slide/bactrio/adenovirus.gif

contains a double-stranded linear DNA genome, as shown in Fig1.2. The capsid is built up from 252 capsomers (*T*=25), of which 240 are hexavalent (called Hexon) and 12 are pentavalent (called Penton base). The virion also has a unique "spike" (called Fiber) associated with each penton base that aids in attachment to the host cell via certain receptors on the cell surface. With a total protein mass as 150 MDa (Harrison 2010), the virion is constructed from a total of 13 different protein types. The genome size is about 26 to 45kb in length, which allows the virus to theoretically carry 22 to 40 genes. The genome of adenovirus can be divided into four early transcription regions (E1-E4) and one late transcription region (L). A simple diagram for representing adenovirus genome structure is shown in Fig 1.3. A more detailed introduction about adenoviruses genome structure and organization can be found in the following reviews and text books (Davison, Benko et al. 2003; Knipe 2007). Adenovirus replicates in the nucleus of mammalian cells using the

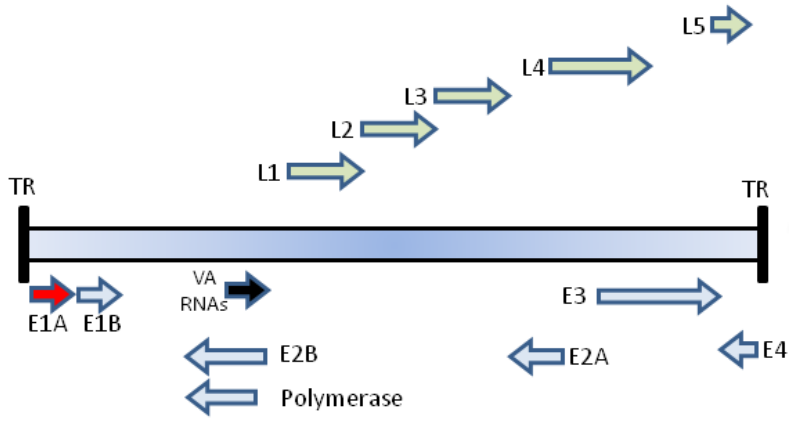


Fig1.3 Adenovirus genome structure. Diagrammatical representation of the adenovirus serotype five genome. The genome of adenovirus can be divided into the regions encoding the early and late transcription events. Those regions below the genome denote early transcription events whilst those above the genome are late transcription events. This image was kindly provided by Dr Ryan Cawood.

host's replication machinery. Once the viral components have successfully been transcribed and translated, the progeny virions are assembled and released from the cell as a result of virally induced cell lysis.

Up to date, there are 57 identified human adenovirus species or serotypes (HAdV-1 to 57). Phylogenetic analysis and haemagglutination capabilities allow them to be classfied into seven subgroups (Human adenovirus A to G) by the International Committee on Taxonomy of Viruses(Jones, Harrach et al. 2007).

1.2.2 Group C adenovirus: Ad5

Most of the oncolytic viruses developed so far are based on group C adenovirus serotype 5 (Ad5). Developed in 1987, ONYX-015 has been genetically engineered to have the E1B55k gene deletion and have been extensively tested in human clinical trials. The first commercialized oncolytic virus, Oncorine (H101), which is very similar to Onyx-015, was approved by Chinese SFDA in 2005 for nasopharyngeal carcinoma combined with chemotherapy (Liang 2011). Since then, a number of oncolytic viruses have been moved into clinical trials.

Ad5 is a good choice of agent for virotherapy (Kevn, 2008), notably because the wild type is only associated with relatively mild disease and its genome has been well characterized, allowing ready molecular manipulations. In addition, Ad5 is easy to produce and purify to a high titre, it is stable in storage and has a relatively wide tropism that allows infection of most types of cancer cells. Nevertheless, shortcomings associated with the use of Ad5 have also been gradually recognized. Many cancers (including gastrointestinal cancers, pancreatic cancer, ovarian cancer and hormone-refractory prostate cancer) do not express the primary receptor for Ad5,

the Coxsackie adenovirus receptor (CAR), limiting virus uptake. Also oncolysis induced by Ad5 has been reported to be slow (Wigand and Kumel 1977). Particular limitations have been identified in the context of intravenous delivery. Poor blood compatibility, high serum prevalence, high neutralising antibody titre, binding to blood cells, sequestration by macrophages and uptake by liver-resident macrophages are all factors that greatly decrease the amount of systemically available adenovirus (Yamamoto and Curiel 2010). Furthermore, intratumoral injection of the virus to human tumour xenograft-bearing immune compromised mice suggested poor spreading of Ad5 in the tumour matrix (Bazan-Peregrino, Carlisle et al. 2008).

There are currently several approaches in development to address these major issues. These include the use of fibre modification (replacement of Ad5 fibre knob domain with that of Ad3) in order to modify the viral tropism and circumvent CAR deficiency in the target cells, leading to improved transduction efficacy (Nandi, Ulasov et al. 2009); chemical/physical modifications such as polymer coating of the Ad5 capsid and retargeting in order to improve blood compatibility and delivery efficacy (Bachtarzi, Stevenson et al. 2011); arming the virus with genes encoding toxins or tumour suppressor genes, including adenovirus death protein ADP and p53, to enhance Ad5's killing potency and accelerate the cell-to-cell spread (Chen, Wu et al. 2011; Toth, Kuppuswamy et al. 2011). These innovations are at the frontier of cancer biotherapy research and will have important impacts to push the technology forward.

1.2.3 Group B adenovirus: Ad11

Switching to alternative human adenovirus serotypes also provides opportunities to avoid some of the problems associated with the use of Ad5. Previous studies have

demonstrated that group B adenoviruses such as Ad11 have much lower seroprevalence in human populations and do not cross-react with neutralising antibodies against Ad5 (Holterman, Vogels et al. 2004). More importantly, they have much wider tropism, higher cellular binding affinity and higher transduction efficiency since CD46 is used as the primary attachment/recognition receptor rather than CAR (Zhang, Mei et al. 2003*)*. Thus, developing group B-based replication-competent adenoviruses could lead to the generation of more potent oncolytic viruses for clinical application.

The structure and biology of group B Ads is similar to that of the group C virus. However, there are aspects of group B Ads life cycle which differ from group C members and remain to be defined. Research interests in Ad11 began only recently as its genome was not sequenced and characterized until 2003 by the Wadell group (Mei, Skog et al. 2003). Ad11p (Ad11 prototype, strain Slobitski) has been shown to have certain similarities with Ad5 with regard to its genome size and organization. Comparison between the hexons of Ad11 and Ad5 reveals a relatively high overall sequence homology (78.8%). Regions containing the lowest sequence homology between these two Ads were noted in the fibre proteins (24.6%) with Ad11 having a much shorter fibre. There are also important differences, for example, the E3 11.6K cell death protein (ADP) which is present in Ad5 genome but not found in Ad11p, two additional E3 cassettes (20.3K and 20.6 K) are found in Ad11 but not in Ad5; the E4 region of Ad11p possesses all the open reading frame (ORFs) that appear in Ad5 E4, however, sequence homology is low (44%). Furthermore, there are six late gene-coding regions in the Ad11p genome but only five are found in the Ad5 genome. Therefore, caution must be taken when predicting the functions of Ad11p gene products based on the knowledge already obtained with Ad5.

1.2.4 Chimeric group B adenovirus: ColoAd1

ColoAd1 is a novel Ad11/Ad3 chimeric oncolytic virus recently developed using the so called bioselection methodology (Kuhn, Harden et al. 2008). Analysis of the genomic sequence revealed that ColoAd1 comprises mostly an Ad11p derivative with an Ad11/Ad3 chimeric E2B region and a complete E3 region deletion. As a result, the genome length of ColoAd1 is about 90% compared to the genome of Ad11. The virus shows a 2-3 log higher potency and selectivity than the parental serotypes or the most clinically advanced Ad5-based oncolytic virus ONYX-15 on colon cancer cells. So far, its behaviour has not yet been systematically investigated, and its mechanism of cell killing remains elusive. The current understanding of the oncolytic mechanism of Ad11 also remains poorly defined and there is a lack of direct comparison between Ad5 and Ad11. The data from different reports are confusing to compare as studies have been performed using different cell lines and varied experimental conditions.

1.3 Programmed cell deaths

As our understanding of programmed cell death has evolved, it has become evident that cells can die by various mechanisms. Before the investigating of oncolytic adenovirus mediated cell killing and their cytotoxity mechanisms, it is necessary to briefly summarize the currently known major cell death types: apoptosis, autophagy, necrosis and necroptosis.

1.3.1 Morphological features of the death types

Historically, three types of cell death have been distinguished in mammalian cells by morphological features and they are classified as: Apoptosis, necrosis and autophagic

cell death (as shown in Fig 1.4). Apoptosis, also termed type I cell death, is defined by characteristic changes in the nuclear morphology, including chromatin condensation and fragmentation, overall cell shrinkage, blebbing of the plasma membrane and formation of apoptotic bodies that contain nuclear or cytoplasmic material. Autophagic cell death, also known as type II cell death, is characterized by a massive accumulation of double-membrane containing vacuoles known as autophagosomes, which subsequently fuse with lysosome vacuoles. Necrosis, type III cell death, is morphologically defined by cytoplasmic swelling, organelle dilation and plasma membrane rupture.

1.3.2 Biochemical characters of the death types

Apart from classification by morphology features, the three death types have distinctive biochemical characteristics.

Apoptosis is a programmed cell death by which the sequence of events is highly regulated and regimented. The apoptosis regulation has been well studied (Majno and Joris 1995). The cellular process can be triggered in a cell through either the extrinsic pathway or the intrinsic pathway. The extrinsic pathway is initiated through the stimulation of the trans-membrane death receptors, such as the Fas receptors and tumour necrosis factor TNF receptor. In contrast, the intrinsic pathway is triggered by cellular stress (including DNA damage and heat shock) which causes mitochondria release signal factors to initiate the apoptosis signalling cascade. Both pathways start from the activation of the initiator caspases (caspase 8 for extrinsic pathway and caspase 9 for intrinsic pathway), which subsequently induce the activation of caspase cascade including the effectors caspase 3 or caspase 7. The cytotoxicity of most chemotherapy and radiotherapy is due to the intrinsic pathway

whilst the killing of cytotoxic T cells belongs to the extrinsic pathway. Several of these physiological events or hallmarks can be used to monitor the progression of apoptosis, including caspase activation, membrane alteration, mitochondria depolarization and DNA fragmentation. Since various apoptosis induction can proceed via different pathways, it is usually necessary to use several methods for confirmation.

Autophagy (meaning self-eating) is classically activated in response to nutrient starvation and various forms of environmental stress. While the predominant function of autophagy is to promote cell survival, excess autophagy will result in autophagic cell death. The formation of autophagosomes is initiated by class III phosphoinositide 3-kinase and autophagy-related gene (Atg) 6 (also known as Beclin-1). The hallmark of autophagic activation is thus the formation of cellular autophagosome punctae containing LC3 II, as a result, autophagic activity is measured biochemically as the amount of LC3 II that accumulates in the absence or presence of lysosomal activity (Tsujimoto and Shimizu 2005).

Necrosis traditionally was considered a sudden or accidental cell death which is a pathological process that occurs when cells are exposed to a serious physical or chemical injury. Unlike apoptosis, necrosis is not energy-dependent. Biochemically, the most prominent features of necrosis include massive energy depletion, the formation of reactive oxygen species and the activation of non-apoptotic proteases. All the events result in a loss of function of homeostatic ion pumps and damage to membrane lipids with cell membrane swelling and rupture (Zong and Thompson 2006).

However, there is increasing evidence that necrosis is more tightly regulated than previously thought with an underlying genetic control that might be relevant in multiple physiological and pathological scenarios. Recently certain necrotic cell deaths have been recognized to depend on particular cellular pathways which can be regulated. For example, the cytotoxicity induced by H_2O_2 to respiratory cells (Nanavaty, Pawliczak et al. 2002) and by asbestos to mesothelial cells both belong to necrosis (Yang, Rivera et al. 2010), they are poly(ADP ribose) polymerase PARP dependent and can be inhibited by PARP inhibitor.

More recently, the concept of "necroptosis" has been introduced which relates to a special type of programmed necrosis that depends on serine/threonie kinase RIP1 activity. Like apoptosis, it can be executed by regulated mechanisms which are mediated by an extensive network of genes. Necroptosis is induced by external stimuli in the form of death domain receptor engagement by their respective ligands, TNF-α, FasL and TRAIL, under conditions **where apoptosis is prevented** (Degterev, Hitomi et al. 2008; Christofferson and Yuan 2009; Vandenabeele, Galluzzi et al. 2010). However, necroptotic cell death lacks the clear hall marks as apoptosis, and it is characterized by the same or similar morphological features as unregulated necrotic death (Berghe, Vanlangenakker et al. 2010), including rounding of the cell, cytoplasmic swelling, rupture of the plasma membrane and spilling of the intracellular content. Currently the small molecules RIP1 kinase inhibitors (necrostatin) are the major way to analysis necroptosis (Degterev, Hitomi et al. 2008; Miao and Degterev 2009).

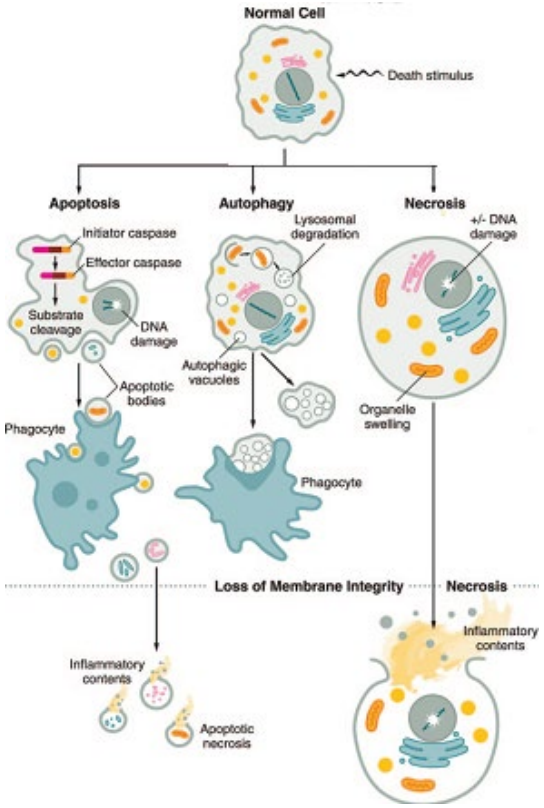


Fig1.4 The three different cell death types. Healthy cells respond to death-inducing stimuli by initiating a variety of molecular pathways leading to cell death, can be divided by apoptosis, autophagy and necrosis. They have distinct features of the dying cells and different pathology significance for the dead cells. The figure was referenced from (Fink and Cookson 2005).

1.3.3 Biological consequences of the death types

The fates of cells that undergo apoptosis or necrosis are totally different. Apoptosis and autophagy are peaceful cell deaths. Apoptotic cell is disintegrated and the cellular contents are encapsulated with intact plasma membrane and formation of apoptotic bodies. These apoptotic bodies are rapidly recognized, ingested and cleared up by phagocytic cells without any leakage of cellular contents, therefore, without provoking an inflammatory response. Moreover, the engulfment of apoptotic cells by macrophages triggers the production of anti-inflammatory cytokines. Autophagic cells can also be taken up by phagocytosis (Fink and Cookson 2005). On the

contrary, necrosis is dangerous and necrotic cells are immunogenic. When cells swell and burst, they spill their contents over in the vicinity of others and thus elicit a damaging inflammatory response. The currently identified endogenous dangers include the extracellular release of Heat shock protein HSP70, high-mobility group box1 (HMGB1), calreticulin and uric acid.

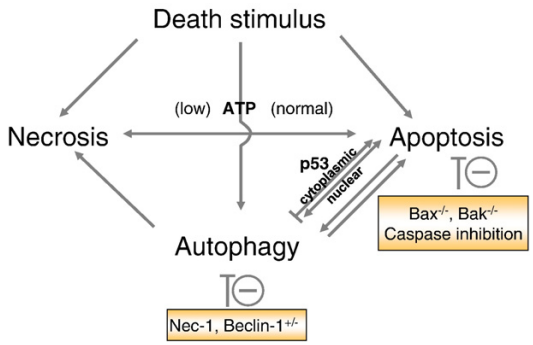


Fig 1.5 The cross talks between different death types, copied from Cell death mechanisms: Cross-talk and role in disease, Exp Cell Res,2010,V36(8)

1.3.4 The crosstalk of the different death types

It is noteworthy, that in reality the cell death mechanisms are often much more complicated and ambiguous to be a clearly defined. Researchers usually found that the same stimulants are able to induce different death types, or that more than one death types occurs concomitantly in the same dead cells (Krumschnabel, Ebner et al. 2010; Peri, Nuutila et al. 2011). The complexicity largely comes from the crosstalk between various modes of cell death. Depending on the nature and severity of the stimulus, or the cell type, the crosstalk may result in different cell modalities. In some cases suppression of the function of a particular intracellular compartment

might switch one mode of cell death to another. As shown in Fig 1.5, inhibition of mitochondrial energy metabolism (lowering of ATP) can change the mode of cell death from apoptosis to necrosis. Similarly, inhibition of caspase activity might change apoptosis to necrosis or autophagic cell death, whereas activation of calpain-mediated cleavage of autophagy-regulated protein, Atg-5, switches the mode of cell death from autophagy to apoptosis (Zhivotovsky and Orrenius 2010).

1.4 Oncolytic virus mediated cell death

Understand the mechanism of virus mediated cytotoxicity is crucial in oncolytic virus development. Closely related with virology and tumour cell biology, the death mechanism could be provide valuable information for optimizing virus genetic manipulation, enhancing therapeutic potential, rational designing therapy procedure and eventually predicting the clinical outcome.

Compared to chemotherapy drugs which mainly work by inducing apoptosis mechanism, oncolytic viruses mediated cell deaths are much more complicated. Through Evolution, viruses have gained the ability to manipulate the host cell machinery at the different levels, in order to maximize progeny virus production and dissemination. However, many previous oncolytic virotherapy studies most focus on virology side while neglect the host cellular response and pathway regulation. The concept of “lysis” or oncolysis, the key step after a successful infection and replication before dissemination, has been oversimplified for long time. Oncolysis was always regarded as the equivalent to necrosis (Liskova, Knitlova et al. 2011), moreover, the direct killing ability was assumed to be mainly responsible for the viral potency. Only recently, more and more evidences based on cell biology studies

have revealed the multiple natures of oncolytic virus induced cell death, depending on viral type and host cell factors.

1.4.1 The cytotoxicity, viral replication and host cell status

Viral mediated cell death is dependent on viral replication. Usually, no tumour cell cytotoxicity is observed when using non-replicating viral vectors or physically inactivated (either by heat or UV radiated) virus; oncolytic adenoviruses are able to infect normal cells but cytotoxicity is found rather week because of low replication. However, it is of noted that there is limited link between cytotoxicity and viral replication titre, cytotoxicity does not always correlate with the extent of viral growth and replication, and infectivity alone is a poor predictor of cell sensitivity to virus induced death. This observation has been recorded in both Sindbis virus and Ad5 studies.

Sindbis produces high titre of virus in HSC-4 cell along with in 12 other oral squamous cell carcinoma cell lines, however it causes little cytotoxicity in HSC-4 cells. In contrast, viral titres were low in Sa-3 and H-1 cells but it cause high cytotoxicity was observed (Saito, Uzawa et al. 2009). Similarly, in one recent Ad5 based study on the sensitivity of ovarian cancers to adenovirus infection, the viral mediated cytotoxicity was found to vary greatly, even in cells with similar infectivity. Using both the adenovirus E1A-CR2 deletion mutant *dl*922-947 and WT adenovirus serotype 5 in a panel of human ovarian cancer cell lines that cover a 3-log range of sensitivity, profound overreplication of genomic DNA was found only in highly sensitive cell lines including TOV21G and HCT116, but not in non sensitive cell lines including A2780 and Skov3 (Flak, Connell et al. 2010.). The authors believe this was associated with the presence of extensive genomic DNA damage and

overreplication. The cellular DNA repair mechanisms ataxia telangiectasia and Rad3-related checkpoint kinase 1 (ATR-Chk1) and Cdc25 are key determinants of oncolytic adenovirus activity.

The functional p53 (Hall, Dix et al. 1998) and p21(Flak, Connell et al. 2010.) levels of the infected cells have been identified to play a necessary part in mediating cellular destruction to allow a productive adenovirus infection. Cells expressing wt p53 (including A549, 293, HepG2, HT1080), as well as p53-defective cells (including IIICF/c and HT1080 6TGc5) allow adenovirus replication, but only cells expressing wt p53 show evidence of virus induced cytopathic effect. This correlates with the ability of adenovirus to induce cell death. The defect in adenovirus-induced CPE in mutant p53 cells is not due to an absence of virus infection or growth, but instead, it results from a defect in the ability of these cells to die.

1.4.2 Oncolytic RNA viruses induce apoptosis

Currently RNA viruses are composed of the majority part of oncolytic virus development. Various RNA viruses have been intensively investigated in oncolytic virotherapy, including: Sindbis (SIN), Respiratory syncytial virus (RSV), Newcastle disease virus (NDV), Vesicular stomatitis virus (VSV) as well as reovirus. The advantages of RNA viruses relay on their specific selection in tumour cells, fast oncolysis and short, simple genomes which are easily manipulated. Viral RNA genomes undergo robust transcription/replication in the cytoplasm without nuclear involvement. Cytotoxicity induction starts from just a few hours after infection, for example, 6 hours in the case of SIN (Saito, Uzawa et al. 2009).

Most RNA oncolytic viruses induced cell death type belongs to apoptosis. Depending on the specific virus, the apoptosis can go through either the intrinsic (mitochondrial dependent) pathway or extrinsic (death receptor dependent) pathway. On multiple human tumour cell lines such as HeLa, HepG2, CaCO2, PC3 and HT29, the oncolysis induced by NDV is thought to be multiple caspase-dependent pathways of apoptosis, and is independent of interferon signalling competence (Elankumaran, Rockemann et al. 2006). Apoptosis triggered by NDV appeared from 6 hours after infection, since then the cells displayed typical Annexin V positive labelling, DNA laddering (8 hours post of infection). TNFα was induced as early as 12 hour post of infection with the level increasing, and TRAIL was induced at 48 hours post of infection but there is no correlation between TNFα and TRAIL levels in the different cell lines. In the mean time, caspase-8 is found activated but dispensable for apoptosis induction after NDV infection of tumour cells. These results indicate that activating apoptosis by death receptor signalling (extrinsic pathway) plays a minor role in cell death and is late cellular events. On the other hand, NDV triggers death by rapid loss of mitochondrial membrane potential and the subsequent release of the mitochondrial protein cytochrome c ; Caspase-9 is activated early after infection, followed by the effector caspase 3 activation. The killing is entirely caspase dependent and the broad-specificity caspase inhibitor zVAD-fmk is able to inhibit the oncolysis completely until 48 hours post of infection. This has proved that apoptosis, especially the intrinsic pathway plays a major role in NDV oncolysis. The mitochondrial membrane destabilization may be related with the double-stranded RNA intermediates during viral replication and their cause endoplasmic reticulum stress.

Similarly, the intrinsic apoptosis pathway mediated by oncolytic RSV is considered as the major route to kill the tumour cells (Echchgadda, Kota et al. 2009). In PC-3 human prostate cancer cells, RSV infection was found to activate caspase-3, increasing pro-apoptotic protein Bad and Bax expression levels and decreasing anti-apoptotic protein Bcl level. Blocking caspase9 and 3 results a drastic decline (by 75-85%) in apoptosis. The extrinsic pathway may have minor function because blocking caspase 8 is only associated with 15% reduction of cell death. In addition, the minor extrinsic pathway is found exclusively induced by the paracrine/autocrine action of TNF generated by the infected cells, and not by TRAIL and FASL. Further study suggested the RSV induced apoptosis is triggered by the down-regulation of nuclear factor-κB (NFκB) activity. Further more, the intrinsic apoptosis also has been evidenced as contributing the major part of SIN and VSV(Cary, Willingham et al. 2011) mediated tumour cell oncolysis.

As a contrast, for Reo virus (Errington, White et al. 2008) and VSV(Cary, Willingham et al. 2011) the extrinsic pathway has been identified as the major apoptosis route. Reo virus induces the releasing of TRAIL and up-regulation the related receptor DR5 on the infected cells. The consequence of the binding of TRAIL and DR5 then promotes FADD association and activation of caspase 8. Blocking the caspase activity by the inhibitor ZVAD-fmk can protect 90% virus kill on melanoma cell lines.

1.4.3 Oncolytic DNA viruses mediate complicate cell deaths

Adenovirus (Ad), Vaccinia virus (VV) and Herpes Simplex virus (HSV) are the three commonly used DNA oncolytic viruses. Compared to ordinary RNA viruses, the three DNA viruses have a large and complex genome, which affects host cells

metabolism at many different levels. Apoptosis is normally considered a defense mechanism of infected cells that minimizes the spread of viral progeny by limiting cellular production of virus. In order to achieve the maximum progeny virus production, the DNA viruses have evolved to encode various genes, the products of which exert anti-apoptotic properties at the replication stage. During infection stage, the viral proteins act in concert with several host cell-encoded key apoptotic regulators in a sort of cell death balancing act, leading to the time delay of cell death and allowing efficient replication and generation of viral offspring. However, at the late replication stage and once the mature virions finish assembly, the lytic virus will try to destroy host cell to facilitate virions release. Despite the known apoptosis-regulatory function of individual viral genes, it is currently unclear that, at the last stage of infection, named oncolysis, whether the disruption of tumour cells employs the basic apoptotic machinery of the host cells.

1.4.3.1 Vaccinia and HSV

VV has multiple gene products that inhibit the extrinsic apoptosis pathway (SPI-2 inhibits caspase8 and caspase1) and intrinsic apoptosis pathway (F1L inhibits Bax, Bak and caspase 9, N1L is similar to Bcl-2 and E3L prevent activation of PKR). Additionally, VV interferes with apoptosis indirectly by inhibiting or modifying various host antiviral immune response (Liskova, Knitlova et al. 2011).

During oncolysis, VV (strain WR) has recently been reported to induce apoptosis in Hela cells but necrosis in BSC-40 cell, although both are epithelial cell lines. The induced death of HeLa cells are characterized as caspase 3 activation, PARP cleavage and the morphological observation, typical of apoptosis, ZVAD also can effectively reduce the caspase activity; moreover, these features were not seen on

BSC-40 cells although it shows the similar cytotoxicity degree and some caspases 2 and 4 activation. The difference of host cell metabolism could be owing to divided death routes, for instance, lack of caspase activity in BSC-40 cells; the kinetics of VV growth and gene expression are slower in HeLa cells than in BSC-40 cell; VV encoded anti-apoptosis genes at early infection stage have higher expression in BSC-40 cells than in Hela cells, consequently, it more potently inhibits caspase activity; expression of VV-encoded genes and negative effects on the host cell metabolism may be faster and more profound in BSC-40 cells, thus BSC-40 cells should be more prone to necrosis. In contrast, the expression of VV-encoded genes, including the anti-apoptotic ones, is slower in HeLa cells, therefore increasing the chance for apoptosis to occur.

HSV-1 can prevent the apoptosis induced by hyperthermia, osmotic shock, or exposure to C2-ceramide, tumor necrosis factor α as well as FASL antibody. The cellular response to HSV-1 infection includes phosphorylation of eukaryotic initiation factor-2α, which shuts off protein synthesis and terminates the lytic cycle of the virus. To counteract this apoptotic response, HSV-1 has evolved to include genes such as γ_1*34.5*, which encodes the ICP45 protein and prevents phosphorylation of eukaryotic initiation factor-2α and thus precludes the host cell shut off of protein synthesis. Several other HSV-1 genes and proteins are involved in preventing the host apoptosis response such as *ICP4*, *Us3* and *Us5*, and *ICP27*, underscoring the importance of apoptosis to viral propagation(Stanziale, Petrowsky et al. 2004).

During oncolysis, HSV-1 virus was reported to elicit apoptosis in infected cells but induces apoptosis in uninfected, cocultured cells. Apoptosis inhibition (10 mM *N*-acetylcysteine NAC) of this response improves virus production and tumor kill(Stanziale, Petrowsky et al. 2004). Nevertheless, any soluble mediator from

infected cells that causes the indirect apoptosis has not been found. It also may be explained by abortive viral transcription or assembly resulting in nonproductive infection, however neither heat-inactivated nor UV-inactivated HSV virus is able to induce apoptosis.

A herpes simplex virus type 2 (HSV-2) mutant, DeltaPK, was reported to have strong oncolytic activity for melanoma. Cell death was due to activation of calpain as well as caspases-7 and -3, and it can be abolished by the combination of calpain (PD150606) and pan-caspase (zVAD-fmk) inhibitors (Colunga, Laing et al. 2010). Up regulation of the autophagy protein Beclin-1 and the pro-apoptotic protein H11/HspB8 accompanied DeltaPK-induced melanoma oncolysis whilst the exact contribution of these death-related proteins to melanoma oncolysis is still currently unclear. This suggests both autophagy and apoptosis can be involved HSV oncolysis

1.4.3.2 Adenovirus

The last stage of the adenovirus replication cycle, oncolysis, is considered inefficient (Bardell and Metcalf 1972) and remains poorly understood.

As Adenovirus serotype 5 (Ad5) has the historically importance in gene therapy, virotherapy and cell biology, its genome have been most intensively investigated. Multiple viral gene products and their functions play important roles to participate in the host cell death manipulation, depending on the infection stage(Braithwaite and Russell 2001). The viral encoded proteins can be divided as pro-apoptotic and anti-apoptotic. Most notably, E1B-19KD, E1B-55KD in complex with E4orf6, and the E3-10.4KD and E3-14.5 KD proteins which are encoded by early transcribed genes, act as anti-apoptotic proteins and are responsible for the prevention of premature oncolysis or cause immune suppression; E1A-12S, E1A-13S, E4orf4 and E3-11.6 act

as pro-apoptotic or death promoting proteins at late stages of infection. Thus, during Ad infection, the viral proteins act in concert with several host cell –encoded key apoptotic regulators in a sort of cell death balancing act, leading to the time delay of cell death and allowing the efficient replication and generation of viral offspring. Among the viral encoded death promoting factors, E3-11.6 (named as adenovirus death protein ADP) and E4orf4 are most interesting and have been considered as the major effectors contributing to oncolysis.

Although it is an early gene product, E3-11.6 is expressed at low levels at early times in the lytic cycle, but synthesized in large amounts from mRNAs derived from the major late promoter. It is an integral membrane glycoprotein that initially localises to the ER and Golgi apparatus; ultimately it accumulates at the Golgi apparatus and nuclear membrane. While ADP is not required for lysis of the infected cell, its presence makes the release and spread of viral progeny much more efficient (Tollefson, Scaria et al. 1996; Yun, Kim et al. 2005). Overexpressing of ADP with replicating adenovirus vector elicits enhanced cytopathic effect (CPE) by induction apoptosis, but the cells killed by Ad5 (with wild type of ADP) lack to show typical apoptosis signs, neither morphological characters nor DNA laddering have been observed. Since that, introducing membrane permeability increase by ADP at the last stage of adenovirus replication has been speculated (Doronin, Toth et al. 2003).

The E4orf4 protein also triggers a novel death program that bypasses classical apoptotic pathways in human cancer cells. It is associated with distinct apoptosis-like morphological features (membrane blebbing with nuclear shrinkage) and kinetics, while the cell death is not inhabitable by pan caspase inhibitor zVAD-fmk. The hallmark of the cell death program is deregulation of the cell cytoskeleton and relies on Src family kinase and E4orf4 phosphorylation. Activation of the Rho GTPase is

required for the death induction and inhibition of actin dynamics dramatically impairs E4orf4 killing (Robert, Smadja-Lamere et al. 2006).

Since these so many viral gene products interact with cellular regulators, it is not surprising that wild type adenovirus mediated cell death is not classified as a classical apoptosis. The Ad5Δ24 infected H460 cells, before oncolysis, show rounding, blebbing with slightly swollen nuclei (probably due to virus replication and assembly), without DNA fragmentation. The oncolysis is independent on caspases and Bcl, with low levels PARP cleavage although with some PS externalization. E1 Hassan named it " necrosis-like" programmed cell death, in order to differentiate with the basic apoptosis programmed cell death (Abou El Hassan, van der Meulen-Muileman et al. 2004). Similar observations have also been recognized by Baird when studying the virus killing on ovarian cancer cells. They confirmed the classic apoptosis does not occur and neither mitochondrial plays any determining role, or does autophagic cell death. By excluding a role for proteases such as cathepsins, lacking the falling of intracellular ATP levels, they further suggested the pure necrosis is not evident (Baird, Aerts et al. 2008).

Interestingly, contrast to many recombinant Ads with overexpression of cytotoxic or therapeutic transgenes induced a typical apoptosis mechanism (through ADP, p53, TRAIL), the recombinant adenovirus AdYB-1 is the few one to report inducing necrosis-like cell death (Glockzin, Mantwill et al. 2006). The E1/E3 deleted Ad expresses the human transcription factor YB-1 under the cytomegalovirus CMV promoter control. This is not only facilitating viral replication, but also involved in the induction of cytopathic effect and cell killing and release of viral particles. The death is not associated with apoptosis, but with a robust extracellular progeny virions release.

Contrary to Baird's conclusion, currently a strong popular opinion insists that autophagic cell death can be the main contributor to adenovirus mediated oncolysis. This theory was first published by the Ito group, who used a conditionally replicating adenovirus with human telomerase reverse transcriptase (hTERT) promoter to treat malignant glioma cells(Ito, Aoki et al. 2006). This is also consistence with some other research groups, demonstrating this death mode is not limited to certain recombinant adenoviruses but also applied to wide type Ad5; what's more, the death is a common feature of different type of cancer cells when infected (Jiang, White et al. 2011; Rodriguez-Rocha, Gomez-Gutierrez et al. 2011) . Their supporting evidences include:

(1) Autophagy morphology increase with Ad infection, hallmarked by the development of acidic vesicular organelles and double layered autophagosomes in the cytoplasm;

(2) Observed by TEM, development of autophagy was seen accompanied by destruction of cellular structure and release adenoviral progenies. Autophagosomes formation is sufficient to disrupt the integrity of membrane structure in the cells. Fusion of the autophagosome with the lysosome is not always necessary for the induction of efficient cell lysis.

(3) Biochemical analysis demonstrates: the remarkable upregulation of Atg12-Atg5 complex, LC3-1 enzymatic cleavages into LC3-II, which is associated with the autophagosome membrane formation. The autophagy inhibitor 3-MA have certain attenuation effect to virus induced cytotoxicity; In addition, the mammalian target of rapamycin (mTOR) is activated by infection, while

it's inhibitor rapamycin stimulates autophagy and therefore enhances viral replication and promote cell lysis.

(4) Autophagy triggered caspase activity also contributes to cell lysis in some cell types. For example, in leukaemia A3 cells, caspase 8 is activated part of the extrinsic FADD/Caspase pathway. ZVAD-fmk treatment can reduce the amount of cell lysis by 40%. This indicates there exists the conjunction of autophagy and apoptosis in adenovirus induced oncolysis.

It is worthy to note, overexpression of nuclear Survivin by CRAd24 was reported to abrogate multiple cell cycle checkpoints and enhance the viral oncolysis(Connell, Wheatley et al. 2008). Survivin is a member of the BIR-containing apoptosis inhibitor family; however, apoptosis is not the primary mode of cell death. In a similar study which employed the surviving promoter in the adenovirus vector induce glioma oncolysis, occurred a process via a beclin-dependent process, autophagy was evident (Ulasov, Tyler et al. 2009).

For a long time, autophagy has been considered as a cell survive strategy when fighting with viral infection (Sir and Ou 2010). On the other hand, autophagy may play a critical role in viral replication by degrading intracellular components for building progeny virus particles (Jiang, White et al. 2008). It is known that excessive autophagy will induce cell death, nevertheless it is still arguable that autophagy could be the basic mechanism for adenovirus induced oncolysis, because it is still unclear that whether autophagy is the cause or the companied phenomena during viral infection.

1.5 Thesis objective

In this thesis, the oncolytic behaviour of the novel Ad11/Ad3 chimeric adenovirus ColoAd1 was investigated. The study would be used to collect the basic information and provide materials for the pre-clinical trial in the near future, and it also would be helpful for the next generation oncolytic virus development based on ColoAd1 prototype. The study included four parts:

- Characterization of ColoAd1 based on its basic virology;
- Investigation the modification of host cell biology with the progression of ColoAd1 infection, particularly at the oncolysis stage
- Identify the cellular death pathway involved in oncolysis by specific inhibition
- Initial exploration of the application of ColoAd1 induced oncolysis in advanced cancer virotherapy.

Understanding the virology aspects is fundamental for an oncolytic virus development. With the side by side study with Ad5 and its parent virus Ad11, we assessed a wide features of ColoAd1 as an effective oncolytic virus, including cellular uptake rate and infectivity, relative potency and killing kinetics, the selectivity of replication and cytotoxicity in tumour cells versus normal cells, the resistance to neutralisation by blood factors and IFN as well as the spreading ability of progeny virus.

Investigation of the host cell biology aspects is the next important step to understand ColoAd1 induced cytotoxicity mechanisms, since the outcome of the virus life cycle (infection, replication and oncolysis) is highly dependent on cellular response. Depending on by the host cell and virus types, the adenovirus replication has

profound impact on cellular DNA damage, cytoplasm membrane leakage, cell and nuclear morphology, cell death key regulator and enzyme expression levels, as well as intracellular ATP and Ca^{2+} levels. Measurement of the change of these cellular factors with virus infection progression revealed the source of ColoAd1 potency, which could be associated with the specific pathway used in ColoAd1 mediated cell death: apoptosis, necrosis or autophagy.

Identification of the cellular pathway is further critical to elucidating oncolysis mechanism and using synthetic small molecular weight inhibitors to specifically inhibit the key enzymes in the cellular pathways provided an effective tool. The inhibition effects of a panel of inhibitors, including the inhibitors of caspase, PARP, RIP1,Rho kinase were investigated.

Finally, as an initial preliminary study, in the last part of this thesis the potential of ColoAd1 is assessed in: (1) circumventing drug resistance (2) activating an immunogenic signal in the tumour micro-environment. Both of these subjects represent the current frontier of cancer virotherapy and show great potential for using oncolytic viruses as lethal weapons to combat cancer.

Chapter 2: Materials and Method

2.1 Materials and methods

2.1.1. Virus and cell lines

The Adenovirus serotypes Ad5, Ad11, ColoAd1 and ONYX-015 were all purchased from The Native Antigen (UK). The viral stocks were propagated on HEK293 cells and purified on CsCl gradients. For determining stock viral genome copies concentration, Picogreen assay was used to quantify the viral particles number (VP/ml) by measuring DNA content; for determining viral biological titre, TCID50 assay was used to measure the infectious particles number or plaque forming unit (PFU/ml).

The tumor cell lines A549 (human lung adenocarcinoma epithelial cell line), HepG2(human liver heptocellular carcinoma) and normal cells human lung fibroblast WI-38 were purchased from ATCC, cultured and passaged in Dulbecco's modified Eagle's Media (DMEM) containing 2 mmol/l glutamine supplemented with 10% foetal calf serum(PAA, UK). The other normal cells human umbilical vein endothelial cells HUVEC and human hepatocytes were purchased from Lonza (UK), cultured or maintained in their special medium supplied by the cells supplier. Cell phenotypes of the cell lines were analyzed every passage; WI-38 and HUVEC were used for experiment between passage 4-8. Hepatocytes was used and maintained for 3 days after thawing from the liquid N2 storage state.

CAPAN-1 (pancreatic cancer cell line) and CAPAN-1 res (CAPAN-1 cisplatin resistant strain) both are kindly gifts from Professor Thomas Helleday (Gray Institute for Radiation Oncology and Biology, University of Oxford, UK). The cells were maintained and passaged in DMEM with 10% FCS.

HCT 116 (colorectal carcinoma cell line) and it drug resistant sub lines HCT-OX (Oxaliplatin resistant) and HCT-5FU (5FU resistant) are kindly gifts from Professor

Patrick Johnston (Department of Oncology, Queen' University, Belfast, Northern Ireland). The cells were grown in McCoy's 5A medium, supplemented with 10% FCS, 50 μg/ml penicillin-streptomycin, 2mM L-glutamine and 1mM sodium pyruvate (PAA, UK). HCT-OX were found to be stably resistant and therefore maintained in oxaliplatin-free medium that was spiked every 4 weeks with 8 μM oxaliplatin (Sigma Aldrich, UK and prepared 50mM in DMSO); HCT-5FU were maintained in the presence of 2 μM 5FU (Sigma Aldrich, UK and prepared 50mM in DMSO) and stepwise increasing concentration of 5FU to 5 μM over a period of 2 months. The drug resistant status of the cell lines was confirmed by inclusion of the relevant drugs as an experimental control.

The stable NFKB Macrophage reporter cell line U937-NFKB-Luc cells is the kindly gift from Dr Kerry Fisher. It was cultured in RPMI medium (PAA, UK) with the supplements of 10% FCS, 1% P/S and 0.2 mg/ml hygromycin (Sigma Aldrich, UK) which was used as selection antibiotics.

Cells were maintained at 37ºC, 5% CO_2 in a humidity-controlled incubator and handled using sterile techniques in a class II laminar-flow cabinet. Cells were split once they were confluent. All the tissue culture plasticware are supplied by Corning (UK).

2.1.2 Picogreen assay

Viral stock was diluted and lysed in SDS-TE buffer at 56ºC for 30min, then the double strand DNA content of the virus quantified with Picogreen kit (Invitrogen, UK). The picogreen dye bind with double strand DNA leads to a strong fluorescent emission maximum of 530 nm which was read out by a fluorescence microplate reader (Wallac Victor 1420 multilabel counter). The concentration known purified bacteriophage λ DNA was used as standard, according to the kit supplier's protocol.

The virus particle number was calculated according to adenovirus genome molecular weight. The viral stock diluted in TE buffer were also measured by Picogreen, the obtained DNA content represents the free double strand DNA(unpacked virus) in the stock.

2.1.3 TCID50 assay

A549 cells were seeded at the density of 10,000 cells/well in 100 µl DMEM with 10% FCS and 1% penicillin-streptomycin in a 96 well plate a day before the experiment. The virus was 1:10 serial diluted in 200 µl DMEM with 2% FCS and 1% penicillin-streptomycin to prepare the infection medium. The medium of the cells was removed and cells were washed by PBS twice and then were added in with the infection medium. At the post infection day 4, another 100 µl fresh medium was topped up. Each virus dilution was replicated in 12 wells of one row and repeated in three plates. CPE was observed at post infection day 7 under the microscopy and the plate was stained by 10% formaldehyde-1% crystal violet (Sigma Aldrich, UK) solution. The wells which has turned up the CPE and just below the row of the totally cell death were counted, then the infectious particle unit (PFU/ml) calculation was done by equation $T=10^{1+d(s-0.5)}$ of Karber formula (Karber 1931) (d: dilution factors; s:sum of infection well ratio.

2.1.4 Cell viability assay (MTS)

The viral oncolysis potency was measured using the 5days (unless specified) MTS assay (cellTiter 96 aqueous Non-Radioactive cell proliferation assay, Promega, UK). To perform this assay, the cells were seeded at the density of 10,000 cells/well in 100 µl DMEM with 10%FCS and 1% penicillin-streptomycin in a 96 well plate a day before the experiment. Started from 500 viral particle per cells (unless specified) , the virus was 1:5 or 1:3 series diluted in 200 µl DMEM with 2% FCS and 1% penicillin-

streptomycin to prepare the infection medium. The medium of the cells was removed and cells were washed by PBS twice and then added in with the infection medium. The plate was then incubated at 37^0C with 5% CO_2 and the MTS assay was performed at the time points indicated for the tested cells. The infection medium was removed, the wells were washed PBS twice and re-added with 100 µl warmed DMEM without phenol red medium (with 2% FCS and 1%P/S). Then 20 µl of MTS reagent was added into each well, and the plate was incubated at 37^0C for 1 hour. The colour change was read out by a microplate reader (Wallac Victor 1420 multilabel counter) at 490 nm. The reading of mocked cells served as negative controls and established 100% survival point for the given assay, and the reading of the medium alone with MTS reagent was used as 0 survival point. The number of the cells in the tested wells was calculated according to these two end points.

2.1.5 DNA extraction and quantitative PCR (QPCR)

Viral genome in all the complex samples including intracellular and cell culture supernatant was quantified by QPCR. The samples were extracted with the GenElute^{TM} mammalian genomic DNA Miniprep Kit (Sigma Aldrich) according to manufacture's instructions. Extracted DNA samples were stored at -20^0C. For QPCR DNA amplification, sequence specific FAM-TAMRA labelled probes and primers (Sigma) were designed according to the fragment of the adenovirus fibre gene. Analysis both Ad11 and ColoAd1 containing samples were used forward primer-TACATGCACATCGCCGGA, reverse primer CGGGCGAACTGCACCA, Taqman probe CCGGACTCAGGTACTCCGAAGCATCCT; Analysis Ad5 containing samples was used forward primers TGGCTGTTAAAGGCAGTTTGG , reverse primer GCACTCCATTTTCGTCAAATCTT , Taqman probe TCCAATATCTGGAACAGTTCAAGTGCTCATCT which was labeled at the 5'

end with the FAM fluorophore and at the 3' end with the TAMRA quencher. Primers and probe were purchased from Sigma Genosys (UK). Reactions were carried out in a total volume of 25 µl, primers and probe with Rox dye(Invitrogen, UK) were added to SensiMix NoRef (Quantace, UK) master mix and toped up with distilled water to 20l µl per well to obtain final concentrations of 0.125 µmol/l,1.25 µmol/l and 0.5 µmol/l respectively. 5ul of sample was added and QPCR performed on an ABI PRISM 7000 (Applied Biosystems, UK) starting with 50^0C for 2min and 95^0C for 10 min followed by 40 cycles of 15 sec at 95^0C for denaturation and 60^0C for 60 sec for annealing and extension. Data was analyzed using 7000 system SDS software (Applied Biosystems, UK), test samples compared to standards of known viral content based on Picogreen analysis.

2.1.6 Neutralization assay

Virus infection was carried out in the infection medium which include 1/25 (V/V) neutralization factors, including serum, erythrocyte, interferon, etc. The fresh blood from a healthy donor with high ad neutralization effect was collected in a heparin blood tube(BD, UK), the plasma was isolated from the supernatants of the blood tube after 5min centrifugation (3000 rpm); the RBC was isolated from the cell part of the tube followed by twice PBS wash.. A pooled human serum with 11 donors was purchased from Serum Lab (UK). Interferon α recombinant was purchased from Sigma. The infection medium was kept in the well for 5days before MTS assay, except the experiment with blood cells because the remained blood has cytotoxicity effect to the targeted tumour cells. In this case, the blood containing infection medium was removed after 2 hours of infection, 300 µl PBS was used to wash the wells twice, and 200 µl of fresh medium (DMEM with 2% FCS and1% P/S) was

added in to maintain the cells for 5 days, then the cell viability was measured by MTS assay.

2.1.7 Viral spreading assay and Plaque assay

Viral spreading assay in 96 wells plate was followed the method used by Sauthoff and Toth (Sauthoff, Pipiya et al. 2002; Toth, Djeha et al. 2004). Similarly to TCID assay, the cells (A549) were seeded at the density of 10000 /well, 24 hours before the infection. The virus was from 1:2500 dilution of the stock and then further 1:5 diluted in the infection medium. After PBS wash, 50 µl infection medium was added to the wells after the removing the previous medium, and then the plate was incubated at 37^0C, 5% CO_2 for 2 hours for the infection. After infection, the infection medium was removed and followed by PBS wash to get rid of unbinding virus. 20 µl of fresh 2% FCS DMEM was then added into the wells to maintain the cells for 7 days. At day 4 another 100 µl fresh medium was topped up in each well. When at the end point of the assay, all the supernatant was removed, cells was fixed by 10% buffered formaldehyde solution and stained by 1% crystal violet.

In plaque assay, A549 cells were seeded at the 0.5million cells/well in 6 well plates a day before the infection. A 10 folds serial dilution of virus from the stock was used to prepare 1ml infection medium. The infection was carried out for 2 hours, and then the cell monolayer was washed by PBS twice. After remove any supernatant, 2ml of 1% agar (Noble agar, Sigma Aldrich, UK) in DMEM with 2% FCS and 1% P/S) was carefully lay on the top of the cells. The plate was let it cooling down and solidify at the room temperature for 15 min, and another 2ml agar was layered again on the top by the similar way. The plate was then incubation at 37^0C, 5% CO_2 for 10 days. At day 4 and 7, when the color of the agar change from pink to yellow, 2 ml of fresh agar was applied on the top to supply the nutrition to the cells. The plaque can be

observed from day 5, and the size grew with the extension of the incubation time. At day 10, all the agar overlayers were removed; the cells were fixed and the wells were stained by crystal violet before taking pictures.

2.1.8 SDS-PAGE , Western blot and Dot blot

For visualising adenovirus proteins epitopes – human serum IgG binding, 5E10 particles of adenovirus were mixed reducing SDS-PAGE loading buffer and heat denatured (95^0C, 5min) before loaded 10% SDS-polyacrylamide gel. 120 V was applied for the electrophoresis to protein separation. The gel was then transferred to a nitrocellulose membrane (Amersham, UK) with current at 300mA for 4 hours. The membrane was blocked with 5% milk in PBST buffer (PBS with 0.1% Tween-20) for 1 hour, then incubated with the plasma or serum (1:1000 in 2.5% milk in PBST) for overnight at 4^0C with shaking. After incubation, the membrane was washed by PBST for 3 times and incubated with a secondary antibody (mouse anti-human IgG HRP, 1:5000, Santa Cruz) for 1 hour at room temperature. The membrane was washed again with PBST and PBS, stained by a chemiluminescence substrate ECL (Amersham, UK), then visualized and recorded by a digital gel image system with software Fluorchem 8900.

For investigating the key protein expression level in cellular response to viral infection or drug treatment, 0.8 million A549 cells were seeded and treated in T25 flask. At the end of incubation time, the supernatant was removed and floated cells were pelleted by centrifugation (600g, 5min). The pelleted cells and the cell monolayer were direct lysed with RIPA Buffer (Sigma, UK) containing protease inhibitor cocktail (Roche, UK) on ice for 20 min and pooled. After centrifugation at 14,000 rpm for 10 min, the supernatant of cell lysate was collected and stored in -80ºC. A small portion of the cell lysate was used in BCA assay by BCA kit (Sigma

Aldrich, UK) for measuring the protein concentration. The cell lysate was then adjusted by adding RIPA buffer and the SDS-PAGE loading buffer to get the concentration of 2 mg/ml. Then the samples were heat denatured (95ºC, 5min). 20 µl (40 µg) was used to load into the gel well.

SDSPAGE gel running, gel transfer and membrane blotting were the same as previous description. The primary antibodies used included: mouse monoclonal Anti-PARP-1(5A5) IgG1(Santa Cruz sc-56197); rabbit monoclonal IgG anti human cleaved PARP(Cell Signalling D214); rabbit monoclonal IgG anti human cleaved Caspase3 (5A1E), (Cell Signalling 96645); mouse monoclonal IgG3 anti human poly ADP-Ribose (BD Pharmingen, 550781); mouse monoclonal IgG1 anti human p53 (2C3) (AbD Serotec MCA35102); rabbit polyclonal IgG anti human MAP1LC3A/B(N-terminal) (AbD Serotec AHP2167T); mouse monoclonal IgG anti β -actin(AC-74) (Sigma, A2228); rabbit polyclonal IgG anti HMGB1 (Sigma, H9664); Mouse polyconal anti human HSP 70 antibody (R&D systems,841680).. Dilutions were used at 1:1000 except anti cleaved Caspase 3 was used at 1:500. The secondary antibodies were used as goat anti mouse IgG HRP (Santa Cruze) or goat anti rabbit IgG HRP (Promega, UK) by 1:5000 dilution.

The dot blot was prepared by dispensing 1 µl of the cell lysate or protein sample on the nitrocellulose membrane. Once the dot has been dry, the membrane was carried out with blocking, antibody coupling and HRP- ECL staining steps same as West blot.

For direct visualizing the protein bands on the SDSPAGE gel, the gels were stained either by the sliver staining kit (Sigma, UK) or the instant blue kit (Expedeon,UK).

2.1.9 Cell cycle analysis

The A549 cells were seeded 0.1 million cell/well in 12 well plate with 1ml DMEM (10% FCS and 1% P/S) 24 hours before. Next day, the medium was taken off and the cells were washed by PBS twice. ColoAd1 (10 PPC), Ad11 (25 PPC) and Ad5 (100 PPC) were used to infect cells with 2ml infection medium (2% FCS and 1%P/S). Similarly, Cisplatin (50 μM) and H_2O_2 (1mM) were used to treat the cell. The inhibitors, 50 μM necrostatin-1(Sigma, UK) and 5mM 3-ABA (Tocris, UK) were added to the cells 1hour before infection. Then the cells were maintained in the infection medium to the specific incubation time.

At the end of the incubation time, the cells were harvested. The cell monolayer was trypsinized and neutralized with full growth medium and pooled together with the previous supernatant part. The cells were pelleted by centrifugation at 400g for 5min, then were fixed and permeabilized in 70% cold ethanol and stored in -20ºC. When all the samples were collected, the cells were washed by cold PBS and stained with 100 μg/ml PI and 100 μg/ml RNase A (Sigma, UK) at 4ºC for overnight. Cells were then analyzed by flow cytometry FCAS Calibar (BD Biosciences, UK) with Cell QuestPro software. A minimum of 10,000 events were counted for each sample. Percentages of cell cycle distribution in the phases: SubG1 phase (hypodiploid, DNA content <2N), G0/G1 phase (resting/gap phase 1, DNA content = 2N), S phase (DNA synthesis phase), G2 phase (gap phase2, DNA content = 4N) and M phased(Mitosis phase, DNA content > 4N) were calculated.

2.1.10 Annexin V/ PI stain

The cells were seeded and treated as the same described in cell cycle analysis.

For the samples used in microscopy analysis, the medium was then carefully aspirated and the cells were washed by PBS to get rid of the floating cells. 100 μl binding buffer containing with 1μl AnnxinV-flurorescein and 1μl PI from the

Annexin V/PI kit (Roche, UK) was used to stain the cells. The staining was carried out by the incubation under the condition of the dark, room temperature for 15min. After that, the wells were observed under a Zeiss Axiovert 25 Invert light/fluorescence microscope in 1 hour, the images were recorded by a Nicon DS-U2 camera and processed by a NIS-element AR 3.00 software.

For quantification of apoptosis and necrosis by flow cytometry analysis, the cells were harvested via mild trypsinisation, including with any floating cells, centrifuged and resulting pellets washed twice in ice-cold PBS (5% FCS). The cell pellets were then re-suspended in 100 µl binding buffer containing 1 µl AnnexinV-FCS and 1 µl PI in FACS tubes. Cells were gently vortexed and incubated for at room temperature in the dark for 15min. Following this, 400ul of the binding buffer was added to each tube before analysis. The samples were run using Dako Cyan flow cytometer with 488nm excitation laser and 530/30nm (FL1, green), 585/42nm (FL2, red) filters. With gating out the cells debris, a minimum of 10,000 events were quantified for each sample. The data was analysed using Summit 4.3 software to quantify the percentage of apoptosis and necrosis in the cell population. Comparisons were made with untreated mock cells and Cisplatin or H_2O_2 treated cells.

2.1.11 Intracellular ATP measurement

The cells were seeded as 10,000 cell/well density in a 96 well plate. The virus infection was carried out as in previous description. At the end of incubation time, the supernatant was removed and intracellular ATP was measured according to the commercial kit manufacture instruction (Intracellular ATP kit HS, Biothema 266-111, Netherland). Briefly speaking, the well was washed, added with 20 µl fresh medium and 20 µl ATP eliminating regent, incubated for 10 min at RT which enzymatically degraded the extracellular ATP. The cells were then lysed by 20 µl Extractant B/S

for intracellular ATP release and stabilization. Then 15 µl of the lysate was taken to mix with 160 µl ATP reagent HS containing luciferase and luciferin, finally, the light emission is measured by a microplate luminometer (Vector). The protein concentration was measured by BCA assay. The data was analysis by luminometer reading deduction of the background, normalized by the protein concentration and finally expressed as the percentage of the control wells.

2.1.12 Intracelluar Ca^{2+} measurement

The intracellular Ca^{2+} level was measured by FluoForte ^{TM} calcium assay HT kit (Enzo, UK). The treated wells are removed medium and washed by PBS. 100 µl FluoForte dye loading solution was added into the well. The plate was incubated at 37ºC for 45min then moved to RT for another 15min. At the end of the incubation time, the well was observed under the Zeiss Axiovert 25 Invert light/fluorescence microscope and the plate was read by Vector microplate reader with green florence filter. The data was analysed by the reading normalized with protein concentration and expressed the percentage of the mock control wells.

2.1.13 Enzyme Linked Immuno Sorbent Assay (ELISA)

The cellular and extracellular HSP70 was quantified by DuoSet IC Human/Mouse/Rat total HSP70 ELISA kit (R& D Systems, UK) according to the manufacture manual. The supernatant of the wells was collected and stored at -80C. The cells were lysed by 100 µl reporter lysis buffer (Promega, UK). The ELISA ImmunoMaxiSorp plate(Corning, UK) was coated with 50 µl capture antibody at the working concentration of 2 µg/ml in PBS overnight at RT. Next day, the plate was aspirated, washed by PBST and blocking with 1% BSA for 2 hours. The 50 µl of cell lysate or supernatant was added into the well with the HSP standards 1:2 serial dilution (started from 10 mg/ml), then the plate was incubation at RT for 2 hours.

After the incubation, the plate was aspirated and washed by PBST for 3 times. 50 µl detection antibody at the concentration of 100 ng/ml was added into each well and the plate was incubation further 2 hours. After aspirate and wash by PBST, 50 µl of streptavidin-HRP was added and the plate was incubated for another 20min. repeat aspirate and wash, finally 50 µl of TMB substrate was added to each well. The plate was incubated at RT for another 20 min, then 25 µl of the stop solution was added to the well. The plate was read by the microplate reader Vector at 450nm wavelength. The standard curve was constructed by plotting the log of the HSP concentrations versus the log of O.D. The HSP 70 concentration of the sample was then calculated based on the standard curve.

2.1.14 NFKB activation assay

The U937-NFKB-Luc cells were seeded as 1 million / 1ml concentration in 12 well plate. 50 µl cell lysate or cell culture supernatant is added in to stimulate the cells. The plate was incubated at the cell incubator for 8 hours. Then the cells were collected by centrifugation at 1000 rpm for 5min. The cells pellet was washed by cold PBS twice, and was added 100 µl of Promega reporter lysis buffer then stored at -80ºC for overnight. Next day, 25 µl cell lysate was mixing with 25 µl luciferase assay substrate (Luciferase assay kit, Promega) and the luciferase gene expression signal measured with luminometry (Berthold Technology, UK). Another 25 µl of the cell lysate was used in BCA assay to measure protein concentration. The final results were obtained by luciferase reading normalized with protein concentration.

2.1.15 LC-MS analysis

The medium supernatant of the cultured cells were collected and stored in -80˚C until further analysis. Immediately prior to LC-MS analysis, the thawed supernatants were centrifuged at 4,000 rpm for 15min in a spin filter with 3000 Da cut off (Millipore, UK) to obtain the filtrates. 50ul of the filtrate was then analysed on LC-MS (column:

Agilent Zorbax RP C18, 150x4.6mm, 5µm). An Agilent 1200 HPLC coupled with a Bruker HCT-Ultra-ETD mass spectrometer was employed. The target compound was eluted with a gradient of water (A)-methanol (B) both with 0.1% NH_3 added, flow rate was set at 1ml/min and 20% of the flow diverted to the MS. (Gradient: 0-5 minutes, 100% A, 5-30minutes 100%A to 100% B, then isocratic for 5 minutes before equilibrate back to initial condition in 5 minutes). Mass spectrometer was operated in negative electrospray mode, settings are: nebulising gas 40 psi, dry gas 10 l/min, dry temperature 300˚C, MS scan range 50-1500m/z. Uric acid standard was analysed in parallel with all samples.

Chapter 3:

Characterization of the Virology Aspects of ColoAd1

3.1 Introduction

Based on the oncolytic virus life cycle, there are a number of basic selection criteria to decide whether an oncolytic virus is suitable as a cancer therapeutic agent.

- Firstly, the virus should have a wide tropism among various types of tumour cells, and also have an effective infection ability;
- secondly, the virus should have efficient replication to generate the maximum quantity of progeny; the replication must be selective and confined only to tumour cells, with limited replication and no toxicity in normal cells;
- thirdly, a shorter viral life cycle and complete oncolysis are the main contributors for virus potency and the ability to destroy the target cell;
- and finally, progeny virions should able to spread efficiently from cell to cell within the tumour microenvironment.

Additionally, there are also other important considerations which must be satisfied, including safety, genetic stability, suitability for genetic manipulation and GMP manufacture. In order to treat metastatic or inaccessible tumours, a virus that can be given systemically would be greatly beneficial, therefore there would need to be a high degree of blood compatibility.

Among the broad types of oncolytic viruses, adenovirus serotype 5 certainly has several features that meet the above selection criteria and has over time become the most intensively studied and used virus. However, the performance of Ad5 is far from satisfactory and is in urgent need of further improvement. The disadvantages of Ad5 have been identified as relatively narrow infection tropism, slow oncolysis and incomplete progeny virus release, limited tumour tissue spreading and poor blood compatibility. Some of the problems associated with Ad5 might be overcome by switching to an alternative serotype such as group B adenovirus, although

understanding of the oncolytic behaviour of those adenoviruses (such as Ad11) remains limited.

In this chapter, the oncolytic properties of ColoAd1 were assessed according to the above criteria, compared with its parent virus Ad11p and with Ad5. The objectives of the study included: viral uptake and infectivity, viral killing potency and kinetics, viral replication efficacy and tumour selectivity, viral cell to cell spreading ability as well as the neutralisation susceptibility by blood factors. The results revealed that ColoAd1 in general has superior potency over both Ad5 and Ad11, and is able to overcome the major shortcomings of Ad5. It is a promising candidate with significant potential as a novel oncolytic virus in future virotherapy studies.

3.2 Results

3.2.1 Titre of the stock viruses

The titres of stock adenoviruses were quantified by two different assays. Virus particle number/ml (VP/ml) was supplied by the manufacturer and was checked by DNA content measurement using the Picogreen assay. This assay also can be used to measure the proportion of free DNA present and thus indicates the percentage of the intact virions present in the whole virus sample. Infectious particle number/ml (PFU/ml) was determined by TCID50 assay on A549 cells. As shown in Table 3.1, the three adenoviruses Ad5, Ad11 and ColoAd1 have high levels of intact virions in their CsCl-purified stocks (about 95%). The ratios of viral particle number to infectious plaque forming units (VP/PFU) of the three stocks are very close. Therefore, in order to simplify the calculation, the particle number per cell (PPC) rather than infectious particle unit per cell (PFU) was used as the unit for calculating

virus multiplicity of infection (MOI) in all the following experiments, unless otherwise specified.

Table 3.1. Particle number and infectious titre of virus stocks

	Particle number/ml (VP/ml)	Intact virions percentage	Infectious particle number/ml (PFU/ml)	VP/PFU ratio
Ad5	2.50E12	95.5	7.07E10	35.3
Ad11	1.90E12	94.8	6.13E10	31.0
ColoAd1	1.65E12	95.0	4.77E10	34.6
Ad3	1.45E12	ND	ND	ND
ONYX-15	4.88E12	ND	ND	ND

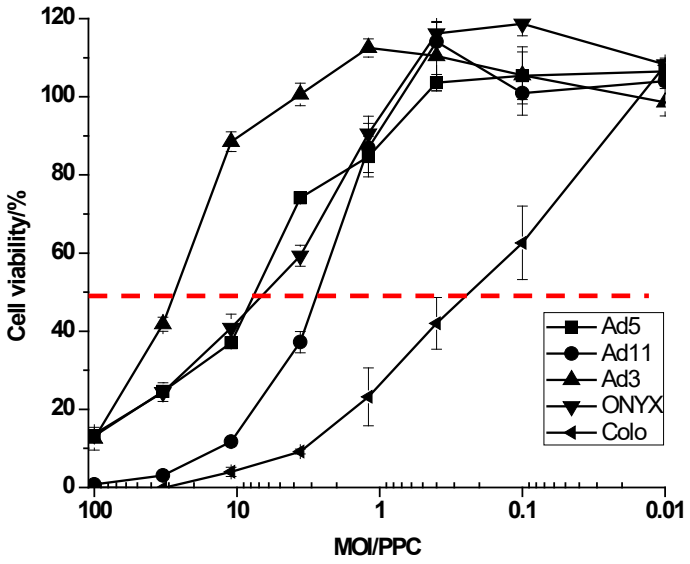


Fig 3.1. **Comparison of the cytotoxicities of five oncolytic adenovirus by MTS assay on HepG2 cells.** HepG2 cells were seeded at 10000 cell/well in 96 well plates 24 hours prior to infection. After washing the wells by PBS, a 1:3 serial dilution of the virus started from 100PPC of the different virus (200 µl in DMEM with 2% FCS and 1% P/S) were used to infect the cells. The infection medium was left on for the remaining incubation time. The cells were incubated for 5 days after infection. MTS assay was used to measure cell viability. The IC50 value can be obtained from the MOI that achieved 50% cell killing (therefore 50% cell viability) in the specific curve (red line). Mean data ± SD are presented, *n* =3.

3.2.2 The potency and kinetics of viral oncolysis

The superior potency of ColoAd1 to Ad5 on its cognate cell line HT29 was first described in Kuhn's paper published in 2008 (Kuhn, Harden et al. 2008). ColoAd1 was found to be over 2 logs more potent than Ad5; additionally, it also demonstrated potency equivalent to or greater than Ad5 on other human tumour cell lines (e.g.PC-3, MDA-231, Ovcar-3 and DU-145, but was attenuated on the Panc1 cell line). ColoAd1 displayed significantly increased potency (9-100 folds) relative to Ad5 on all colon cancer tumour cell lines screened, with the exception of Colo320DM. In this study, human hepatocellular carcinoma HepG2 and human lung adenocarcinoma epithelial cell line A549 were used as the target cells to compare the lytic potency of these oncolytic adenoviruses.

3.2.2.1 Comparison of the viral potencies by end point MTS assay

As demonstrated in Fig 3.1, the order of killing potency of the adenoviruses was: ColoAd1>>Ad11> ONYX ≈ Ad5 >Ad3. The IC50 values were 0.2, 2.2, 8, 6, 30 PPC respectively, which means the cell killing activity of ColoAd1 is approximately 10-fold higher than that of Ad11, 40-fold higher than that of Ad5 and 150-fold higher than that of Ad3. The oncolytic potency of ONYX, an Ad5-based type oncolytic virus, was similar with Ad5 on HepG2 cells. The results indicated that ColoAd1 not only showed superior cell killing ability compared to Ad5 and ONYX-015, it also showed greater activity than its parental group B viruses Ad11p and Ad3; as expected, the potency of ColoAd1 was closer to that of Ad11p rather to Ad3, which correlated to the higher sequence homology between ColoAd1 and Ad11p.

Similar results were also observed using A549 cells; supplementary material S1 showed MTS assay results from days 2 to 5. At the day 5 time point, the IC50 values

obtained using A549 cells were 0.5 PPC for ColoAd1, 5 PPC for Ad11 and 200 PPC for Ad5.

3.2.2.2 Comparison of the killing kinetics of the viruses by xCelligence

The automatic real time recording of the cell proliferation and events by the Roche xCelligence system has provided more precise and detailed information to assist in the understanding of the killing kinetics of these oncolytic viruses. As demonstrated in Fig 3.2, ColoAd1 displayed a very clear dose-dependent cell lysis effect, which was evident even at the low infectious viral dose of 0.8 PPC; a complete cell killing can be achieved at day 5 at this dose. With Ad11, PPC 20 was required to achieve a complete cytotoxicity at the same time course. At the higher infection doses ColoAd1 mediated cytotoxicity was slightly more pronounced than Ad11, however, they shared similar replication kinetics and most cell death occurs at day 3-4 post-infection. Importantly, this pattern appeared distinctly different from the case of Ad5. Cell killing achieved by Ad5 was more time-dependent rather than dose-dependent, as there was no major difference observed between the high dose (500 PPC) and the low doses (20 PPC). Most of the cell death occurred at day 6 regardless of the infectious dose; in addition, Ad5 required a much longer incubation period to achieve cell killing. When infected at the same dose (20 PPC), most of the cells treated by the three adenoviruses started to show cytotoxicity at 46-48 hours post-infection. From the first sign of cytotoxicity, ColoAd1 was able to achieve complete cell killing over the following 47 hours with a rapid decrease of cell index and steep slope on the proliferation curve; the equivalent time course of cell killing for Ad11 was 75 hours. In contrast, Ad5 required the longest time to achieve cell killing (103 hours).

3.2.2.3 Comparison of the killing kinetics of the viruses with chemotherapy drugs and H_2O_2

When the kinetics of virus-mediated oncolysis was compared with chemotherapeutic drugs such as Cisplatin, 5-fluorouracil (5FU) and Camptothecin, virus induced oncolysis (especially ColoAd1 and Ad11) was shown to be significantly more efficient. As demonstrated in Fig 3.3, A549 cells were not sensitive to the DNA crosslinking reagent Cisplatin and the pyridine analogue 5FU. The IC50s values were determined by a 5 day- MTS assay and were around 50 μM.

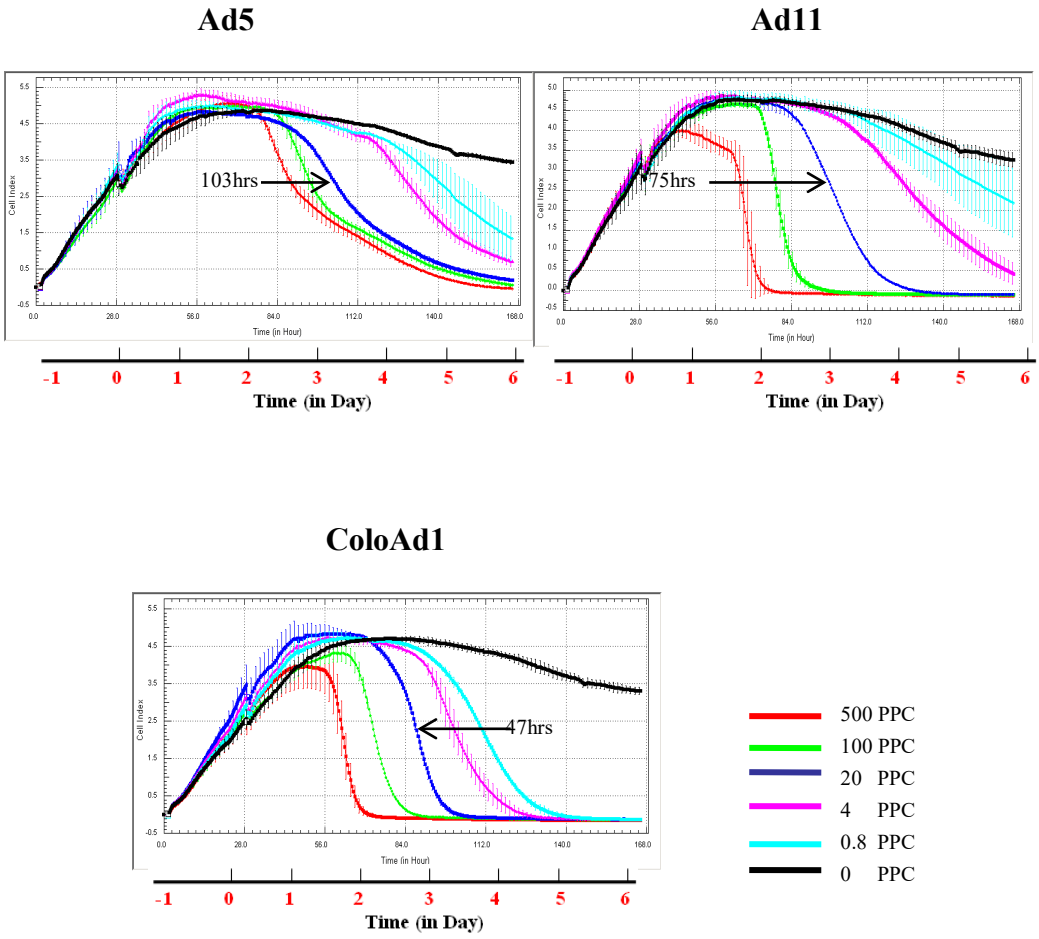


Fig 3.2. Proliferation curves of A549 cells infected with different doses of oncolytic adenoviruses, recorded by Roche xCelligence. The number labelled on the curves refers to the virus infection dose by the unit of PPC. Virus infection was carried out at 24 hours after cell seeding (time 0 hr or day -1), and cell index data was recorded until 168 hours (6 days post infection). Mean data ± SD are presented, *n* =3.

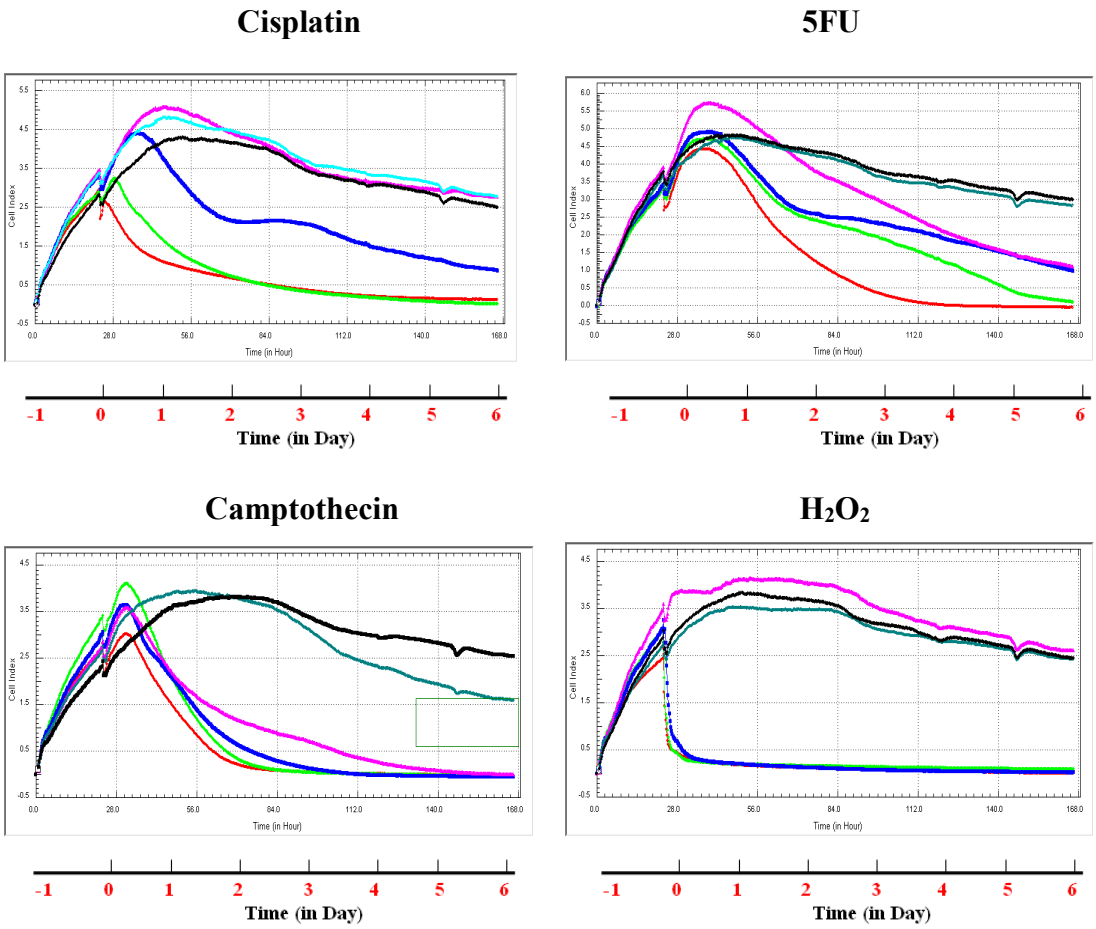


Fig 3.3 Proliferation curves (viability/time) of A549 cells treated with chemotherapeutic drugs or H_2O_2, recorded by xCelligence over a period of 7 days. Cells were seeded at 10,000/well, the respective reagents were added at the 24th hours. Drugs were applied at serial 5-fold dilutions starting from 500 µM (Cisplatin, 5FU), 50 µM (Camptothecin) and 5 mM (H_2O_2). The coloured lines refer to the serial concentrations of the reagent and are in the same order as Fig 3.2.

The cells began to respond shortly after the start of each drug treatment, as evidenced by the decreasing cell index in Fig 3.3; however, the decrease in cell index is a long process occurring over a period of 4-5 days even at the conditions of highest concentration of the drugs. At the lower concentration of 20 µM of Cisplatin treatment, some cells were found to show resistance and even recover proliferation, as indicated by the broad shoulder peaks which appeared around the 100th hour in

the Cisplatin plot. The topoisomerase inhibitor Camptothecin was the most effective of the drugs tested (cytotoxicity observed in the 2-50 μM range), but its cell killing ability was not as efficient as ColoAd1 and Ad11 (50 hours to achieve a completely killing at 50 μM concentration). On the other hand, H_2O_2-mediated killing (DNA oxidation-induced necrosis) is very toxic to A549 cells at all concentrations above 0.2mM, and complete cell death was achieved in 6-8 hours after treatment. When the H_2O_2 concentrations used were below 40 μM, there was no observable cell death.

3.2.3 Virus infectivity and cellular uptake

The uptake of the three Adenoviruses by A549 cells quantified by QPCR is shown in Fig 3.4. At an infection dose of 100 PPC, Ad11 had a high uptake efficiency which reached nearly 34% of the input virus at the 2 hour post-infection time point and then 80% of input dose at the 6 hour post-infection time point. In contrast, the uptake of

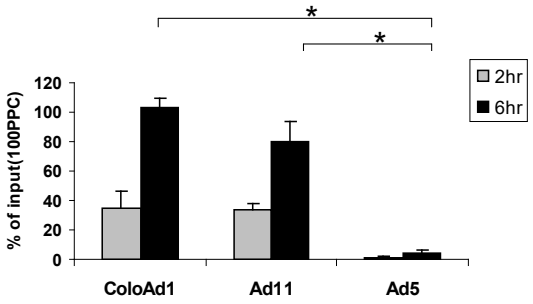


Fig 3.4. **The cellular uptakes of the three adenoviruses on A549 cells**. Cells were infected with ColoAd1, Ad11 or Ad5 at 100 PPC. At 2 or 6 hours post infection the infection medium was removed and cells were washed by PBS twice. The cells were lysed and DNA was extracted. Virus genome number was then detected and quantified by QPCR from the extracted DNA samples. The input virus number is used as 100%. Mean data ± SD are presented, *n* =3.Statistical differences between the two groups were determined using Student's t-test.*: P< 0.05.

Ad5 was very low. At 6 hours post infection, its uptake was only 5% of the input

virus. Interestingly, ColoAd1 shows the same high cellular uptake efficacy as Ad11, with similar or even slightly higher entry than Ad11 in A549 cells.

3.2.4 Virus selective replication and cytotoxicity

In order to compare virus activity in normal versus tumour cells *in vitro*, the HepG2 cell line was used with normal primary human hepatocytes as its counterpart, the A549 cell line and the normal lung-derived WI-38 fibroblasts cells as its counterpart, along with human umbilical vein endothelial cells HUVEC.

3.2.4.1 Comparison of the relative cytotoxicity of the viruses on normal cells versus tumour cells

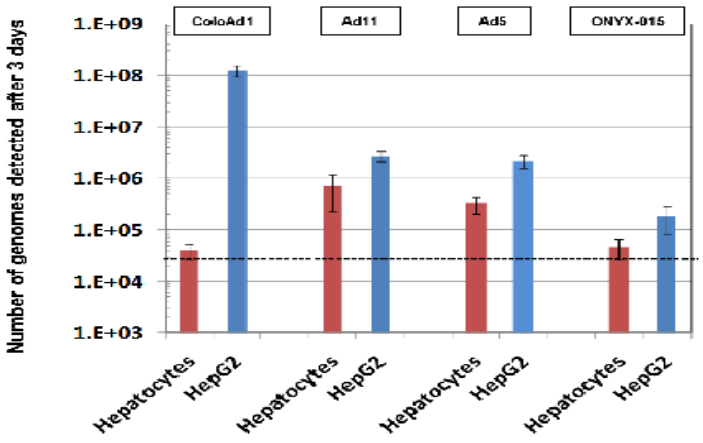
The viruses, especially ColoAd1, had very low IC50 values on tumour cell lines such as HepG2 and A549. In contrast, all viruses had high IC50 values in the normal cells, as shown in the supplementary materials S2 and table 3.2. The ratio of IC50 values in normal versus tumour cells was between 10 and 5000. This likely reflected the intrinsic selectivity of all the oncolytic viruses used in this study. The relative cytotoxicity varied depending on the specific normal cells., For example, on normal hepatocytes Ad11 showed the highest cytotoxicity, followed by Ad5 and then ColoAd1; on HUVEC the order of cytotoxicity is Ad11>ColoAd1>Ad5. ColoAd1 has a wider therapeutic window considering the relative ratio of IC50 of tumours to normal cells. The combined data suggested that ColoAd1 had the highest potency as well as selectivity in tumour cells compared to Ad5 and Ad11; this would give it a much improved therapeutic window.

Table 3.2 IC50 summary and analysis for virus on normal cells and tumour cells

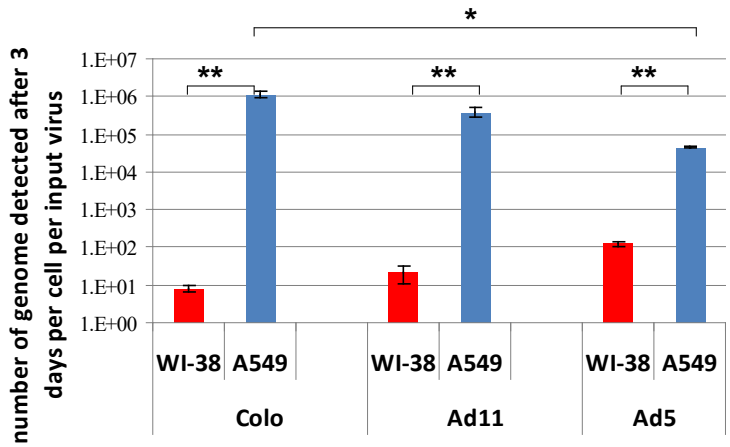
	HepG2	Hepatocyte	**Hepatocyte / HepG2**	A549	WI-38	**WI-38/A549**	HUVEC
Ad5	8	105	**13**	200	>5000	**25**	200
Ad11	2.2	10.9	**5**	5	>5000	**1000**	10.9
ColoAd1	0.2	1000	**5000**	0.5	300	**600**	65

4.2.4.2 Comparison of the replication of the viruses in normal cells versus tumour cells

Based on the cytotoxicity study, virus replication in these cells was investigated. Fig 3.5A showed that ColoAd1 had the highest virus production in the tumour cells and was over 2 logs higher than the other adenoviruses. On the other hand, it had the lowest virus production in the normal cells - it was 1.5 logs lower than Ad5 and Ad11. Its replication in human hepatocytes was even lower than ONYX-015, which is Ad5 based and been genetically modified to improve the tumour selectivity by removing E1B 55K. Data in Fig 3.5B also demonstrated that ColoAd1 showed very little replication in normal lung WI-38 cells but had remarkable amplification in the tumour cells, with a difference of about 5 logs. In contrast, the selectivity of Ad5 was relatively poor. Interestingly, ColoAd1's selectivity was once again proven to be enhanced compared with its parental virus Ad11. ColoAd1 reached similar or even higher virus production in A549 cells compared with Ad11 even at an infectious dose as low as 10 PPC. The results were similar when based on the same virus input dose (PPC 20, see supplementary material **S3**). This suggested that ColoAd1 is not only more selective but also replicates much more efficiently in tumour cells compared with the other adenoviruses.



A. **Heptatocytes vs HepG2**



B Fibroblast vs A549

Fig 3.5 Comparing replication of ColoAd1, Ad11, Ad5 and Onyx-015 in tumour versus normal cells. WI-38 and A549 cells were seeded at 10000 cells per well in 96 well plates. Hepatocytes were seeded at 50000/well 24 hours prior to virus infection. 20 PPC of each virus was used to infect hepatocytes and HepG2. ColoAd1 PPC 10, Ad11 PPC 25 and Ad5 PPC 100 were used at to infect the fibroblast and A549 to achieve a similar degree of virus-mediated cell killing at three days post infection. Data obtained using 20 PPC of each virus is shown in the supplementary materials (S3). Three days after infection the medium was removed and the viability of remaining living cells was measured by the MTS assay. After the assay, cells were lysed. The cell lysate and medium were pooled for DNA extraction then QPCR to measure the number of virus genome copies in each sample. The data was normalized as the virus yield per cell and per input virus. Mean data ± SD are presented, *n* =3. Statistical differences between the two groups were determined using Student's t-test.*:$p<0.05$, and **: $p<0.01$.

3.2.4.3 ColoAd1 mediated bystander killing of adjacent infected cells

In the fibroblast/A549 overlay co-culture model, the cytotoxicity of ColoAd1 was compared with cisplatin, using either A549 tumour cells alone, WI-38 fibroblasts alone or a co-culture system.. As previously discussed, A549 cells appear to exhibit a certain resistance to Cisplatin-induced killing. Fig 3.6 shows that when Cisplatin was used at 20 μM, the fibroblasts were very sensitive to the cytotoxic effects of the drug while the A549 cells were not as susceptible.

On the basis of IC50 values already determined, treatment with Ad5 and ColoAd1 would be expected to induce tumour-selective cell killing while sparing normal cells. This selectivity of ColoAd1 was apparent in the experiments where it was incubated with tumour cells alone. However ColoA1 mediated almost complete cell killing of both tumour cells and fibroblasts in the co-culture system when used at the dose of 20 PPC, despite having minimal cytotoxicity on the fibroblasts monolayer when used at this dose in the absence of tumour cells. A much weaker cytotoxicity is achieved with Ad5. ColoAd1 tumour cell oncolysis appears to produce a bystander killing on the adjacent fibroblast, and this observation may be related to an unusual mechanism of ColoAd1 oncolysis. In other words the oncolysates produced as a consequence of ColoAd1 tumour killing may induce apoptosis in fibroblasts adjacent to the tumour cells. Considering that the tumour associated fibroblasts can constitute a large proportion of the tumour mass, it is hypothesised that ColoAd1 may therefore be less restricted in its penetration and could spread more efficiently through the tumour matrix *in vivo* than Ad5.

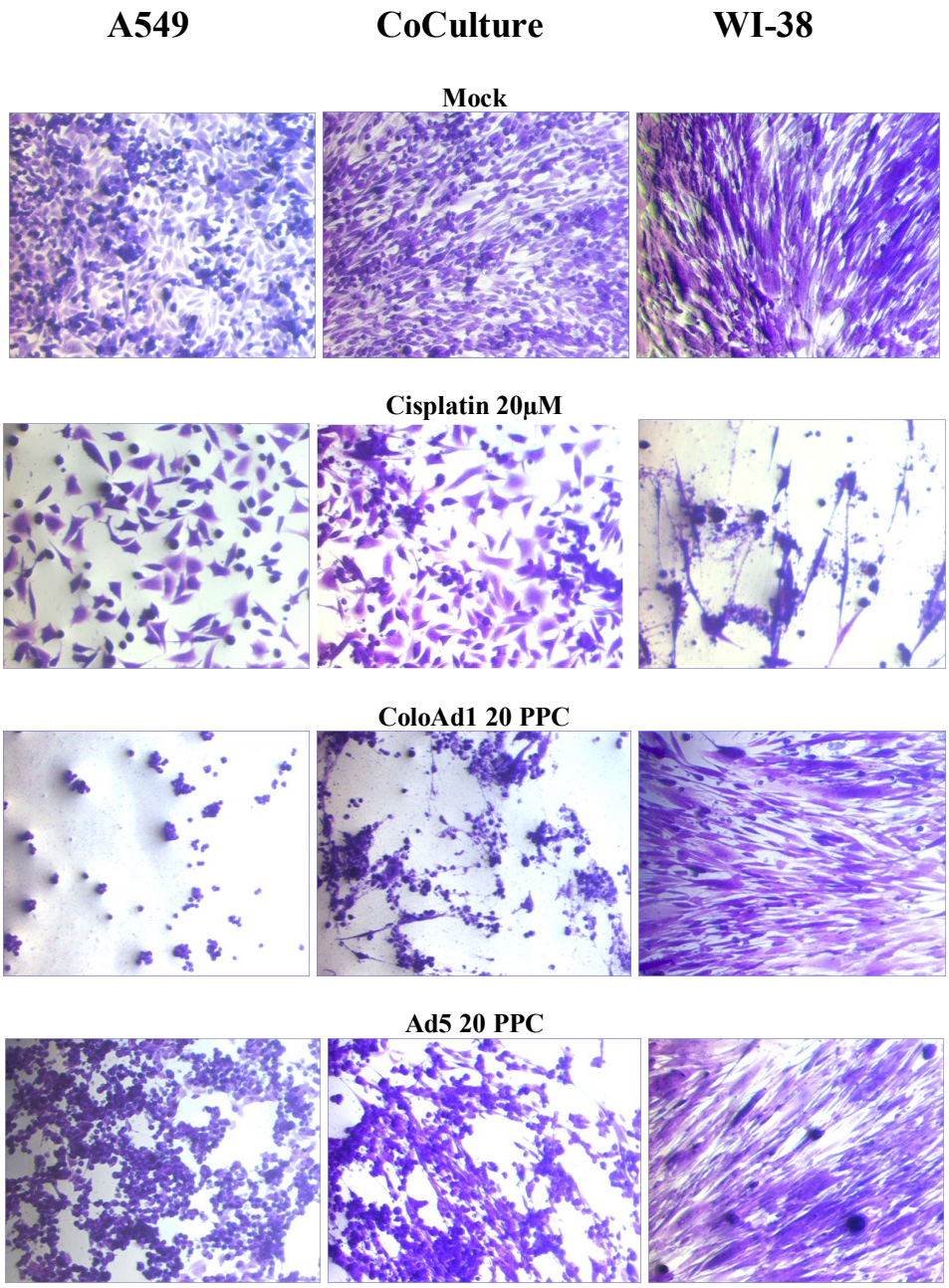


Fig 3.6 The viruses and Cisplatin killing on Fibroblast WI38/A549 overlayer. WI-38 was seeded 10000 cell/well 48 hours before, then the same density of A549 was seeded on the top of WI-38 monolayer 24 hours before. Virus 20 PPC (calculation based on A549 cell number) in 200 µl DMEM (2% FCS with 1% P/S) was used for infection. For Cisplatin treated wells, Cisplatin 20 µM in 200ul medium was added in. The assay was terminated at day 5. The wells were washed by PBS, fixed by formaldehyde and finally stained by crystal violet before imaging. The pictures were taken with a Zeiss Axiovert 25 microscope (with 10X magnification lens) coupled with a Nikon DS –U2 camera.

3.2.5 Susceptibility to neutralization by blood factors

Ad5-based oncolytic viruses are highly susceptible to blood factors as neutralising anti-Ad5 antibodies are present in a high percentage of human populations (50-90%) due to previous exposure to this serotype in the environment. In contrast, the group B adenovirus serum prevalence is much lower (18-31%). Therefore, it is expected that ColoAd1 could inherit the good serum-compatibility properties associated with Ad11. The serum and erythrocytes (red blood cells, RBC) sample from a high Ad5 neutralising donor have been used in the present study to assess the neutralising resistance of the three viruses.

3.2.5.1 Resistance of the adenoviruses to serum neutralisation

As shown in Fig 3.7, the neutralizing serum has a significant impact on Ad5, causing a 2000-fold increase of its IC50 value on HepG2 cells. The virus has therefore probably lost most of its infectivity. The IC50 value of Ad11 also increased, with a 750-fold reduction of its infectivity; In contrast, the IC50 of ColoAd1 only increased slightly and its infectivity was reduced by only 12-fold. Interestingly the effect of neutralizing antibodies on Ad11 was greater than on ColoAdl1 despite having the same coat proteins. These results probably reflect the fact that the ColoAd1 replicates at a faster rate and kills cells more quickly with fewer particles.

3.2.5.2 Resistance of the adenoviruses to erythrocytes binding

As shown in Fig 3.8, erythrocyte-binding also leads to the reduction of adenovirus infectivity and therefore the reduction of cytotoxicity. However, as seen by the right shift of the proliferation curves, the erythrocyte-binding which causes the IC50 value to increase varies remarkably according to the different adenoviruses. Among them, Ad5 showed a 1000-fold increase in IC50 value; by contrast, both group B

adenoviruses had minor increases in their IC50 value; Ad11 gave a 20-fold increase while ColoAd1 only gives a 5-fold increase.

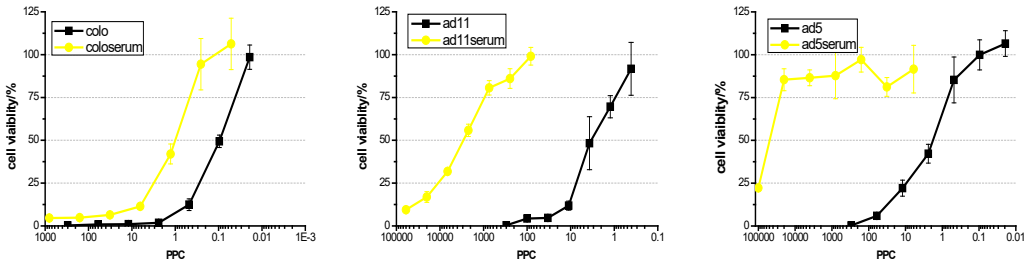


Fig 3.7 5 days MTS assay of HepG2 cells infected with adenovirus with or without the presence of neutralizing serum in the infection medium. HepG2 cells were seeded at 10000/ well 24 hours prior to infection. Virus infection was carried out in 50 µl infection medium with or without 1:25 (V/V) human serum and infected for 2 hours. After 2 hours the medium was replaced with 150 µl fresh DMEM with 2% FCS and 1%P/S. Cell viability was assayed by MTS assay on day 5. Mean data ± SD are presented, *n* =3.

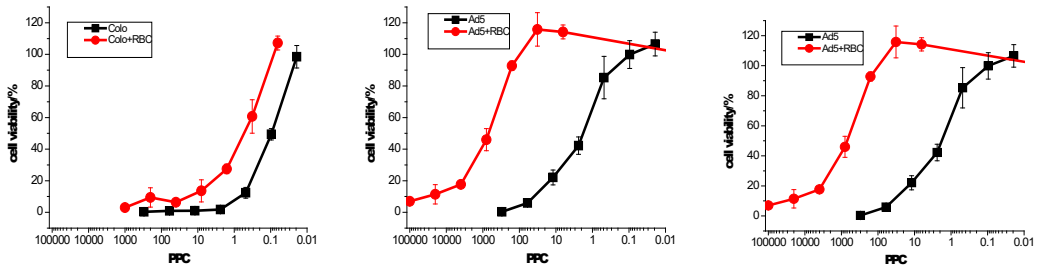


Fig 3.8 5 days MTS assay of HepG2 cells infected with adenovirus with or without the presence of human erythrocytes in the infection medium. HepG2 cells were seeded at 10000/ well 24 hours prior to infection. Virus infection was carried out in 50 µl infection medium with or without 1:25 (V/V) human erythrocytes and infected for 2 hours. After 2 hours the medium containing RBC was removed and the HepG2 cells monolayer was washed by PBS three times. Then 200 µl fresh DMEM with 2% FCS and 1% P/S was added. Cell viability was assayed by MTS assay on day 5. Mean data ± SD are presented, *n* =3.

ColoAd1 displayed the highest resistance to erythrocyte-binding amongst the three viruses tested, and was more resistant than its parental virus Ad11 despite having the

same capsid. Again, these results probably reflected the fact that the ColoAd1 replicates at a faster rate and kills cells more quickly with fewer particles.

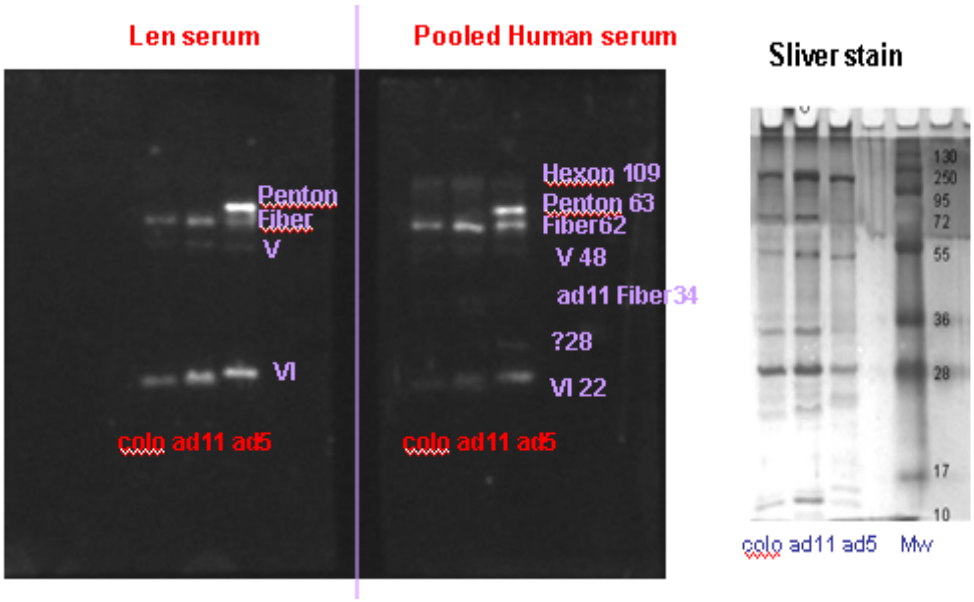


Fig 3.9 Neutralizing serum IgG binding patterns for capsid proteins from three adenoviruses, Ad5, Ad11 and ColoAd1. A. Western blotting for the capsid proteins (which are assigned in the image) exposed to two sources of neutralizing serum. $10E^{10}$ virus particles were denatured and loaded onto a 10% SDS-PAGE gel. B. Silver stain of the ad proteins. $5E^{10}$ virus particles were loaded to SDS-PAGE, and the gel was stained by silver staining kit according to the manufacturer's recommended protocol.

3.2.5.3 Binding patterns of IgGs in neutralizing serum with the virus proteins

Western blotting for whole virus proteins with neutralizing serum revealed the antibody binding epitopes of the virion proteins. Fibre and protein IX are two major capsid proteins which have low sequence homology between Ad5 and Ad11. It should be noted that the fibre of Ad11 and Ad5 differ substantially in size as there are 325 and 585 amino acid residues, respectively, with molecular weight roughly around 34 kD and 62 kD respectively (Mei, Skog et al. 2003). As demonstrated in Fig 3.9, the IgGs in the human serum had a strong affinity to Ad5 fibre, penton base III, capsid cement protein IIIa and capsid cement protein VI. The IgGs had much

weaker binding affinity to group B adenovirus capsid proteins, mostly binding to the protein bands at IIIa area but not the penton. IgG binding to ColoAd1 was weaker than Ad11, mainly with protein VI There was an indication of weak binding around 34 kD (the fibre band for Ad11 and ColoAd1) on the pooled human blot for Ad11 proteins, although the fibre protein bands at the silver stain were strong. This may explain why group B adenoviruses are less susceptible to neutralisation compared with Ad5. However, it should be noted that the specific binding patterns were found to vary greatly with different serum samples. For instance, the pooled human serum showed more binding to adenovirus hexon than serum from one particular individual, which has more binding to protein VI areas than pooled human serum.

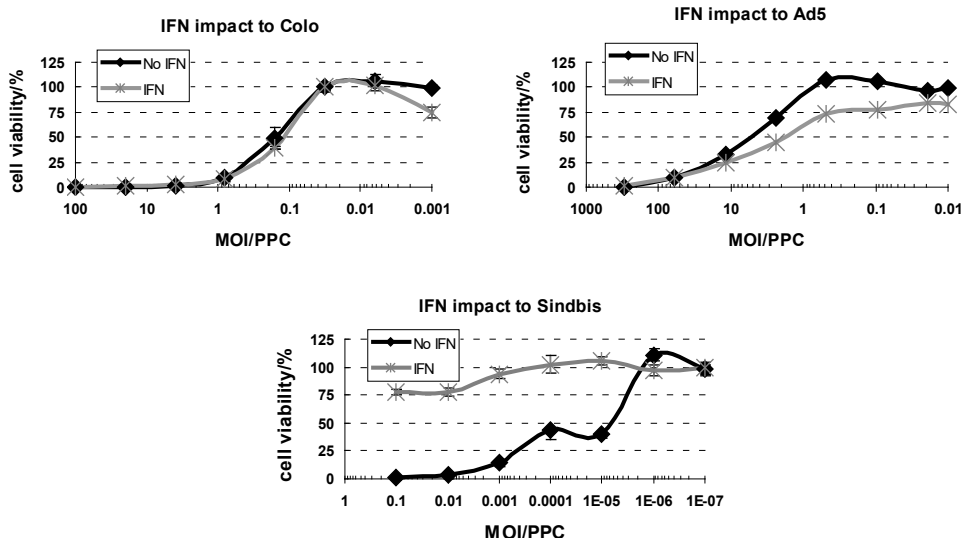


Fig3.10 Effect of IFNα on the virus cytotoxicities. A549 cells were infected with the virus, with and without incubation of IFNα, and after 5days the cell viability was assessed using the MTS end point assay. IFNα concentration was used at 1μg/ml, and the virus was used at the starting concentration of 500 PPC, and then with 1:10 serial dilution. Mean data ± SD are presented, *n* =3.

3.2.5.4 Resistance of the adenoviruses to Interferon α neutralization

As shown in Fig 3.10, IFNα had no neutralizing effect on adenovirus, and can itself have some cytotoxicity to the tumour cells; on the other hand it greatly affected Sindbis, an RNA virus, which was neutralized completely under the experimental conditions.

3.2.6 Comparison of virus spreading through tumour cell monolayers

The ability of these viruses to spread through an A549 monolayer culture was investigated by non-restricted spreading assay and agar overlay restricted spreading assay.



Fig 3.11 Non restricted spreading assay. The A549 cells monolayer after infection by 5 fold series dilution from the stock virus was maintained in 2%FCS DMEM medium for 7 days incubation. At the end point of day 7, the medium was removed and plate was fixed and stained to visualize the remaining area in the wells.

From non-restricted virus spreading assays demonstrated in Fig 3.11, the results provided clear evidence that ColoAd1 spreads better laterally than both Ad11 and Ad5. As seen from Fig3.11, in the control samples and samples receiving very low doses of virus (row 7 and 8) when there was only one plaque forming unit in the well,

ColoAd1 showed much more efficient lateral spread than Ad5 and Ad11, while Ad5 showed the poorest spread; in samples containing low doses of virus (such as row1-5), almost complete cell killing was achieved in ColoAd1 but not seen in the case of Ad11 and Ad5. However, the supplementary material S5 showed that from the plaque forming assay of the three viruses, ColoAd1 produced a larger plaque size than Ad11, whilst the latter is smaller than Ad5.

3.3 Discussion

The data reported here indicate that the group B adenoviruses Ad11 and ColoAd1 both have superior oncolytic capability compared with the widely used Ad5. Ad11 and ColoAd1 have demonstrated higher transduction efficacy, more specific and efficient replication in tumour cells, better resistance to various pre-existing neutralizing factors as well as more potent cell killing or oncolysis. Altogether, these factors contribute to an improved ability of these viruses to spread from infected to adjacent uninfected cells. It is therefore of particular interest to investigate the factors contributing to the increased potency of the group B viruses compared with other members of the adenovirus family. It is also worth noting that other group B adenoviruses such as Ad3 have been shown to be less potent than Ad5, despite sharing similar genomic arrangements with Ad11 and ColoAd1.

Undoubtedly, a major factor contributing to the higher potency of ColoAd1 is its use of CD46 as a cell entry receptor as opposed to using CAR as the primary attachment/entry receptor. CD46 is often up-regulated in cancer cells, possibly because increased CD46 expression aids tumour evasion and destruction by the complement system (Hall, Blair Zajdel et al. 2010). On the contrary, CAR has been

shown to be down-regulated during tumour progression. Loss of CAR appears to correlate with increasing aggressiveness of tumours, with the most aggressive tumours displaying the lowest levels of CAR. As CAR functions in cell adhesion, it was suggested that loss of CAR may reduce contact between cells, therefore increasing cellular proliferation and promoting migration. Indeed, as cancer cell lines age, their cell surface receptor profile may change and this can impact on the ability of the virus to infect the cells. Older cells were found to have greater sensitivity to Ad11 and ColoAd1 but less sensitivity to Ad5. Moreover, it was recently found that Ad11, Ad3 and Ad7 are capable of utilizing both CD46 and Desmoglein 2 for attachment (Wang, Li, et al 2011). The use of different receptors could offer more opportunities for virus entry, which could explain the higher transduction capacity of Ad11 and its wider tropism. ColoAd1 has inherited the same entry receptors as Ad11. The high binding and uptake of the two group B viruses were observed in these studies, displaying a 20-fold higher infectivity than Ad5 on A549 cells. These observations are in agreement with previously published results (Zhang, Mei et al. 2003).

Regarding tumour selectivity, the data demonstrated that all viruses tested, including wild type Ad5, showed tumour-selective replication and oncolysis. According to previously published studies, Ad5 is considered to have intrinsic selectivity in killing tumour cells rather than normal cells (Yamamoto and Curiel 2010), which could be attributed to more efficient virus replication in tumour cells which usually have increased metabolic activity as well as mutations in the tumour suppressor genes p53 and/or Rb. It has been reported that Ads do not achieve nuclear localization during infection of primary normal cells, such as fibroblasts and endothelial cells, yet

staining of the nuclear periphery has been observed following adenovirus infection of transformed cell lines (Leopold and Crystal 2007). Some strategies are used to further restrict Ad5 based oncolytic virus's selectivity, such as mutations or removal of the viral E1A or E1B oncogene.

The data demonstrated that group B viruses have shown a more enhanced selectivity than Ad5 without compromising their replication and oncolytic ability in A549 tumour cells. Within the group B viruses, ColoAd1 exhibits greater potency and selectivity than its parental virus Ad11. Some strategies to improve Ad5 selectivity for tumour cells most commonly make the virus less cytopathic (efficacy reduced). For example, ONYX-015 has an overall attenuation of the virus by deletion of the E1B 55kD gene and thus reduces the efficiency of the nuclear export of viral RNAs. The mechanisms which lead to improved potency of Ad11 and ColoAd1 are yet to be explained, but it is likely to be at least in part due to the use of the ubiquitously expressed CD46 as the attachment/entry receptor. Furthermore, mutations in the E2B gene in ColoAd1 could account for its increased potency compared with Ad11, as this may lead to modified pTP-CAD interactions (Kuhn, Harden et al. 2008). It is worth noting that Ad11 is able to transduce primary cells including smooth muscle cell, synoviocytes, dendritic cells and cardiovascular tissue with higher efficiency than Ad5 (Holterman, Vogels et al. 2004), and also displays markedly higher binding for endothelial cells (Zhang, Mei et al. 2003). However, the high binding, infection and transduction or even gene expression does not necessarily mean high replication and high virus-induced cytotoxicity. For example, in a study comparing infection and killing of multiple myeloma by Ads, the results revealed that Ad11 and Ad35 attached to multiple myeloma cells 10-100 times better than adenoviruses from other

serotypes. However, following the efficient virus binding to the cell surface, viral DNA did not undergo successful replication and cell killing was not achieved. (Senac, Doronin et al. 2010).

The seroprevalence of Ad11 is significantly lower (18-31% range) than that of Ad5 (50-90% range), and neutralizing antibody titre against Ad11 is typically 3-10 fold lower than that against Ad5. Therefore it is not surprising that Ad11 and ColoAd1 both have shown high resistance to neutralizing serum. Western blot analyses on serum IgG binding to capsid proteins from Ad5, Ad11 and ColoAd1 have revealed that the epitope binding properties are also important in influencing neutralization by serum. Fig 3.9 demonstrates that different serum samples show varying binding properties, while in general the intensity of the binding signal decreased in the order of Ad5>Ad11>ColoAd1, which reflects the order of neutralizing antibody titre to the three Ads.

With regard to the aspect of inert immune factors, the investigation undertaken so far was only confined to human erythrocytes and interferon binding in vitro. ColoAd1 has proved that it is able to overcome these neutralizations. The human erythrocytes binding and inactivation of Ad5 was reported by our group in 2009 (Carlisle, Di et al. 2009) as occurring through the interaction of CAR and the complement receptor CR1 with Ad5 capsid. This finding provides an Ad5 sequestration mechanism that can protect against system infection, which is one of the major barriers to system delivery. Due to the differences between the capsid proteins of group B adenoviruses and Ad5, particularly the fibre region, the binding of Ad11 and ColoAd1 to erythrocytes could be much weaker than that of Ad5. This could be the reason why the higher resistance to inactivation happens to Ad11 and ColoAd1. Many group B Ads

have shown a lower affinity for the blood coagulation factor FX compared with Ad5 (Greig, Buckley et al. 2009). It is to be expected that ColoAd1 has similar behaviours to Ad11, while the high affinity of Ad5 hexon for coagulation factor may lead to liver sequestration following delivery to the blood stream, again reducing the virus' ability to target cells. Furthermore, ColoAd1 shows similar neutralization resistance to IFNα as Ad5, which is the main advantage of adenovirus against RNA virus (such as Sindbis which loses infectivity completely in the environment with IFNα). Therefore, taken together, ColoAd1 has shown the best blood compatibility among the three Ads and it more likely to be amenable to intravenous administration.

Virus release and spread from cell to cell are critical for effective cancer therapy, as only a minority of tumour cells can be infected initially, even with direct intra-tumoral injection. The virus spreading ability in the monolayer tumour cells model is normally closely related to the virus killing potency or lysis ability. ColoAd1 and Ad11 were naturally expected to have a greater spreading potential than Ad5, since they are able to kill more efficiently and rapidly; in particular ColoAd1 induces oncolysis even at a very low MOI. It needs to be pointed out that the viral spreading undoubtedly also requires efficient replication and propagation of a viable virus. ColoAd1's higher replication rate than Ad11 and Ad5 in A549 cells has been evident in the experiment (see Fig 3.5). However, by agar plaque forming assay, ColoAd1 did not perform better than Ad5, while by the non strict cell spreading assay it did display more potential. This could be explained by the fact that the three dimensional burst and disperse of virions maybe an important feature unique to ColoAd1's oncolysis.

In this experiment it was observed that Ad11 induces much smaller plaque morphology than Ad5, although it mediates much more potent killing than Ad5. This is in agreement with the previous reports which state that the plaque sizes of group B adenoviruses are smaller than those of group C adenoviruses (Green, Pina, et al 1967). The agarose overlay prevents the release of virus particles into the culture medium, thereby restricting the spread of progeny virions to cells immediately adjacent to the originally infected cell. Without the agarose overlay, the virus is not prevented from spreading laterally to adjacent cells.

It must be borne in mind that the tumour cell monolayer model is far too simple accurately to mimic a real tumour in vivo, the latter being a more complex system comprising a number of key factors apart from tumour cells that influence virus replication, killing and spread. These include hypoxia, high interstitial fluid pressure, stroma cells and extracellular matrix, immune components etc. In addition tumours are three dimensional structures whereas cell monolayers are essentially in two dimensions. Three dimensional models which are able to display relevant cell-cell and cell-matrix contacts and inform about spreading of oncolytic virus through tumour mass in particular are currently very limited. Using the tumour cell/fibroblast co-culture model in the experiment design has led to speculation about the enhanced spreading potency of ColoAd1 in a real tumour environment. In contrast to Cisplatin, the virus's killing involves multimodal anti-tumour actions; it not only kills tumour cells efficiently, but also spontaneously kills the co-cultured fibroblast despite the virus having very limited replication in those fibroblasts. The death of the fibroblast is as a result of apoptosis activated by virus lysis tumour cells. It can be hypothesized that the cytokines and IFNs secreted by the stimulated fibroblast would induce further cell death (particularly apoptosis) in the environment. The responses occur in

the vicinity of the transduced tumour cells, rather than at a specific cell, non-transduced cells are also susceptible. Thus the enhanced killing has been effectively controlled within the tumour. It has been found that ColoAd1 has displayed a stronger cytotoxicity than Ad5, and the cell lysate produced by ColoAd1 probably has a greater ability to modulate the immune response and stimulate cytotoxicity of the tumour. In fact, construction replication-deficient Ad5 based Ads with gene encoding secreted factors such as GM-CSF (granulocyte macrophage colony-stimulating factor) and IL-12 (interleukin-12) (Chang, Chen et al. 2007), or with soluble TRAIL (tumour-necrosis-factor-related apoptosis-inducing ligand) (Bremer, van Dam et al. 2008) have already been reported, and were found to have improved cytotoxicity. This additional killing and spreading characteristic of ColoAd1 will be a a great advantage for the clinical application potential, considering the inoculated virus is always so small and as it is impossible to successfully transduce each cell within a tumour.

3.4 Conclusion

In the current study the potential of ColoAd1 was investigated as an oncolytic virus in studies comparing ColoAd1 with Ad11 and Ad5. The data has revealed that ColoAd1 has largely inherited the features of Ad11, with high cellular uptake (infectivity), strong resistance to neutralizing factors as well as higher selectivity for tumour cells, all of which are advantages over the widely used oncolytic virus Ad5. Moreover, ColoAd1 also showed greater replication efficiency, oncolytic potency and improved ability to spread through cell cultures. Cell killing mediated by ColoAd1 was shown to be most potent of the three oncolytic agents studied. Furthermore, it was shown to be more effective than conventionally used

chemotherapeutic drugs Cisplatin, 5Fu and Camptothecin on A549 cells, as demonstrated by its superior cell killing ability and kinetics. The virus also is able to produce a bystander killing effect in the fibroblasts/tumour coculture system, although it does not show strong cytotoxicity and replication in the fibroblasts alone.

The next question to be addressed is what factors can account for the high potency of this virus. Possible explanations could be higher cellular uptake, faster viral replication and/or different mechanism of virus-induced cell killing. Some of the experimental results achieved indicate that ColoAd1 induced cell death occurs via a different mechanism compared with drug-induced apoptosis; it also differs from Ad5-mediated cell death, and may be more similar to H_2O_2 induced necrosis, however so far there is insufficient data to explain the mechanism of ColoAd1-mediated killing. As the mechanisms of cell death induced by Ad5 and group B viruses such as Ad11 have not yet been explained, characterising the pathways responsible for virus-mediated cytotoxicity remains an important research area. Understanding the mechanisms of oncolysis may provide valuable information to assist future designs of oncolytic platforms, agents to synergise with virotherapy as well as aiding progress towards rational design of combination therapies. For instance, activating multiple death pathways (apoptosis, autophagy and necrosis) is an effective way to bypass cancer drug resistance (Hu and Xuan 2008). Induction of necrosis or programmed necrosis (named "necroptosis") has also been shown to circumvent the drug resistance. Cancer cells resistant to apoptotic inducers such as anthracycline antibiotics were found sensitive to necroptotic inducers. In the meantime, certain cell death mechanisms have been shown to be responsible virus-induced immunotherapeutic effects. Necrotic cell death produces highly

immunogenic signals and provokes an inflammatory response; anti tumour activity could be improved by local immune activation in the tumour. On the contrary, apoptotic cell death tends to be anti-inflammatory.

Therefore, the next part of this project will focus on identifying the mechanisms of ColoAd1-mediated oncolysis. The study will be carried by comparing ColoAd1 with Ad5 and Ad11. It is hypothesized that ColoAd1-induced cell killing involves necrosis and this could be an effective way to overcome drug resistance as well stimulating tumour immune suppression.

Chapter 4:

Investigation of the Cellular Responses during ColoAd1 Oncolysis

4.1 Introduction

4.1.1 Aim of this chapter

According to the previous data in Chapter 3, two group B adenoviruses particularly ColoAd1 demonstrated a significantly enhanced cytotoxicity for inhibition of tumour cell proliferation and selective killing compared to Ad5. In order to understand the mechanism of ColoAd1 mediated cell killing, it is essential to monitor the cellular responses with the progress of viral infection and replication, especially at the late stage of the viral life cycle: oncolysis.

Conventionally, cell death is loosely classified into three different types: Apoptosis, necrosis and autophagic cell death. These modes of cell death are characterised by different cellular pathways and different points of regulation. The cytotoxicity of oncolytic viruses was initially assumed as just simply by "lysis" the cell at the end of infection and replication, not necessarily reflecting any conventional death mechanisms, however recently some types of oncolytic viruses have been shown to kill cells with all the hallmarks of apoptosis. Autophagic activity has also been associated with the oncolytic cell death exerted by adenovirus serotype 5, facilitating release of progeny virions. To date, there is no clear consensus on the death mechanism(s) associated with general adenovirus oncolysis, especially the group B adenoviruses such as Ad11 and ColoAd1 which are presented in this thesis.

Due to the significance of the three different types of cell death in cell biology, features associated with each mechanism are now well established. In this chapter, some well knew methodologies have been used to investigate the mechanism of ColoAd1 induced oncolysis. In most studies ColoAd1 oncolysis has been compared with the oncolysis induced by Ad5 and Ad11, as well as the killing by Cisplatin (used as a positive control for apoptosis) and H_2O_2 (positive control for necrosis).

Cellular targets monitored in our study include: morphology, plasma membrane alteration and leakage, regulation of key proteins, maintenance of intracellular ATP and Ca^{2+} levels as well as cell cycle disturbance and cellular DNA damage. These features are all significantly affected by viral replication and oncolysis. Detailed observation of these targets may well provide further insights to help elucidate the killing mechanism of ColoAd1.

4.1.2 Investigation of characteristic features of different cell death mechanisms

Changes in morphology can provide a lot of information about death mechanisms. Apoptotic cells are characterised by cytoplasmic shrinkage, plasma membrane blebbing, chromatin condensation and fragmentation, formation and shedding of apoptotic bodies that contain nuclear or cytoplasmic material. In contrast, necrosis is defined by cytoplasmic swelling, dilation of organelles and gross swelling/rupture of the plasma membrane but with conserved chromatin. Autophagy is distinguished by a massive accumulation of double membraned autophagosomes that subsequently fuse with lysosomes. These morphological features are conventionally observed either by light microscopy, transmission scanning electron microscopy (TEM), or by fluorescence microscopy using immunostaining methods. DAPI nuclear staining is the most used technique to visualize nuclear morphology changes. The recent development of live cell imaging technology using time lapse microscopy provides a powerful tool for studying cell death, because all the dying events are dynamic processes and highly time dependent. The ability to study individual cells in a population provides much more information than measurements using cell lysates, as cell death is unlikely to be accurately synchronised between different cells.

Early leakage of the cytoplasmic membrane is the second critical hallmark to distinguish necrotic death from apoptosis, in which the membrane is kept intact at early stages. The leakage can be identified by membrane-impermeable DNA-intercalating fluorescent dyes such as propidium iodide (PI) or 7-Aminoactinomycin D (7-ADD), since theses dyes only have chance to enter into the cells and intercalate binding to DNA to induce fluorescence signals when the cell membrane is permeable (Darzynkiewicz, Bruno et al. 1992).

In apoptosis, a second characteristic feature related to the cell membrane is translocation of the phospholipid phosphatidylserine (PS), a class of acidic phospholipids. In cellular plasma membranes, PS is normally located on the internal leaflet of the lipid bilayer. During apoptosis, activation of ICE family proteases (such as caspases) leads to PS externalisation (Naito, Nagashima et al. 1997). The process can be detected using Annexin-V (a PS-binding protein) conjugated with a fluorophore.

Double staining the cells with PI and Annexin-V is a widely used basic experimental method to distinguish apoptosis, necrosis and viable cells, using either fluorescence microscopy or flow cytometry analysis. In principle, viable or healthy cells have negative staining signal with both dyes (Annexin V-/PI-). Apoptotic cells display a positive signal for Annexin V binding but negative signal to PI staining (Annexin V+/PI-). In contrast, necrotic cells display a positive signal for PI staining and variable Annexin V staining. However, it is important to note that this assay itself has limitations. Firstly, in the case of necrosis, although PS is not externalized, Annexin V may access the inner membrane of the cell from the ruptured cytoplasmic membrane and bind to PS, giving double positive signal; secondly, at the late stage

of apoptosis where without the presence of macrophage, the cells undergo the secondary necrosis, still resulting in a necrosis staining pattern(Annexin V+/PI+).

The third cellular feature used to discriminate death mechanisms relates to the expression levels of key cellular proteins. Immunoblotting methodology can be used to monitor oncolytic progression at different times. Candidate proteins include p53, PARP (including full length PARP, cleaved PARP and PARP product PAR), caspase3 and LC3.

P53 activates in response to a variety of stresses such as DNA damage, oxidative stress, oxidative stress, osmotic shock and ribonucleotide depletion. This activation is marked by two major events: First, the half-life of the p53 protein is increased drastically, leading to rapid accumulation of p53 protein in stressed cells; secondly, a conformation change forces p53 to be activated as a transcription regulator in these affected cells (Maddocks and Vousden 2011). When DNA damage occurs, p53 can induce growth arrest by holding the cell cycle at the G_1/S regulation point while DNA repair systems are activated. When DNA damage proves to be irreparable, p53 will initiate apoptosis.

Poly (ADP-ribose) polymerase PARP activation is an immediate cellular response to metabolic, chemical, or radiation-induced DNA damage. The main role of PARP is to detect and signal single strand DNA breaks (SSB) to the enzymatic machinery involved in the SSB repair. Once PARP detects a SSB it binds to the DNA and begins the synthesis of a poly(ADP-ribose)chain (PAR) as a signal for the other DNA repairing proteins. The amount of PAR formed is commensurate with the extent of damage. It is the activation degree of PARP that determines cell death modes : (i) when PARP is activated by mild genotoxic stimuli, it facilitates DNA repair;(ii) more severe DNA damage induces apoptosis, during the process caspases

inactivate PARP by cleaving it into p89 and p24 fragments; (iii) extensive DNA breakage triggered by a massive degree of oxidative or nitrosative stress causes PARP over activation, which depletes the stores of cellular NAD+ (which is the substrate for generating PAR) and induce a progressive ATP depletion, promoting cell necrosis (Ha and Snyder 1999; Pagano, Pitteloud et al. 2005).

Caspase-3, belongs to the Caspase family, is the main executioner used in both extrinsic and intrinsic apoptosis pathways. Caspase-3 is formed from a 32 kDa zymogen cleaved into 17 kDa and 12 kDa subunits to activate. Cleaved caspase 3 plays a dominated role in apoptosis signaling cascade, and is responsible for chromatin condensation and DNA fragmentation (Porter and Janicke 1999). Thus, it is another hallmark for identifying apoptosis besides PARP cleavage.

During autophagy, the double-membrane containing vacuoles known as autophagosomes form a massive accumulation and subsequently fuse with lysosome vacuoles. The cytoplasmic form of microtubule-associated protein light chain 3 LC3 (LC3 I, 18KD) is processed and recruited to the autophagosomes, where LC3 II (16DK) is generated by site specific proteolysis and lipidation near to the C-terminus. Similar as PARP cleavage is used a classical apoptosis hallmark, the formation of cellular autophagosome punctae containing LC3 II is widely accepted as the specific hallmark for autophagy activation (Ju, Miller et al. 2009).

The fourth target for investigation, intracellular ATP level, is the factor determining which cell death mode will be adopted at the death road junction. Apoptosis is an ATP dependent process. The presence of ATP is necessary for activation of the caspase cascade, apoptosis signalling, chromatin condensation and nuclear fragmentation. In the early stage of apoptosis, loss of mitochondrial membrane

potential halts mitochondrial ATP production. Despite this, glycolysis is still able to provide the ATP required for apoptosis. In contrast, necrosis is a passive process and therefore does not require ATP. For instance, the DNA random fragmentation which occurs in necrosis is not ATP dependent. On the contrary, intracellular ATP depletion leads to necrosis (Leist 1998; Zhao, Wieman et al. 2008). Therefore, a decrease in intracellular ATP levels is frequently considered an important biochemical marker of necrosis.

A low intracellular ATP level observed in tissue culture condition can be caused by several reasons: (1) intracellular ATP supplies are rapidly exhausted due to rapid consumption of glucose, especially for the cell lines which are more dependent on mitochondrial ATP production; (2) mitochondrial injury may cause ATP production to shut down; (3) induced by severe cellular DNA damage, PARP activation causes its substrate NAD+ depletion and then consumes a large amount of ATP; (4) intracellular ATP leakage caused by increased permeability of the cytoplasmic membranes. During necrosis, the decrease of intracellular ATP level always is connected with calcium level disturbance. When depletion of ATP impedes the function of membrane channels, increased calcium activates calcium-dependent proteases like calpains and cathepsins. These factors involve complex and interactive feedback loops that self-amplify and potentiate each other, finally leading to exaggerated cell death (Lemasters, Qian et al. 2002; Criddle, Gerasimenko et al. 2007)

The fifth target for investigation in this chapter is the cell cycle. Compared to MTS assay and xCelligence which measure cell proliferation either by metabolism or by cell morphology, cell cycle analysis by flow cytometry provides a parallel study that

gives more insight into cellular events responsible for cytotoxicity. Flow cytometry has proved to be a popular tool in conventional chemotherapy and radiotherapy research and often plays critical roles in drug discovery. It not only describes the cell growth alteration by the specific treatment, represents a sensitive marker of the cytotoxicity, but also characterises the cellular genome damage and therefore indicates the death mechanisms.

The final target is the profile of release of progeny virions. Release and spread of progeny virions represents one of the most critical steps of the oncolytic virus' life cycle (replication, cell lysis, viral exit). They are the determining factors to decide the viral potency. Spread relies both upon release of virus from initially infected cells as well as upon subsequent infection of neighbouring cells. The virus release and subsequent spread may be influenced by the different death modes. For example, apoptosis has been believed to be an important means for both viral lysis and spread (Roulston, Marcellus et al. 1999; Mullen and Tanabe 2002). During the process of apoptosis, the cell is disintegrated by the formation of the apoptotic bodies; a small vesicle enveloped by the intact plasma membrane which contains the cellular content. The apoptotic bodies are then phagocyted by macrophages and the adjacent cells to prevent the induction of an inflammatory response. Thus, apoptosis has been considered as a strategy for survival and propagation of intracellular infectious pathogens including adenovirus. By the engulfment of apoptotic bodies, the viruses are able to achieve dissemination without initiating a concomitant host response. Conversely, necrotic cell death releases the virus progeny and other cellular contents which disperse from the plasma membrane, simultaneously causing immune-activation by DSR and TLR ligation. Contrary to cell to cell spreading of enveloped

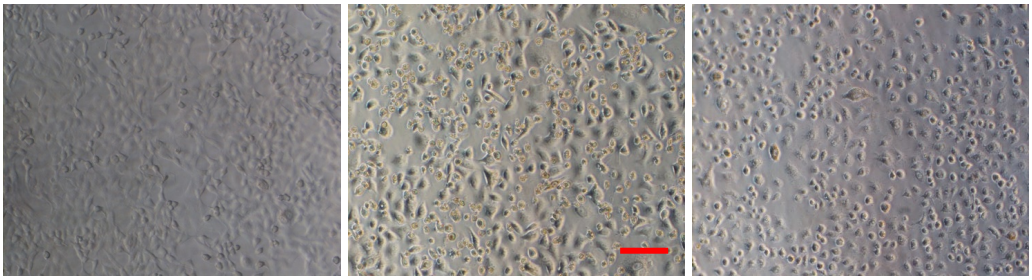
virus that occurs in apoptosis, the extracellular release of virus during necrosis is obviously more disruptive and may be seen as more “dangerous”.

4.2 Results and discussion

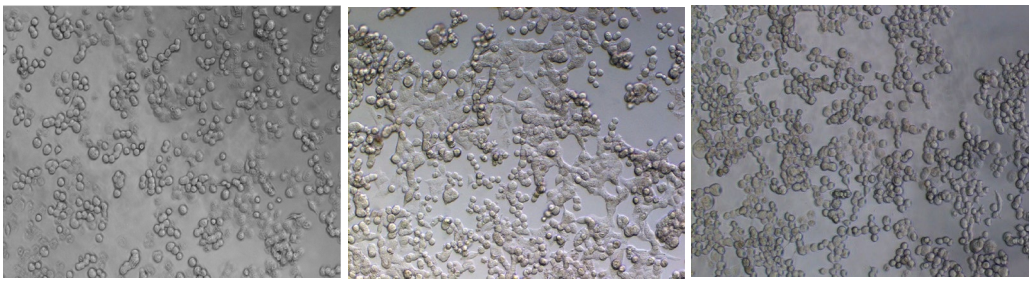
4.2.1 Morphological observations of adenovirus oncolysis

4.2.1.1 Light microscopy observations of cell deaths

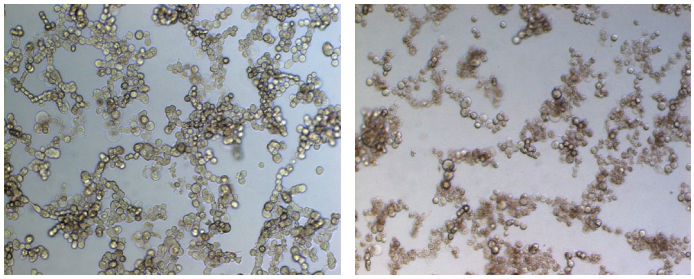
Images of cells dying or dead were taken using light microscopy under various treatment conditions, and were shown in Fig 4.1. Following Cisplatin treatment (Fig4.1B), most of cells showed characteristic cytoplasmic shrinkage and floating into the medium, while a small percentage of cells were still adherent to the surface and maintained apparently normal cell morphology; H_2O_2 treated cells (Fig4.1C) rounded up, with blebbing and slightly increased size while keeping adherent. At the onset of oncolysis (day 3 of POI), CPE of the three adenovirus were similar to each other but were distinct from both Cisplatin and H_2O_2 treatment. The cells rounded up, were slightly swollen and appeared to detach from the monolayer. The Ad5 infected cells appeared to be slightly larger while ColoAd1 infected cells were relatively smaller. As oncolysis progresses (day3.5), an increased number of round cells were aggregated into grape like clusters. ColoAd1 and Ad11 treated cells reduced their size faster than those treated by Ad5, and most of them have fallen off the monolayer surface. The remaining cells appeared refractive and were essentially cell debris (day 4). Ad5 treated cells kept floating on the surface until day 4. However, no obvious burst of virion release was observed for any of the three viruses treated cells under the optical microscopy.



A: Mock **B: Cisplatin** **C: H_2O_2**



D: ColoAd1(day3) **E: Ad11(day3)** **F: Ad5 (day3.5)**



G: ColoAd1(day3.5) **H: ColoAd1(day4)**

Fig4.1 Light microscopy images of A549 cells under various treatments. Images were taken directly of the wells and focused to the cell monolayer (at 10X magnification, the red bar present a scale of 100 µm). A. Mock-treated cells; B: cells treated with Cisplatin 50µM at 36 hours; C: cells treated with H_2O_2 1mM at 6 hours; D,G,H: cells treated with ColoAd1, 10 PPC at day 3, day 3.5 and day 4 of POI respectively; E: cells treated with Ad11, 25 PPC, at day3(images at day 3.5 and day 4 similar to ColoAd1); F: cells treated with Ad5, 100 PPC at day3.5 of POI.

4.2.1.2 Time lapse microscopy

The time lapse microscopy results showed some detailed differences between the virus mediated oncolysis and Cisplatin induced cytotoxicity. Cisplatin treated cells underwent blebbing, nucleus and cytoplasmic shrinkage, and then were disintegrated

with formation of small vesicles (apoptotic bodies). These vesicles were phagocytosed by the adjacent cells. In Ad5 infected cells there was a small amount of apoptotic bodies formed, but in ColoAd1 infected cells the apoptotic bodies were not seen. Compared to Cisplatin treated cells, both virus-infected cells were more mobile (similar to control cells), showing the inter cell connection with some cytoplasmic fibrils during the oncolysis. During viral infection, there was large number of small round vesicles appeared in the cytoplasm (these were not further identified but appeared quite stable). Nuclei remained intact and were slightly enlarged compared to those of control cells. At the virus oncolysis stage, a violent burst was recorded associated with sudden eruption of cytoplasmic membrane, especially in the case of ColoAd1. This phenomenon is similar to H_2O_2 caused cell death, which is manifest as rapid breakage of the cytoplasmic membrane.

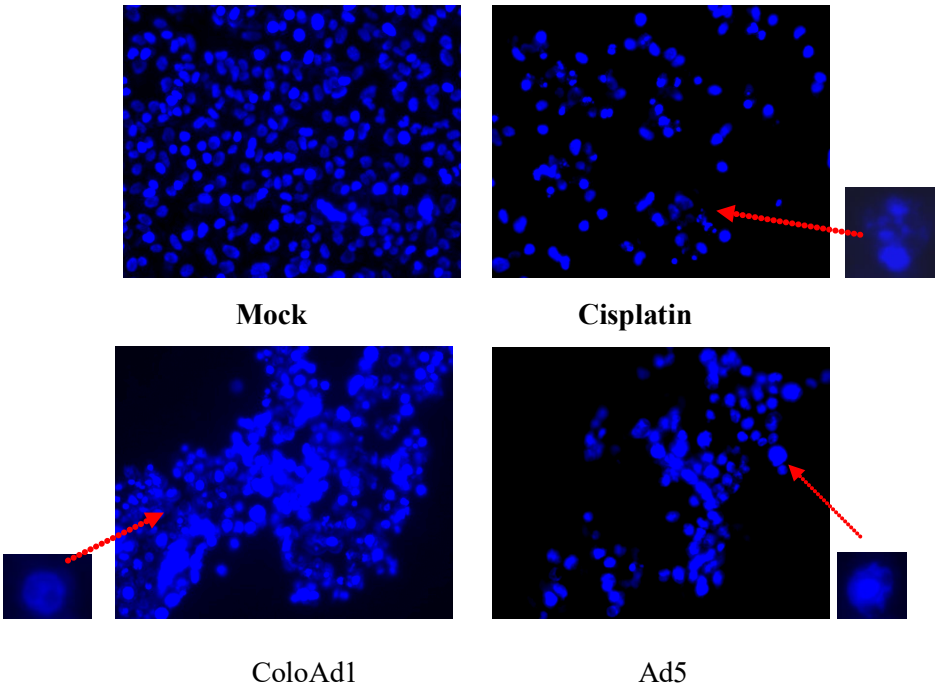


Fig 4.2 DAPI nuclear staining of Cisplatin and viruses treated dying cells. The dose of treatments were the same as shown in Fig 4.1.The pictures of treated cells were taken at 36 hours, day 3 and day 4 for Cisplatin, ColoAd1 and Ad5 respectively (after PBS wash). The small frames are zoomed images from the location where the red arrows indicate.

4.2.1.3 DAPI nuclear staining

No obvious chromatin condensation and fragmentation were found in either ColoAd1 or Ad5 treated cells when dying, whilst they were easily identified in the cells treated with Cisplatin. As shown in Fig 4.2, the small frame of Cisplatin treatment showed the typical nucleus fragmentation into apoptotic bodies. On the contrary, there was very slight condensation seen in both viral treated cell nuclei, but the nuclei were still intact.

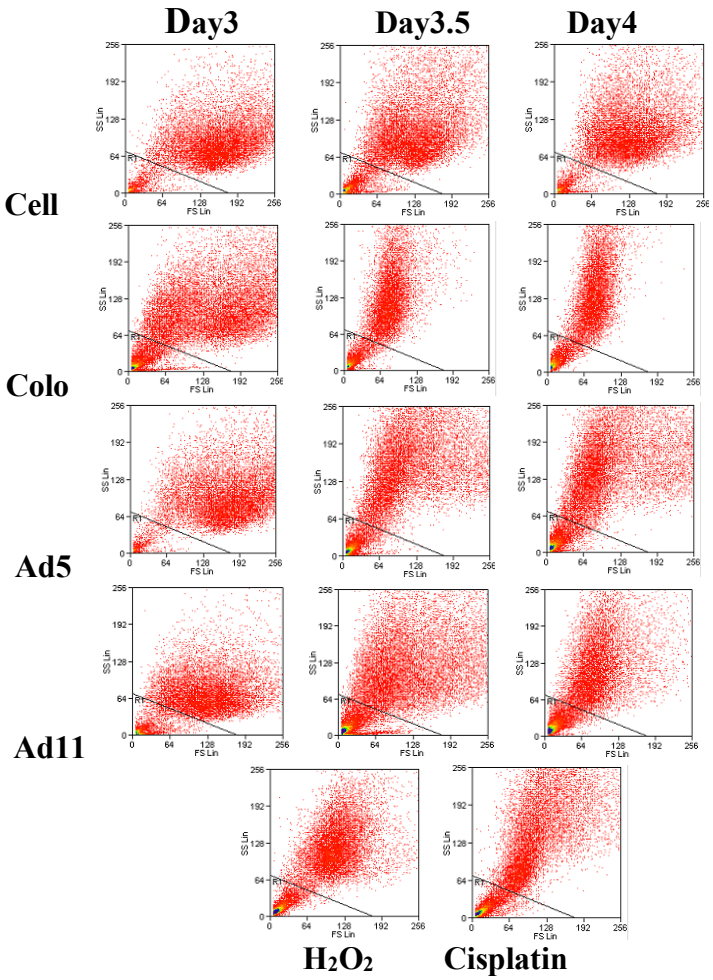


Fig 4.3 Forward and side scatter plots of dying cells. A5459 cells were treated under the same conditions as in Fig 4.1. The cells were harvested and stained by Annexin V/PI for the flow cytometry analysis, the data of Annexin V/PI signals is reported in Fig4.6.

4.2.1.4 Cellular size and granularity change

Flow cytometry analysis revealed that virus oncolysis caused a decrease in forward scatter and an increase in side scatter compared to the mock cells. This demonstrated

that cells gradually shrink and cellular granularity increases during progressive oncolysis. The most drastic changes happened with ColoAd1 treatment, followed by Ad11 and Ad5 treatment respectively. Both Cisplatin and H_2O_2 treatment also caused the cellular size decrease and granularity increase, although they were not as drastic as ColoAd1 induced cell death.

4.2.2 Cytoplasmic membrane alteration and leakage during oncolysis

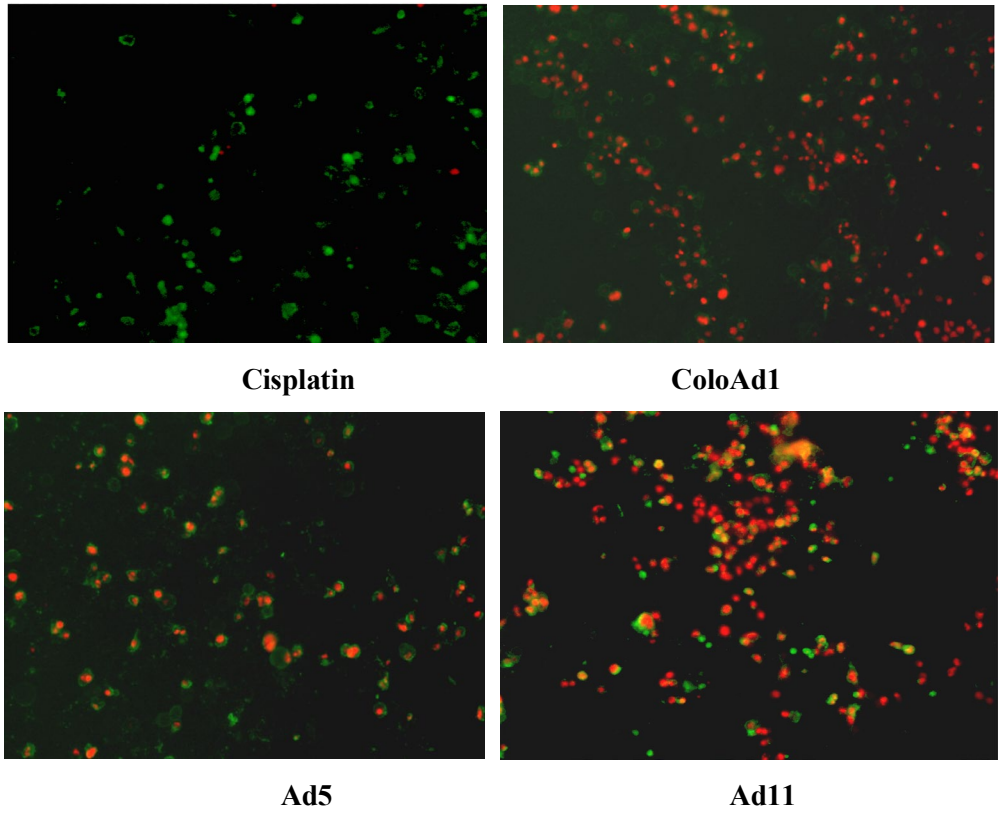


Fig 4.4 Typical Annexin V/ PI double staining images observed by fluorescence microscopy with 10X magnification. Annexin V was labelled by FITC (green color); PI was shown as red color. Low signals were detected in the mock-treated A549 cells(data not shown). Cell treatments were the same as described in the legend to Fig 4.1. The images of Cisplatin treatment was recorded at 24 hours after the start of treatment, the images of the viruses treatments were recorded at day3 after infection. The optical microscopy images can be seen in the Supplementary Materials S5.

4.2.2.1 Fluorescence microscopy observation

Four typical double staining images captured by the fluorescence microscopy were shown in Fig 4.4.

ColoAd1 treated cells displayed a complete PI permeability (red) with a weak Annexin V staining signal (green), which indicated a necrosis pattern. In contrast, Cisplatin treated samples showed a classical apoptosis-related PS externalization with very few cells showing membrane permeability associated with necrosis (almost all the cells stained green). Treatment with Ad11 and Ad5 gave images that fell between these two extremes, with the majority of cells displaying a clear double staining thought to represent necrosis (red overlapped with green or yellow color) and a small population giving a classic apoptotic signal (green color); furthermore, Ad11 gave higher percentage of double staining than Ad5 in the cell population.

4.2.2.2 Annexin V/PI staining characterization by flow cytometry analysis

The microscopy observations were verified by flow cytometry (Fig 4.5). H_2O_2 treated cells and ethanol permeablised cells together with Cisplatin treated cells were used as controls for different type deaths. As shown in Fig 4.5, H_2O_2 induced a completely necrotic pattern, 90% of treated cells were showing intensive PI positive signal (Annexin V either positive or negative, both upper quadrants in the dot plots), but only 4% of cells were apoptotic (Annexin V+/PI-,lower right quadrant). For ethanol permeablized cells, the PI staining was a only positive signal and the cells showed a primary necrotic pattern (95%, upper left quadrant), this indicated PS remained the inner layer of cytoplasm and not enough binding site was available for Annexin V, or the Annexin V were unable to get access inside the cells by ethanol

treatment. In contrast, in Cisplatin treated cells, the majority of population (59%) has fallen into apoptotic category.

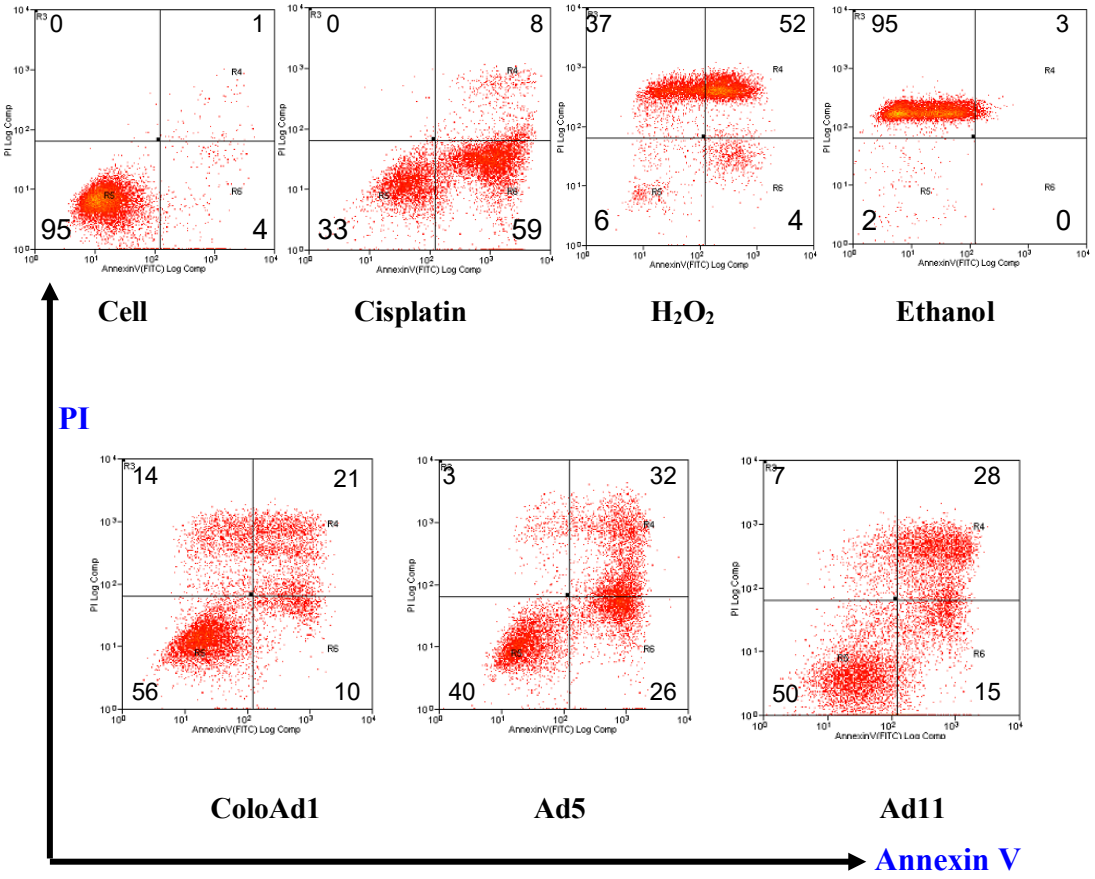


Fig 4.5 Flow cytometry dot plot analysis for cells treated with different cytotoxic agents and dual color stained with Annexin V /PI. Y axis represents the PI signal; X axis represents the Annexin V signal. The numbers in each quadrant refer to the percentage of the whole population and were the mean value of two independent experiments. The cell treatments were the same as described in the legend to Fig 4.1. The samples of ColoAd1and Ad11 treated cells were harvested at day 3 post infection; for Ad5 was harvested at day3.5 to get the similar cell death percentages. Ethanol treatment was the same as preparation of the cells for cell cycle analysis (others conditions were the same as shown in Fig 4.1)

Interestingly, most ColoAd1 killed cells showed a necrotic pattern, with similarity to H_2O_2 and ethanol treated cells where the majority of cells displayed PI positive (approximately 70% both Annexin V+ and -, upper left and right), in the mean time a minor population as 15% occupied apoptosis quadrant (Annexin V+ / PI-, lower right

quadrant). In the case of Ad5 killed cells, there was large quantity of necrotic cells (32%), however apoptotic cells appear presented a higher percentage of the whole population at 26%, in addition, the primary necrosis signal is relatively weak as 3%. Ad11 treated cells had an Annexin V /PI staining pattern between ColoAd1 and Ad5, which was showed as dominated necrotic cells with a small proportional apoptotic cells, however, the primary necrosis remains a very small percentage overall.

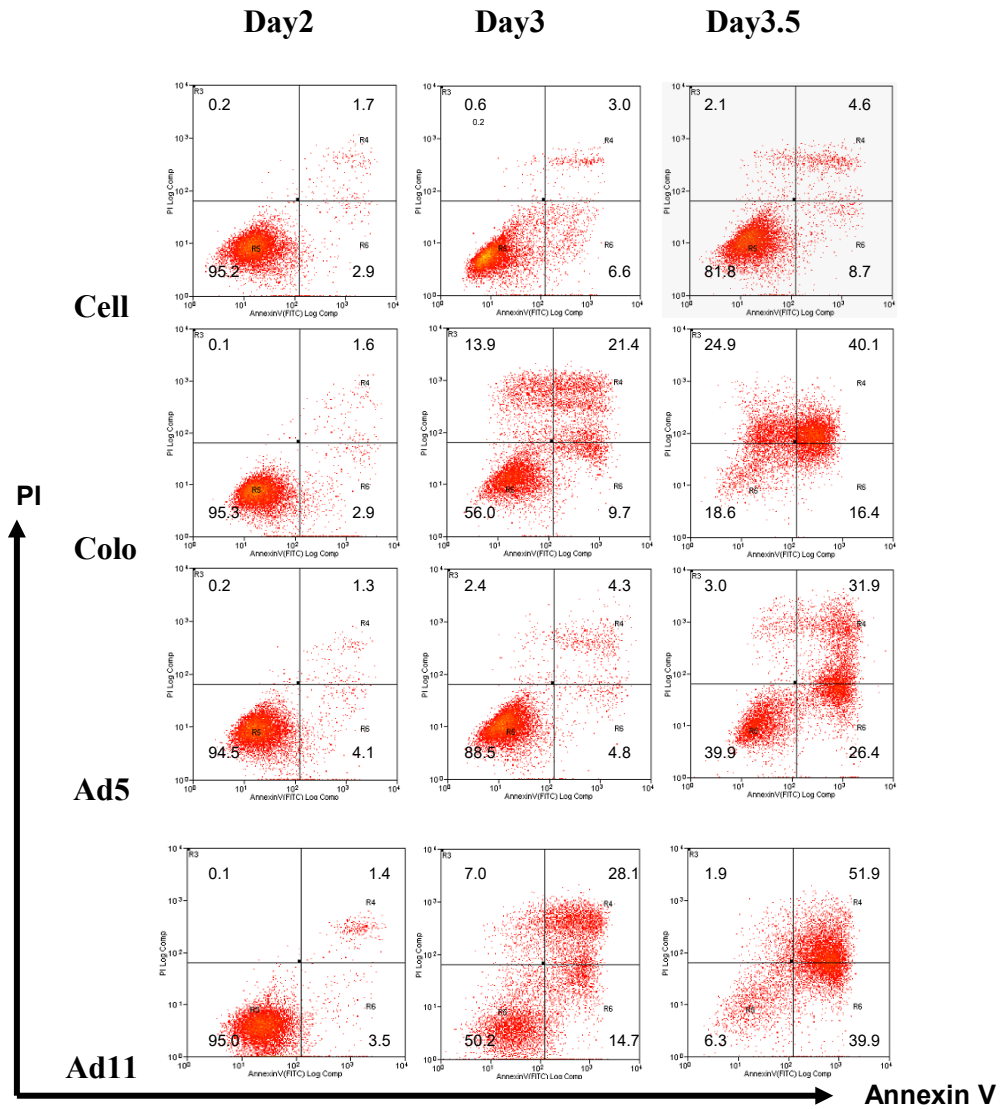


Fig 4.6 Annexin V/ PI staining time course study for Ads oncolysis. The cells treatments and sample preparations were used the same conditions as in Fig 4.5. The experiments were repeated twice and gave the similar results.

Although most literature only showed the end point assay for apoptotic and necrotic Annexin V/PI staining, it would be interesting to know the dynamic status of cells during the dying process. This would be useful to address the question: whether the virus induced necrosis belong to secondary necrosis. With this question in mind, a time course study was carried out to investigate the Annexin V /PI staining patterns of three adenoviruses with the progression of their oncolysis; the results were shown in Fig 4.6.

As seen from Fig 4.6, all the cells (including the viruses treated) were at healthy condition at post of infection day 2. ColoAd1 and Ad11 induced significant a membrane permeabilisation from day3 POI and consequently cell death. The FACS data revealed at time of point of POI day 2.5 all the cells were still in healthy condition; Ad5 only caused cell death at day3.5 when ColoAd1 and Ad11 almost have finished their killing.

Even at the beginning of oncolysis, a large proportion of the whole ColoAd1 treated cell population showed symptoms of necrosis, with 35% cells PI positive and 55% non staining cells (assumed to be still healthy). At 3.5 days post infection there were 68% PI positive cells with only 18% non staining and 16% Annexin V+ PI- (apoptotic) staining. Notably, during treatment with the viruses, there no phase found which had a dominant Annexin V+ PI- pattern, similar to Cisplatin induced early apoptosis. The time course study suggested the necrotic cell death induced by ColoAd1 was more likely attributed to primary necrosis, whereas the death induced by Ad5 could be more related to the late stage of apoptosis and therefore categorised as secondary necrosis. In the case of Ad5 killing, it looked like the early apoptosis

plays an import role from beginning (28%) and then developed into secondary necrosis (26%), though there was still a certain part of primary necrosis (11%) in the whole cell population. The necrotic cell percentage analysis can be seen in Fig 4.7.

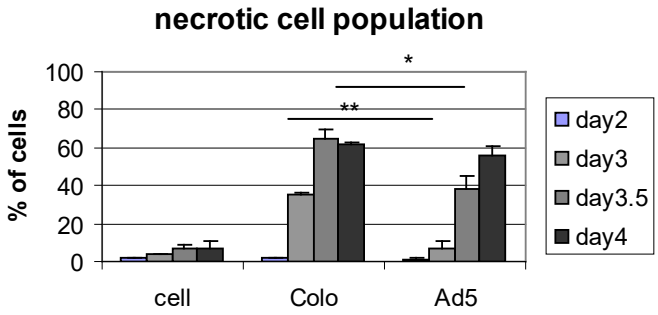


Fig4.7 Percentage of A549 cells showing positive PI staining at different time points after virus infection, measured by Annexin V/PI staining through FACS analysis. The data were collected as PI positive signal (including Annexin V + and – populations). The data is the mean value of two individual experiments. Mean data ± SD are presented, *n* =3.

Using Annexin V/PI staining assay measured by fluorescence microscopy and flow cytometry, it was found during the progression of oncolysis the plasma membrane permeability increased although it did not occur at the early stage of viral infection and replication. The three oncolytic adenoviruses induced various degrees of cytoplasmic membrane leakage. ColoAd1 mediated a rapid primary necrosis staining pattern similar to H_2O_2 and quite distinct from that of Cisplatin induced cell death. Ad11 treated cells displayed slightly less membrane permeability with more signal for Annexin V staining, suggesting some involvement of apoptosis. Although Annexin V staining intensity gradually increased with oncolysis, which may related with the membrane leakage providing access of Annexin V to internal PS and not with translocation of PS. In the case of Ad5, the primary necrosis and apoptotic

features coexisted with the secondary necrosis signal increasing during the late apoptosis progression.

Because of the lack of published data based on group B adenovirus oncolysis, most literature reports relate to the use of adenovirus 5, although some relevant information can be found to compare with our results. Although the eventual result of viral infection is lysis, the possibility that Ad5 simply mediate necrosis has been questioned because there is no wholesale disruption of cellular membranes observed (Abou El Hassan, van der Meulen-Muileman et al. 2004). On the other hand, according to El Hassan's report, PS externalization was detected starting from day 1 post infection): the majority of Ad5-infected cells showed Annexin V-positive membrane staining in the absence of PI staining. In a small portion of Ad5-infected cells, PS externalization was accompanied by PI staining; this may represent a minorityof cells that became leaky during virus propagation. However, co-exposure with Pan caspase inhibitor zVAD-fmk did not alter the Annexin V staining pattern in the infected cells, the cells were killed by caspase-independent mechanism that resembles necrosis-like cell death.

So far, at least two oncolytic adenovirus have been reported to produce a necrotic profile by FACS analysis of Annexin V /PI staining. One is AdYB-1, an E1/E3 deleted recombinant Ad5 vector overexpressing the human transcription factor YB-1; this virus triggers PI staining accompanied by PS externalization without induction of the classical apoptotic pathway, but mediates a necrosis like cell killing (Glockzin, Mantwill et al. 2006). Another one is Ad-XJ (Yun, Kim et al. 2005), an E3 deleted Ad5 reported to induce 63% necrotic and 23% apoptotic cell death. On the contrary, the oncolysis of some oncolytic adenoviruses expressing transgenes often brings a

complicated mixed pattern on the FACS analysis, or a more dominated apoptosis feature. For example, MUD55-IL-24 (a replicating adenovirus expressing IL-24) induces a profound apoptosis in gastric carcinoma, and flow cytometry shows a dominant Annexin V+ but PI- pattern (Wei, Fan et al. 2010).

4.2.3 Expression of key cellular proteins during adenovirus oncolysis

Expression levels of key cellular proteins were assessed over the three days following infection of A549 cells with the three oncolytic adenoviruses. Mock-treated cells were used as background and Cisplatin treated cells (50 μM, 36 hour) were used as an apoptotic cell death positive control, with β–actin of the cell lysate used as a loading control for SDS-PAGE. Viral infection and progress of replication were also assessed by determining hexon expression level using a Coomassie blue stained SDS-PAGE gel.

As can be seen from the SDS-PAGE gel (Fig 4.8), all three viruses achieved a successful infection and replication. From day 2 post infection (52 hour) onwards, the adenovirus hexon bands (at 109 kD) gradually showed up as a late gene product. The intensities of the hexon bands were similar for the three viruses at day 3 post infection (75 hour), representing a time when many of the cells were undergoing oncolysis. By comparing with uninfected cells, the gel showed that at 75 hours viral hexon proteins represented a significant part of the total cell lysate. Other viral proteins could not be identified on the SDS-PAGE gel by the blue staining. Unfortunately, anti-E1 antibody is not yet available for group B adenovirus so far, preventing its determination by immune blotting of the infected cell lysate.

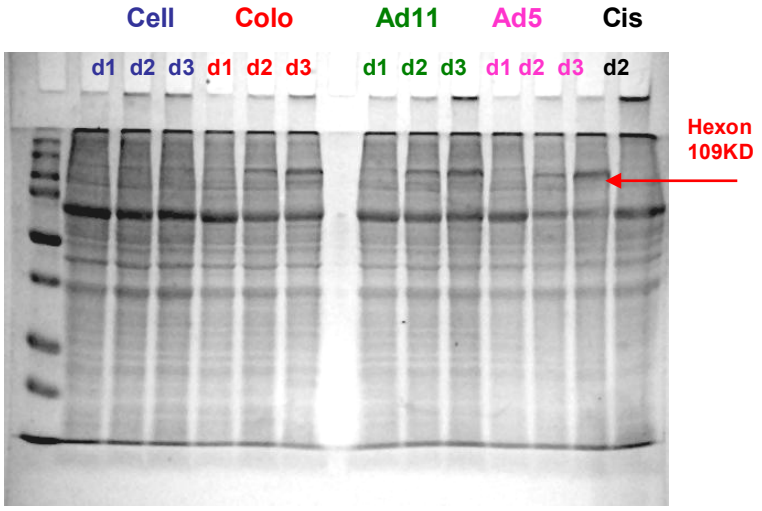


Fig 4.8 The SDS-PAGE gel of A549 cell lysates, stained with Coomassie blue. The Adenovirus hexon band is located at 109 kD and can be differentiated from the cellular proteins. The loading total protein was used at 45 µg/ well.

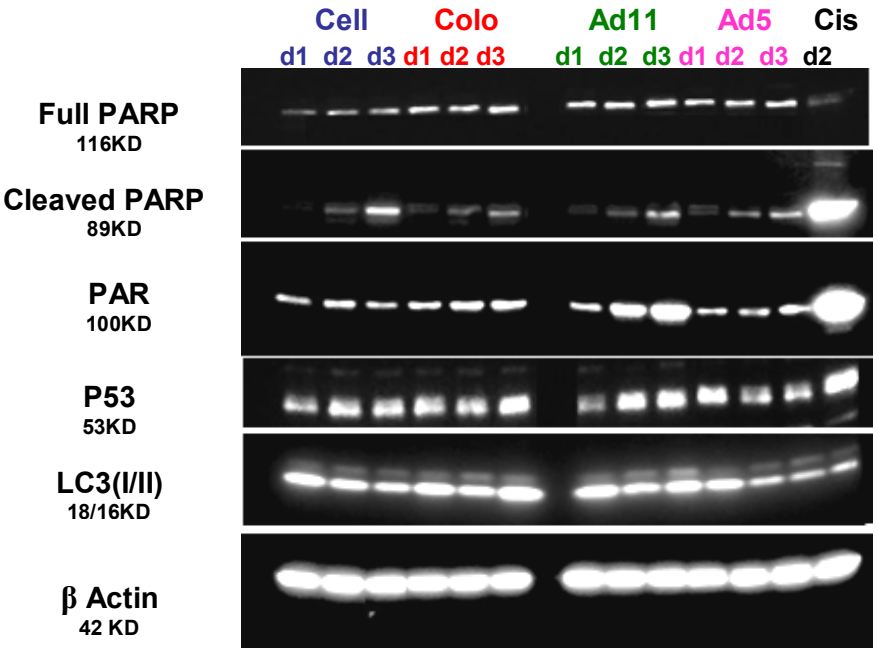


Fig 4.9 Western blots for the key cellular proteins, visualized by Enhanced Chemiluminescence (ECL). The antibodies and detailed staining procedures can be found in the Materials and Methods in Chapter 2. The A549 cell lysates used were the same as in Fig 4.8, and the cells treated under conditions were according to Fig4.1. Cell lysates were all loaded at a concentration of 30 µg/well.

As shown in the western blots (Fig 4.9), Cisplatin treated cells (50 μM, 36 hours) demonstrated some typical hallmarks of apoptosis: there was evidence of cleaved and activated caspase 3 (see supplementary data S6); full sized PARP virtually disappeared and was converted into the caspase cleaved 89 KDa PARP form; the product of PARP activity, PAR is also accumulated; in addition, p53 was up-regulated. Although some signs of apoptosis appeared for the mock-treated cells at 3 days post infection (for example, as seen the cleaved PARP band), however the signal was rather weak. The cleaved PARP and caspase 3 signals from the virus infected cells were not stronger than the mock-treated cells. On the contrary, the adenovirus particularly group B adenovirus infection and replication even up-regulates the level of full-length PARP. Virus infection and replication also caused the slight up-regulation of the autophagy marker LC3, but they did not show significant conversion of LC3 I to LC3II compared to the mock-treated samples. These results suggest that the cell death pathways caused by the three adenoviruses in A549 cells do not represent caspase-dependent apoptosis, nor mainly autophagic death. The lack of PARP cleavage and caspase 3 activation in cells exposed to Ad5 agrees with previous observations (Abou El Hassan, van der Meulen-Muileman et al. 2004; Baird, Aerts et al. 2008), however we didn't find significant evidence of autophagy which has been highlighted in recent reports (Jiang, White et al. 2011; Rodriguez-Rocha, Gomez-Gutierrez et al. 2011).

Both of the group B adenoviruses, ColoAd1 and Ad11, showed some features that were distinct from Ad5. For example they induced PAR accumulation and up-regulation of p53 expression. In contrast, Ad5 causes p53 degradation with viral replication and oncolysis. The same observation has been recently reported by

Forrester (Forrester, Sedgwick et al. 2011). They found during adenoviruses infection, inactivation of the cellular DNA damage response is serotype-specific. Ad5 inactivation is facilitated by the degradation of p53, Mre11 and DNA ligase IV; while Ad11 causes p53 accumulation but does not significantly affect the levels of Mre11 and DNA ligase IV. Although the expression of p53 is increased by Ad11, it does not seem to have transcription-enhancing activity.

4.2.4 Assessment of intracellular levels of ATP and Ca^{2+} during Ad oncolysis

The intracellular levels of ATP and Ca^{2+} were monitored during the progress of adenovirus oncolysis. The observation time started from 16 hour post infection (approximate start of replication) to 68 hours (cells undergoing oncolysis). The results demonstrated dynamic changes of ATP and Ca^{2+} induced by virus replication, and revealed that ColoAd1 causes decrease of cellular ATP early in cell death, followed by dramatic increase in Ca^{2+}.

The data shown in Fig4.10 demonstrated that adenovirus infection (with either virus) caused increases in intracellular ATP compared with control cells at the early stage of the infection (until 24 hours post infection, approximately). This can be explained by adenovirus infection stimulating cell metabolism to facilitate virus production. However, subsequently, ColoAd1 displayed different properties than Ad5. The ATP levels of ColoAd1-infected cells started to drop during the middle stage of replication (24 hours post infections) and it fell to 30% of the starting level at the point of onset of cell death. As a comparison, Ad5 infected cells showed a flatter pattern, perhaps even rising until the onset of cell death, after which the ATP level went down quickly; Ad11 once again displayed a pattern between ColoAd1 and Ad5, it induced ATP dropping at post infection 36-45 hours, then rose slightly before going down.

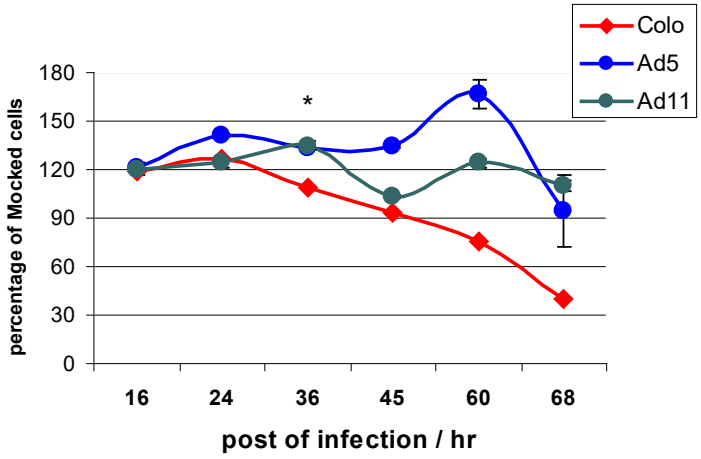


Fig 4.10 Intracellular ATP levels in A549 cells infected with adenoviruses. The doses of the treatments were the same as used in Fig 4.1. The data are expressed as the percentage of control mock-treated cells. Mean data ± SD are presented, *n* =3. Statistical differences between three groups were determined using one way ANOVA.*: p value <0.05.

Intracellular levels of ATP during adenovirus oncolysis have not been widely reported, only in Baird's report it was mentioned the Ad5 based oncolytic virus dlCR2 induced a novel mode of programmed cell death in ovarian cancer. The death pathway was reported to be necrosis-like albeit without falling intracellular ATP level even at the time of cell lysis. In our results, the final drop of intracellular ATP in cells treated with all three viruses is easier to comprehend, and it correlates with the use of MTS assay for measuring mitochondrial activity as a surrogate for cell viability. The early intracellular ATP level falling induced by ColoAd1 infection suggested energy supply shortage, and is probably not due to the malfunction of mitochondria and membrane leakage since the cells still appeared to be in a healthy condition at this stage; more likely the fall was related with both viral rapid replication and PARP activation.

At the point of onset of cell death, intracellular Ca^{2+} levels were observed to increase with all three viruses. There is a greater impact seen in the case of ColoAd1 than with Ad11 or Ad5 (Fig 4.11, the data for Ad11 is not shown).

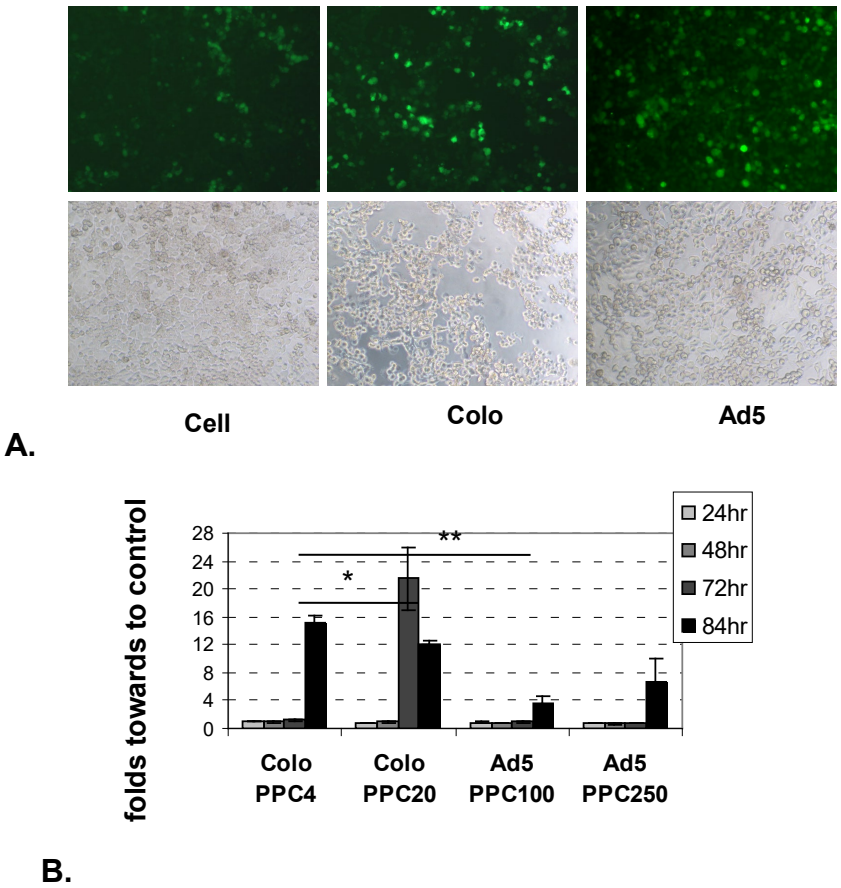


Fig 4.11 Intracellular Ca^{2+} levels detected by Fluoforte ™ dye in virus-infected A549 cells. A. Observed under fluorescence microscopy. Upper three images were the fluorescence images and bottom three were the corresondingly optical images, all with 10X magnifications. ColoAd1 was used at 10 PPC and Ad5 was used at 100 PC for infection, the assays were measured at day 3 post infection. The intensity of the green fluorescence signal indicates the intracellular Ca^{2+} concentration. B. Measured by fluorescence microplate reader. The signals were normalised by protein concentration and calculated as the fold difference compared to the control blank cells. Mean data ± SD are presented, n =3. Statistical differences between two groups were determined using Student's t-test. * = $p<0.05$, ** = $p<0.01$.

According to our observations, increased cytoplasmic calcium level was associated with the progression of all three adenovirus infections. The rise seemed to be related

with the cellular stress and reached a maximum at the onset of oncolysis and then was eliminated when the cells die. Among the three viruses, ColoAd1 gave the strongest effect. Interestingly, this effect has also been observed with another oncolytic adenovirus which was derived from a similar bioselection approach, AT1(Gros, Martinez-Quintanilla et al. 2008). With a E3/19K mutation, this Ad5-based virus was reported to have enhanced antitumour potency. This group reported that the increased intracellular calcium is involved in animal virus-induced cytopathic effects and cell killing, and it may also be used as a tool by the virus to permeabilize the plasma membrane and ultimately cause membrane lesions that allow the release of virus progeny. For example, the Protein 2B from coxsackievirus is a protein with viroporin function that gradually induces the influx of extracellular Ca^{2+} and releases Ca^{2+} from ER (van Kuppeveld, Hoenderop et al. 1997). A rise of intracellular Ca^{2+} level is also usually associated with necrotic cell death usually is associated with a rise of intracellular Ca^{2+} level, which activates, activating the Ca^{2+} dependent proteases such as calpain and caspasine for cell disintegration(Artal-Sanz and Tavernarakis 2005).

4.2.5. Cellular DNA damages during adenovirus oncolysis

4.2.5.1 DNA histograms of virus-infected A549 cells

As can be seen from Fig4.12, during day1-day 4 the mock-infected cells maintain the basic shape of DNA histograms, although the subG1 region gradually increases from day 3.5.

The major changes began at day 3 post infection for virus-infected cells with an increase in S phase coincident with the beginning of oncolysis. During the period

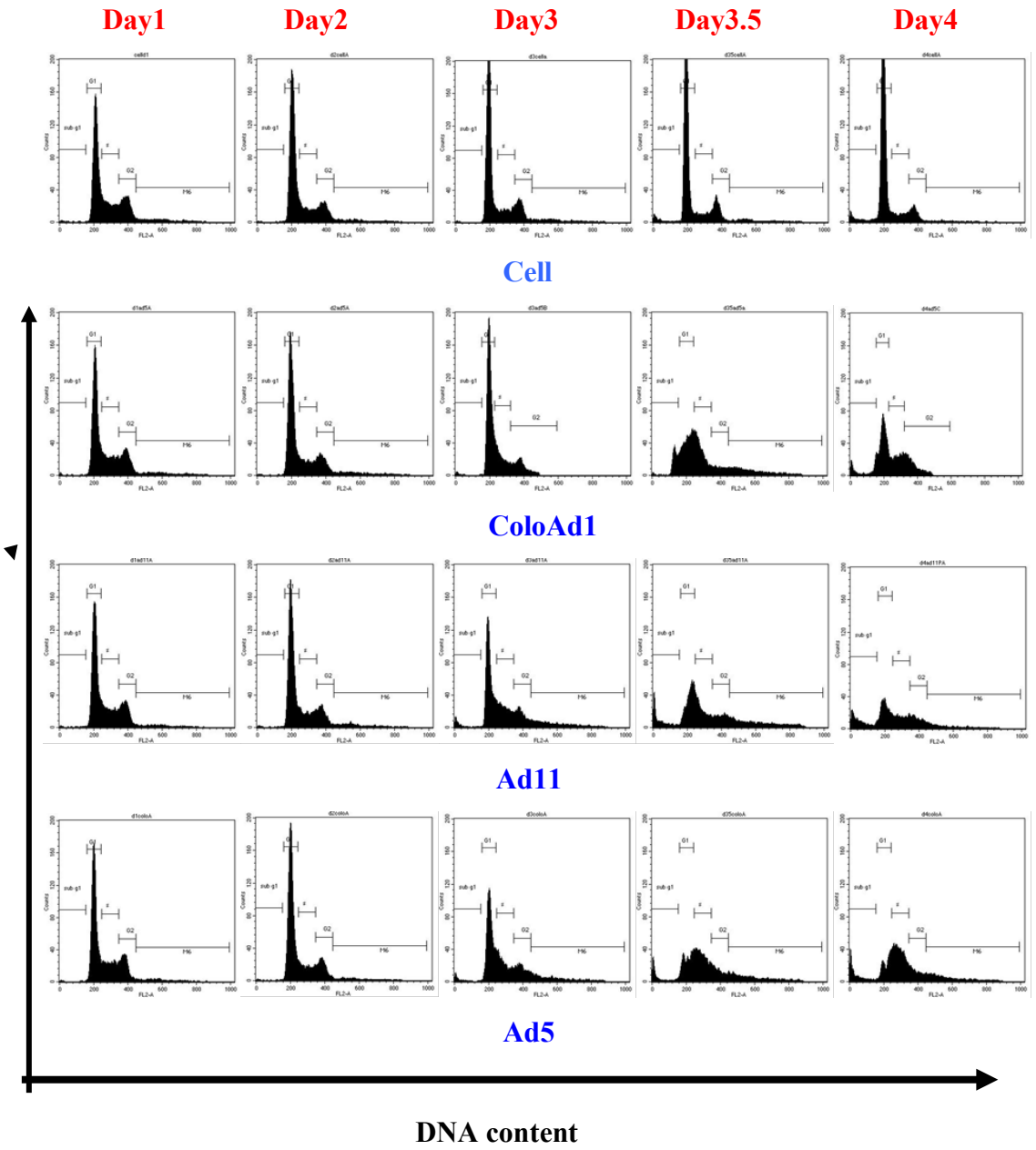
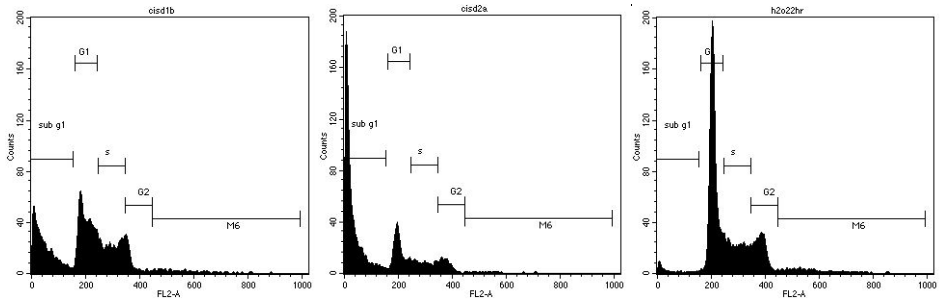


Fig4.12 **DNA histograms of virus-infected cells and mock-treated cells, characterised as cell cycle analysis by flow cytometry**. Each histogram was gated by 5 regions, from the left to the right represented as subG1, G0/G1(2N),S,G2/M(4N), M(>4N) respectively. The doses of viruses applied were: ColoAd1, 10 PPC; Ad11, 25 PPC; Ad5, 100 PPC.

from day 3-3.5 there are remarkable changes in the histogram, corresponding to the time when the majority of cells show cytotoxic effects, according to the kinetic

studies in Chapter 3. During this period from day3-3.5, the G0/G1 peak and G2 of ColoAd1 treated cells almost totally disappeared, instead a new peak arose at S phase.

There also was a significant increase of the >4N (aneuploid) region. In the case of Ad5, a similar phenomenon was observed, although it was less dramatic. The changes induced by Ad11 were weaker than ColoAd1, and it showed a slight remaining G1 peak and a diminished G2 peak at day 3.5. The subG1 area appeared to increase from day 3.5 for all three viruses, and accounted for a higher percentage in Ad11 and Ad5 than ColoAd1, however this did not represent a major population.



Cisplatin, 24hour **Cisplatin, 48hour** **H_2O_2, 6hour**

Fig4.13 **DNA histograms of Cisplatin and H_2O_2 treated cells**. Each histogram was gated by 5 regions, from the left to the right represent subG1, G0/G1(2N),S,G2/M(4N), M(>4N) respectively. Cisplatin was used at 50 μM, H_2O_2 was used at 1mM.

The DNA histograms of adenovirus-infected cells during oncolysis were very different from those treated with Cisplatin. Cisplatin treated cells showed characteristic apoptotic DNA histogram patterns: accumulation at S phase and dominance of Sub G1 population (see Fig4.13, Cisplatin day1 and day 2, sub G1 cells percentages occupy 35% and 67% for day1 and day2 samples respectively). In contrast, H_2O_2 induced cytotoxicity did not show major modification of DNA content and distribution, even at 6 hours after treatment when most cells had died

according to the cytotoxicity MTS measurement and Annexin V/PI staining. Most cell nuclear DNA and chromosomes were still intact at this time (Fig4.13, H_2O_2 6 hours), only a small percentage cells (3%) belonged to SubG1 region.

4.2.5.2 Cell cycle phase distribution

The kinetic change of different A549 cell cycle phases can be seen more clearly in Fig4.14. Under the experimental conditions used (2% FCS infection medium), the mock-treated cells started to show G1 percentage accumulation from day1 to day 4 while S phase and G2/M phase were reduced. Both phenomena are symptoms of G1 arrest under the condition of diminished nutrition.

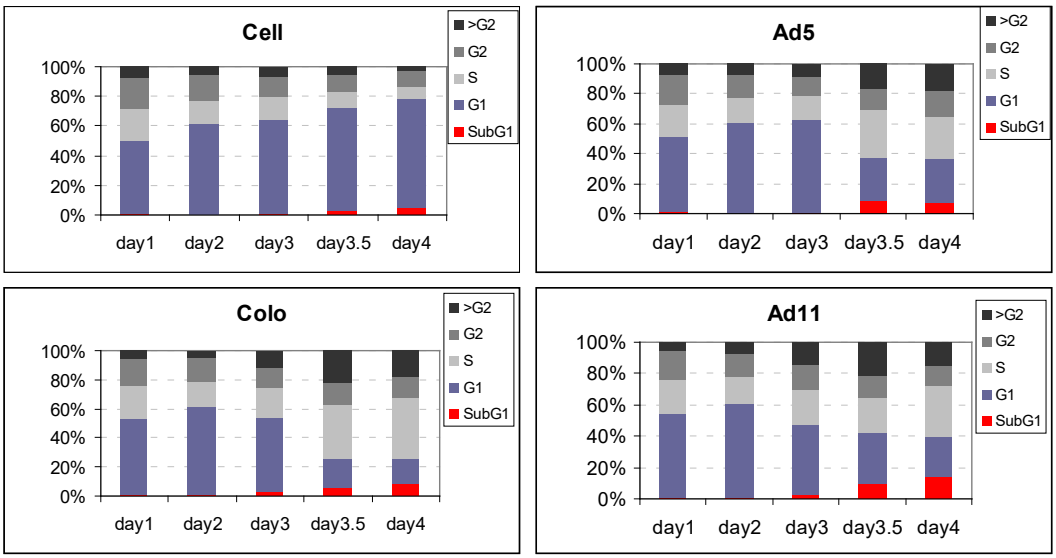


Fig4.14 cell cycle phase distribution

In contrast, the three adenoviruses caused significant shifts in cell cycle phase distribution, forcing cells to abrogate the G0/G1 checkpoint to enter the cycle. Among the three oncolytic viruses studied, ColoAd1 induces the most remarkable modification. The most dramatic changes occurred at the oncolysis stage (from post infection day 3-3.5). Virus infection appeared to override all the cellular check points

(particularly G0/G1), facilitate G1-S transition, and effectively arrest the cell cycle at G2/M, sometimes leading to aberrant mitosis and eventually to polyploidy. The population in G1 fell from 70% in mock-treated cells to 20%, 30% and 30% for ColoAd1-, Ad11- and Ad5-treated cells respectively. There was a simultaneous increase in S phase, which increased as high as 35% (following ColoAd1 treatment) compared to 10% of the mock-treated cells. Similarly, the content of aneuploid cells was ColoAd1>Ad11>Ad5 and reached 20% in cells treated with ColoAd1, compared to 5% in controls. The content of the SubG1 cells was Ad11>Ad5>ColoAd1, however, this is only around 6% (after deduction of the background) of the total population in Ad11-treated cells.

The cell cycle modification pattern induced by adenovirus oncolysis was completely different from Cisplatin (50 μM, 24 hour). Cisplatin treatment induced a dominant SubG1 DNA content (65% of the total cells), and significant decrease of G2/M and S phase indicating G0/G1 phase arrest. The results agreed with previous reports (Almeida, Duarte et al. 2008).

Cisplatin treated A549 cells demonstrated a characteristic cell cycle pattern for apoptosis death mode. The presence of cells with SubG1 DNA content is considered as an indicator of cell death by apoptosis. During apoptosis, breakage of chromatin DNA releases small DNA fragments with in the nucleus. Following the ethanol fixation and permeabilisation with PBS wash, these fragments are lost from the nucleus. As these cells now have a lower DNA content than normal G0/G1 (2N), this population are detected in the sub-G1 region in the DNA histogram. Measuring cellular DNA fragmentation in this way has some advantages over conventional study by DNA gel electrophoresis as it is more sensitive and reproducible.

On the other hand, according to published literature, the addition of H_2O_2 at a sub lethal dose (0.4mM) to A549 cells leads to the prolongation of G2/M phase accompanied by a decrease in the percentage of cells in G0/G1 and S phase, as well as no sign of a subG1 peak that indicates apoptosis. Our results concur with this expectation, albeit our study used a high concentration of H_2O_2 (1mM). This confirms that necrotic cell death does not cause degradation of nuclear DNA.

When combining the data shown in Fig 4.13 and Fig 4.14, it appeared that adenovirus induced cytotoxicity does not show typical apoptotic features (as seen, for example, with Cisplatin treatment). There was a detectable percentage of the total cell population belonging to subG1 (below 10%), however these apoptotic cells never became the dominant fraction. In contrast, viral oncolysis induced a DNA profile that was much more similar to killing of A549 cells by H_2O_2.

In sensitive cells like A549, oncolytic adenoviruses induce deregulation of the cell cycle and appear to promote unscheduled replication of cellular DNA. This activates the DNA damage signalling pathways whose function is to preserve the integrity of the cellular genome. The ability of adenovirus to evade the DNA damage response at early stages of infection has been well recognised, for example, products of the viral E4orf3 and E4orf6 genes have been reported to block signalling of ATR and ATM, the two key kinase central to activating the DNA damage response. These E4 proteins probably function to inhibit cell apoptosis at early stages of infection before reaching maximum production of virions. However, at the late replication stage, and when the virus needs to be released from the cells, it is no longer necessary to maintain cellular integrity; accordingly, activation of DNA damage signalling pathways could be a tool used by the virus for killing the cells.

The correlation between genomic DNA damage and adenovirus cytotoxicity has been recently reported by McNeish's group (Connell, Shibata et al. 2011). Adenovirus-induced cytotoxicity is found be associated with over replication of cellular DNA and therefore extensive genomic DNA damage in sensitive cells; it is initiated by viral DNA replication but only the genomic DNA damage is the direct reason. The major pathway involved is ATR-Chk1 and Cdc25A for virus induced genomic DNA double –strand breaks leading to homologous recombination repair. Thus, virus-induced host cell DNA damage signalling and repair are important determinants of oncolytic adenoviral cytotoxicity. Promoting unscheduled DNA synthesis and/or impeding homologous recombination repair could potentiate the effects of oncolysis.

From our results, ColoAd1 was shown to generate more significant changes to the normal cell cycle on A549 cells than the other two adenoviruses, with increasing S and G2/M cells and those with more than 4N DNA content. This suggested there was extensive genomic DNA damage occurring during ColoAd1 replication, which may be one reason contributing to its enhanced oncolytic potency compared to the other two adenoviruses.

4.2.6. Progeny virus extracellular release and spread

The extracellular release kinetics of the three adenoviruses, ColoAd1, Ad11 and Ad5 were investigated in this study. In contrast to similar studies in the literature, virus genome numbers were measured only in the "extracellular" phase. At the late stage of infection, the infected cells tend to detach from the cell monolayer to enter the supernatant medium. The cell debris and any apoptotic bodies are also suspended in the medium, although they were removed by centrifugation.

In Fig 4.15, for the three adenoviruses, the progeny virions released from the cells into the medium were companied with the progress of oncolysis, cellular DNA damage and permeabilisation of the plasma membrane. A small amount of virus was detected in the supernatant days1-2 post infection, however the majority of virions were released from day 3 onwards when the cells started to die.

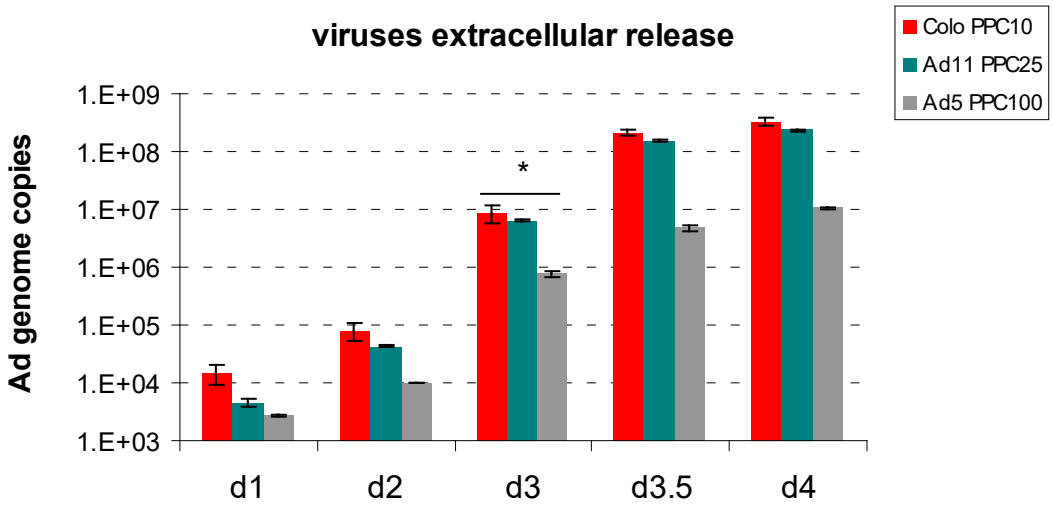


Fig 4.15 Quantification of the extracellular release of progeny virions. A549 cells were infected as described in the legend to Fig 4.1. Samples of supernatant media were collected at the time points indicated and then centrifuged at 6000g for 5 min to remove cell debris. Samples of the supernatant (100 µl) was then used for DNA extraction and virus genomes were quantification using QPCR. Data are presented as mean ± SD, *n* =3. Statistical differences between three groups were determined using one way ANOVA. * = $p<0.05$

Both ColoAd1 and Ad11 have an earlier release profile than Ad5. The extracellular ColoAd1 virion numbers increased 1000 fold at day 3 compared to day 1, and then increased another 10 fold during day 3-3.5 before levelling off afterwards. ColoAd1 induced the most effective release despite being applied at the lowest infection dose (10PPC). Ad11 gave about 80-90% as many virions released when used at 25 PPC. The extracellular release of Ad5 was an average 10-100 fold lower than ColoAd1

and Ad11, even though it was applied at much higher dose of 100 PPC. In addition, Ad5 showed a relatively slow and delayed release kinetics, the highest exit (5000 fold of day1) being detected on day 4, corresponding to cell lysis.

4.3 Summary

In this study, different aspects of the cellular response were monitored with the progress of ColoAd1 oncolysis, compared with the oncolysis of Ad5 and Ad11 as well as treatment with Cisplatin and H_2O_2. The targets investigated included morphology, cytoplasmic membrane permeability, expression levels of key enzymes, intracellular ATP and Ca^{2+} levels, degree of cellular DNA damage as well as release of progeny virions from cells. The most dramatic changes of cellular behaviour always coincided with the onset of viral oncolysis or cell death, whereas there was relatively little change during early infection. The cell killing mediated by the three Adenoviruses shared certain common features, distinct from Cisplatin-induced apoptosis but more similar to necrosis induced by H_2O_2. When cells were treated with equi-cytotoxic doses (ColoAd1 10 PPC, Ad11 25 PPC and Ad5 100 PPC), ColoAd1 oncolysis elicited the most dramatic cellular damages. Ad11 showed generally similar effects, and the cytotoxicity mediated by these two group B adenoviruses appeared similar to necrosis; in contrast, Ad5 oncolysis has milder effects on cell biology and showed some signs of apoptosis.

During ColoAd1 oncolysis, the dying cells demonstrated characteristic necrotic features, including falling intracellular ATP and rising Ca^{2+} levels, PARP activation, early leakage of the cytoplasmic membrane (PI+ staining), violent blebbing of the cell membrane with robust release of intracellular contents, including progeny virus,

HSP70 and HMGB1 (investigated in Chapter 6). On the other hand, these cells did not display typical apoptosis features, such as Caspase activation and PARP cleavage, no pure PS externalization (Annexin V+/PI- staining), few apoptotic bodies, no cellular DNA fragmentation as well as low SubG1 percentage in the whole cell population. However, oncolysis in these cells was accompanied with cytoplasmic shrinkage and increased granularity instead of swelling of the cell and cellular organelles, regarded as typical feature of necrosis.

On the contrary, cells dying from Ad5 oncolysis did not display these features associated with necrosis. Studied by optical microscopy, during early infection the cells appeared slightly larger than ColoAd1 and Ad11 infected cells but during oncolysis they soon shrink to a small size; intracellular ATP levels only fall during terminal cell death; PARP is not overactivated with p53 degradation.; cytoplasm permeability occurs only at a very late stage and consequently the release of intracellular contents is inefficient. However, in agreement with previous reports, the dying cells also lack the signs typical of apoptosis - no DNA fragmentation and a minor subG1 percentage presence, no caspase 3 activation and no PARP degradation. Lastly, there was no evidence in our study of autophagic cell death following treatment with Ad5.

Ad11 and ColoAd1 mediated oncolysis with several common features - they show similar effects on expression of PARP and p53 as well as increased LC3II (possibly indicating raised level of autophagy). However we also found minor differences, for example Ad11 appeared to induce cell permeability by primary necrosis less than ColoAd1, additionally the level of intracellular ATP fell later during oncolysis.

It is noteworthy that all three adenoviruses shared similar effects on inducing cellular DNA damage responses during oncolysis. Replication of the three viruses all led to disruption of the host cell cycle, loss of the G0/G1 checkpoint and abrogation of G1 phase. The measurement of DNA damage response correlated well with the cytotoxicity study in Chapter 3. It is clear that different adenoviruses kill cells in slightly different ways, and the following chapter will evaluate in more detail the virus-induced mechanisms of cytotoxicity.

Chapter 5:

Cell Death Pathway Inhibition and Oncolysis

5.1 Introduction

The key enzymes involved in the different cellular death pathways usually include: Caspase, PARP, RIP1, P13K, Calpain, Cathepsins and Rho kinase. Synthetic inhibitors of these enzymes can be useful tools for elucidating the cell death mechanisms.

Members of the caspase family of proteases form the core engine of apoptosis and are involved in the initiation, execution and regulatory phase of the pathway. zVAD-fmk (carbobenzoxy-valyl-alanyl-aspartyl-[O-methyl]- fluoromethylketone) is a wide used cell-permeable pan caspase inhibitor; it irreversibly binds to the catalytic site of caspase proteases and thus inhibits induction of apoptosis. To avoid any additional cytotoxic effects, its effective concentration in vitro has normally been in the range of 20-100μM (Arnoult, Karbowski et al. 2003). Inhibitors that target the individual caspases are also commercial available. Ivachtin is a potent, reversible inhibitor of caspase-3 (IC_{50} = 23 nM) that displays moderate selectivity over other caspases and exhibits a higher level of protection than zVAD-fmk (Kravchenko, Kuzovkova et al. 2005).

Poly(ADP-ribose) polymerase (PARP) is a nuclear enzyme which plays an important role in DNA repair and is involved in programmed cell death. When activated by DNA strand breaks, PARP cleaves NAD+ into nicotinamide and ADP ribose, and catalyzes the formation of poly-ADP ribose (PAR) polymers. Recently, it has been recognized that PARP is at the junction of different death pathways, so that the cells exposed to DNA damaging agents could enter either apoptosis or necrosis, depending on the degree of DNA damage. Apart from investigating the role of PARP

in the biological process of DNA damage and repair, numerous PARP inhibitors have been developed to try and overcome DNA repair-mediated resistance of cancer cells to cytotoxic therapy. The anti-proliferation agent 3-Aminobenzamide (3ABA) is a potent cell permeable prototypical inhibitor widely used in experiments (Waters, Ramsay et al. 1982). 3ABA has been reported to effectively protect the cells from necrotic death induced by H_2O_2 and asbestos, and the concentration working range for 3ABA is 1-10 mM (Nanavaty, Pawliczak et al. 2002; Yang, Rivera et al. 2010).

Programmed necrosis, so called "necroptosis", has been recognized as an important alternative programmed cell death pathway which plays a role in many human pathologies including viral infections. Although similar to apoptosis in that it occurs under highly regulated conditions, the cell morphology of necroptosis is very similar to that of necrosis. One distinguishing feature is the involvement of the serine/threonine kinase activity of the receptor-interacting protein 1 (RIP1), and necroptosis is also known as "RIP1 dependent programmed cell death". The small molecular compounds called Necrostatins, particularly Necrostatin-1, are potent RIP1 inhibitors and they can protect the cells from necroptosis. Necrostatin-1 was shown to inhibit RIP1 kinase in a T-loop-dependent manner, binding preferentially to and stabilizing the inactive conformation of RIP1 kinase, thereby shifting the equilibrium toward the inactive state (Degterev, Hitomi et al. 2008). The working concentration of necrostatin-1 normally is in the range of 20-100 μM.

Autophagic cell death is characterized by a massive accumulation of double-membrane containing vacuoles known as autophagosomes, which subsequently fuse with lysosome vacuoles. The class III phosphoinositide-3 kinase (P13K) plays a

central role in regulation of autophagy while 3-methyladenine (3MA), the P13K inhibitor, can block early autophagocytic signalling, inhibit autophagy-dependent protein degradation and suppress autophagosome formation. Therefore 3MA has been used as a selective and potent autophagy inhibitor (Ito, Koshikawa et al. 2007). The effective concentration is commonly used as 1-10 mM.

Due to the significantly increased intracellular Ca^{2+} level observed during ColoAd1 oncolysis, the effects of Ca^{2+} related protease inhibitors were also investigated in this study. The lysosomal enzymes, cathepsin and the other cytoplasmic Ca^{2+}-dependent enzyme calpain, are well characterized cysteine proteinases found in mammalian cells. Both of the enzymes normally contribute in protein turnover and cytoskeleton modification, but they also play an important role as the alternatives of caspases to cellular degradation in cell death events, especially in necrosis (Yamashima 2004). MDL 28170 and Calpeptin were chosen as candidate inhibitors. The former is a potent, selective inhibitor of calpain and cathepsin B and the latter is the specific inhibitor of calpain. In addition, the effects on virus toxicity of manipulation using the Ca^{2+} channel blocker Verapamil and Ca^{2+} chelation and also studied in this chapter.

The adenovirus Ad5 early region 4 ORF4 protein (E4orf4) was reported to trigger a novel death program that bypasses classical apoptosis pathways in human cancer cells (Robert, Smadja-Lamere et al. 2006). In this case, the cells show blebbing, nuclear shrinkage and deregulation of cytoskeleton which is similar to apoptosis. However, activation of the Rho GTPases, instead of caspases, is required for the cell death induction. The small GTPases RhoA, Cdc42 and Rac1 are the most studied Rho family members, and they control morphology, motility and vesicle trafficking

via dynamics of the actin cytoskeleton. One of the best characterized ROCK inhibitors, Y-27632, selectively targets p160ROCK from the family of Rho associated protein kinases (Ishizaki, Uehata et al. 2000). The concentration normally applied to inhibit overexpressed E4orf4 is 10μM. It is worthy to note that the E4 region of Ad11 possesses all the ORFs that appear in Ad5 E4, however, the amino acid identity of E4orf4 between Ad11 and Ad5 is only 44.3%; in addition, ColoAd1 has a disrupted E4orf4 region with 24bp deletion. Whether the E4orf4 induced apoptosis-like cell death mechanism contributes to the oncolysis of ColoAd1 and Ad11 is unknown, and this was investigated in this chapter using Y27632.

In this study, a panel of synthetic inhibitors mentioned above were used to investigate the possible key enzymes or proteins involved in adenovirus oncolysis. The specific blocking effect would reflect the different cellular pathways used during oncolysis and therefore indicate the related death mechanisms. The inhibitors impact was mainly measured by MTS cell viability assay in this study; more characterizations were carried out by coupling with other assays to determine killing kinetics, cell cycle analysis, plasma membrane permeability, viral genome replication and release. The impact of the some inhibitors on viral transduction has also been investigated.

5.2 Results

5.2.1 The impact of inhibitors on virus cytotoxicity

5.2.1.1 PARP inhibition

Contrary to initial expectations, the PARP inhibitor 3-ABA demonstrated a significantly reduced cytotoxicity on all three virus incubated with A549 cells at a

wide viral infection doses (ColoAd1 PPC4-100, Ad11 PPC 0.8 -100, Ad5 PPC50-250, Fig 5.1 A-C). The most significant inhibition was on oncolysis of Ad11, followed by ColoAd1, using 5mM 3-ABA. 3-ABA showed similar protection against the cytotoxicity of H_2O_2 (Fig 5.1D), whilst it did not show any protection against Cisplatin (Fig 5.1 E). With Cisplatin, on the contrary, 3-ABA led to enhanced cytotoxicity.

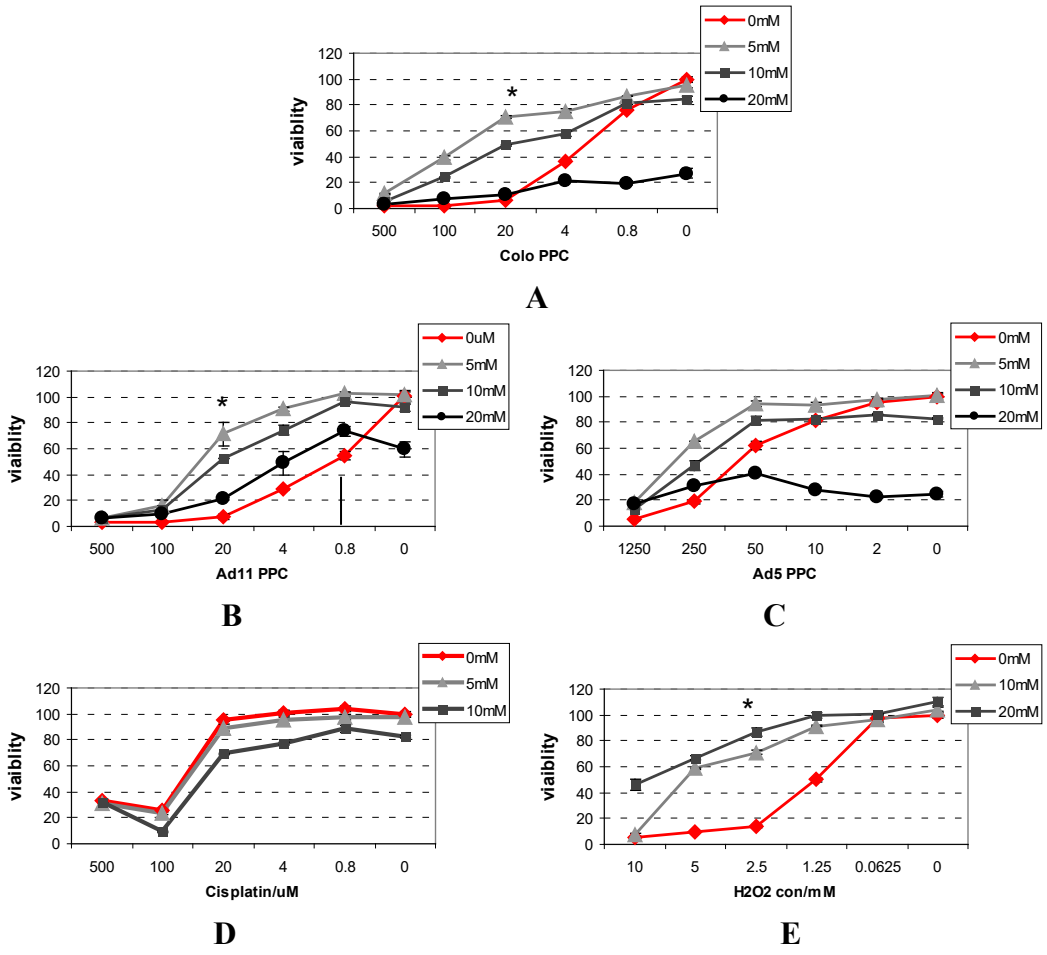


Fig 5.1 The effects of PARP inhibitor 3-ABA on various cytotoxic agents measured by MTS cell proliferation assay. A549 cells were exposed to 5 days incubation for all viruses infections, 2 days incubation for Cisplatin treatment and 6 hours incubation for H_2O_2 treatment. The inhibitor was added 1hour before viral infection or treatment with the reagents at the concentrations indicated. Mean data are presented ± SD, *n* =3. Statistical differences between two groups were determined using Student's t-test. A: ColoAd1; B: Ad11; C: Ad5; D: Cisplatin; E: H_2O_2. The units of Y axis (Viability) represent the percentage of viable cells to control cells, the same in the below figures.

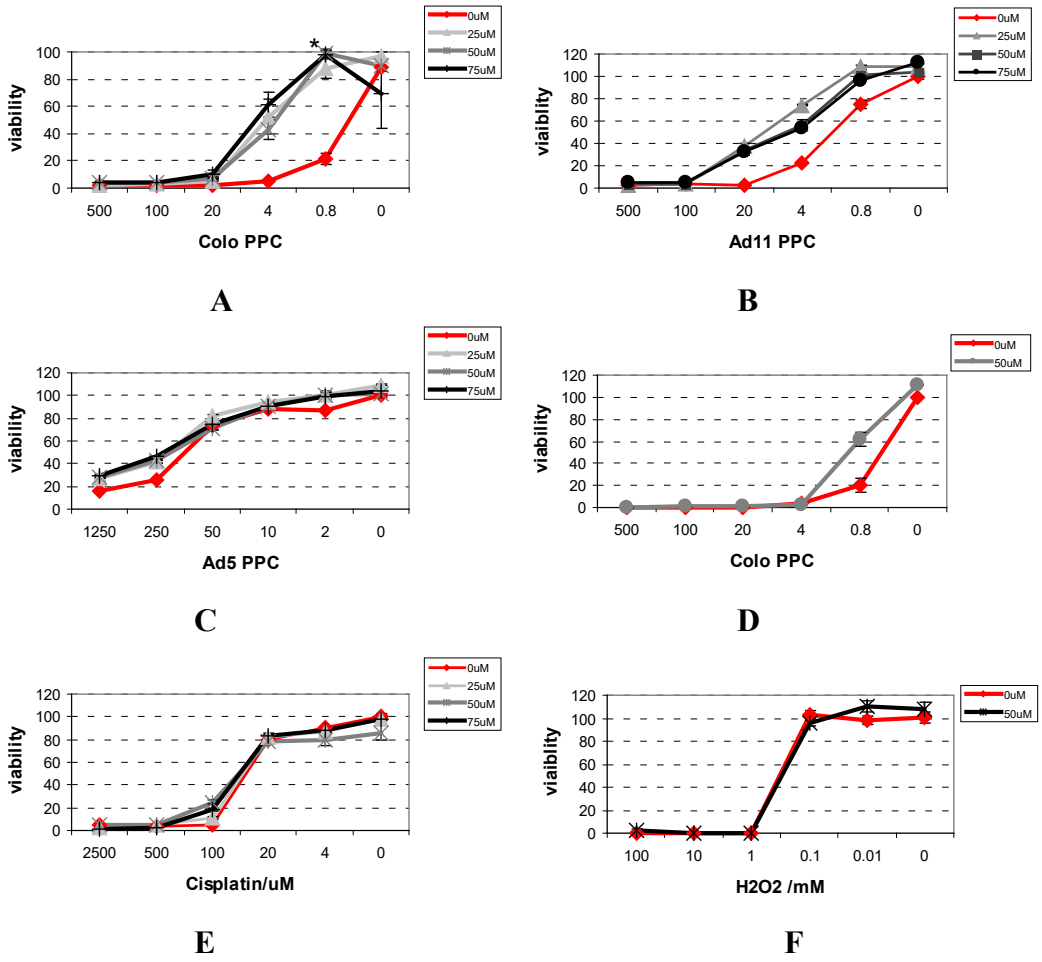


Fig 5.2 The inhibitory effects of RIP1 inhibitor necrostatins on various cytotoxic agents, assessed by MTS cell viability assay. The conditions used are the same as Fig 5.1, only the inhibitor concentrations are different and shown on the graphs. The inhibitors were added 1 hour before viral infection or the reagent treatments. In A-F necrostatin-1 was used, except in D necrostatin-5 was used. Mean data ± SD are presented, *n* =3. Statistical differences between two groups were determined using Student's t-test. A: ColoAd1; B: Ad11; C: Ad5; D: ColoAd1; E: Cisplatin; F: H_2O_2.

5.2.1.2 RIP1 inhibition

Necrostatins also provided significant protection against the cytotoxicity of ColoAd1 and Ad11, whereas they did not show noticeable impact against Ad5 oncolysis (Fig 5.2 A-C respectively), and no effect on Cisplatin (Fig 5.2 E) and H_2O_2 (Fig 5.2 F) treatment either. The effective concentration for necrostatin-1 was as low as 25 µM which reduced the ColoAd1 cytotoxicity from PPC 20-0.8. There was little further

protection when the concentration of the inhibitor was increased. Another necroptosis inhibitor, Necrostatin-5, which inhibits RIP1 kinase indirectly, was observed to have less protection than necrostatin-1 (Fig5.2 D).

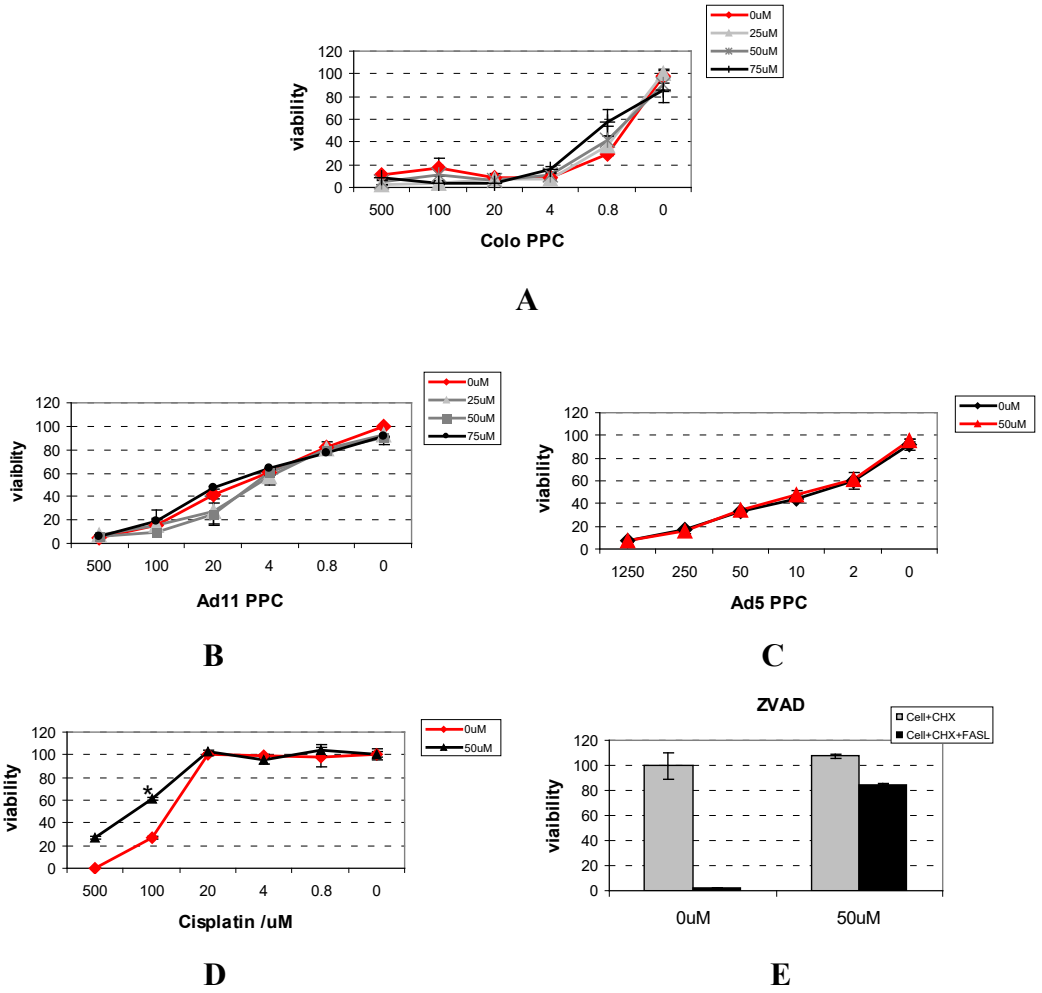


Fig 5.3 The inhibitory effects of Caspase inhibitor zVAD-fmk on cytotoxicity of various agents, assessed by MTS cell viability assay. The conditions used are the same as Fig 5.1, only the inhibitor concentrations are different and shown in the figure legend. The inhibitors were added 1 hour before the virus or drugs treatment. A. ColoAd1 B. Ad11; C: Ad5; D: Cisplatin; E: FASL and CHX. Cells were treated with 25 ng of anti-Fas activating antibody (clone CH11, Millipore,UK.)/ml together with 0.5 µg of cycloheximide (CHX; Sigma, UK.)/ml for 12 hour (Abou El Hassan, van der Meulen-Muileman et al. 2004). Mean data ± SD are presented, *n* =3. Statistical differences between two groups were determined using Student's t-test. * = $p < 0.05$

5.2.1.3 Caspase inhibition

Caspase inhibitors ZVAD-FMK (Fig 5.3 A-D) and Ivachtin (data not shown) were found to give only a limited protection against ColoAd1, Ad11 and Ad5 cytotoxicity, while they showed a greater effect on reducing the toxicity of Cisplatin (Fig 5.3 E). The incomplete protection against cisplatin may mean that caspase inhibition was not complete, or that Cisplatin killing of A549 cells involves a component of caspase-independent apoptotic pathway. FASL+ CHX was used to verify the efficacy of zVAD-fmk and demonstrated it is able to inhibit apoptosis by up to 80% (Fig 5.3 F). zVAD-fmk tested in the experiments were from two independent commercial suppliers (Tocris and Promega, UK), but both gave similar results.

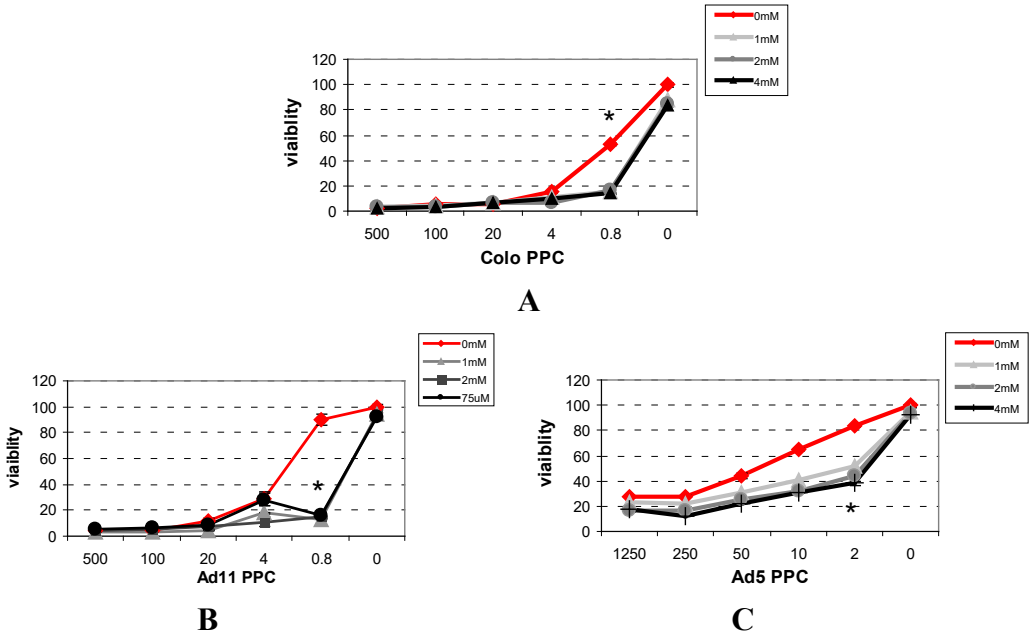


Fig 5.4 The effects of autophagy inhibitor 3-MA on virus-mediated killing after 5 days MTS cell proliferation assay. The inhibitors were added in at 16 hours post viral infections. The conditions used are the same as Fig 5.1, only the inhibitors concentrations were used different and shown on each graph. A: ColoAd1; B: Ad11; C: Ad5. Mean data ± SD are presented, *n* =3. Statistical differences between two groups were determined using Student's t-test. * = $p < 0.05$

5.2.1.4 Autophagy inhibition

Autophagy inhibitor 3-MA was found to have a synergistic effect by promoting cytotoxicity of the three viruses rather than protecting cells against it. The enhanced effect was consistent over the concentration range of 1-4 mM that was tested, as seen from Fig 5.4.

5.2.1.5 E4orf4 inhibition

Rho kinase inhibitor Y-27632 was found to protect Ad5 killing (Fig 5.5 B) with 25 μM of the inhibitor showing a wide protection range from 0.8 -100 PPC for Ad5. Surprisingly, inhibitory-27632 was not able to protect from killing by ColoAd1 or Ad11, on the contrary for Ad11 it even enhanced cell killing (Fig 5.5C).

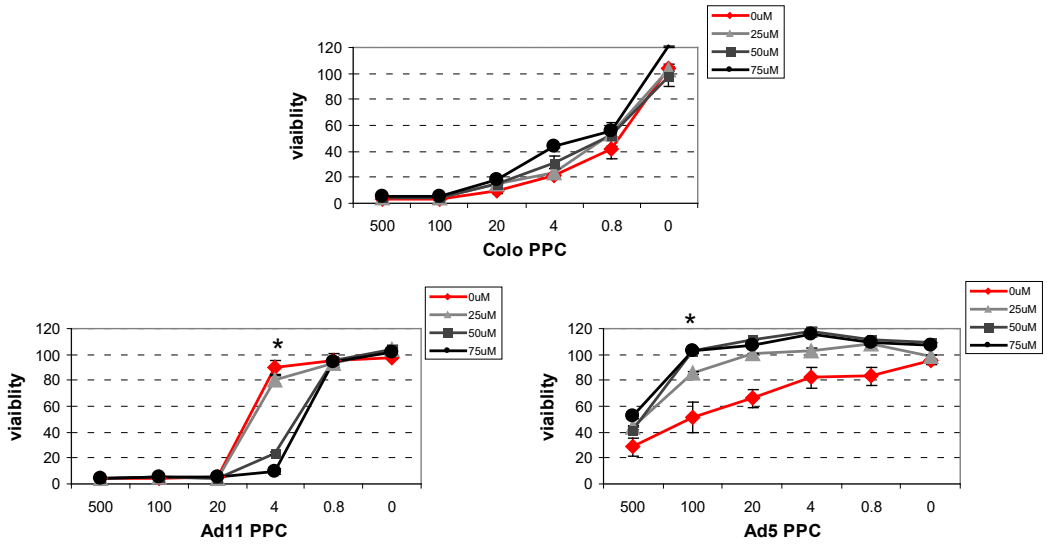


Fig 5.5 The E4orf4 inhibition effects of Rho kinase inhibitor Y27632 on viral killing after 5 days MTS cell proliferation assay. The inhibitors were added in at 2 hour post of infection. The conditions used were the same as Fig 5.1, only the inhibitor concentrations were different and shown in the graphs. A: ColoAd1; B: Ad11; C: Ad5. Mean data ± SD are presented, *n* =3. Statistical differences between two groups were determined using Student's t-test. * = $p < 0.05$

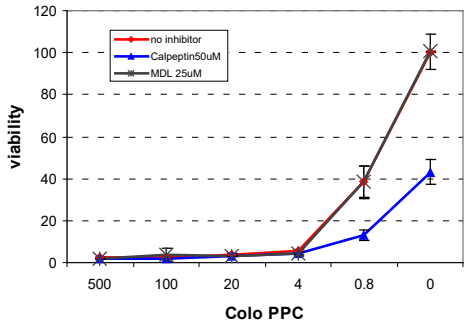


Fig 5.6 The effects of Calpain and cathepsin inhibitors Calpeptin and MDL on ColoAd1 killing. Viability was assessed using the MTS cell viability assay after 5 days. The inhibitors were added at 2 days post of infection. The other conditions used were the same as Fig 5.1, only the inhibitors concentrations were different and shown on the graph. Mean data ± SD are presented, *n* =3.

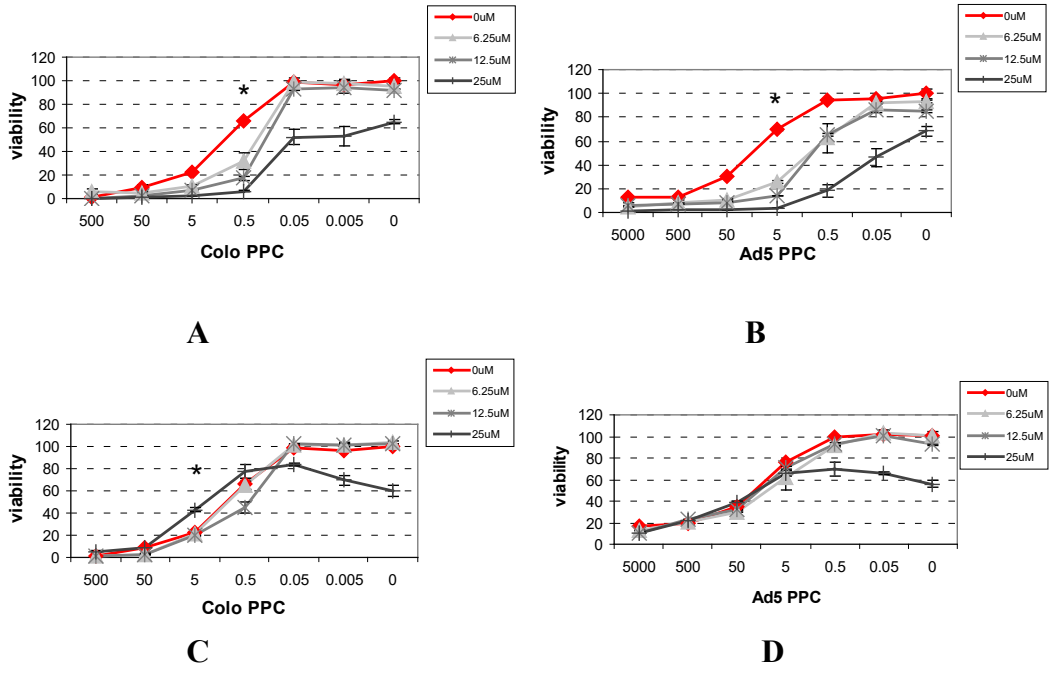


Fig 5.7 Impact of Ca^{2+} blocker verapamil and chelator BAPTA on virus-mediated killing. A. verapamil with ColoAd1; B. verapamil with Ad5; C. BAPTA with ColoAd1; D. BAPTA with Ad5. The concentrations of verapamil and BAPTA are shown on the graphs; the reagents were added 1 hour before viral infection. Other conditions are the same as described in Fig 5.1. Mean data ± SD are presented, *n* =3.Statistical differences between two groups were determined using a two sample Student's t-test. * = $p < 0.05$

5.2.1.6 Calpain and Cathepsin inhibition

Neither Calpain inhibitor Calpeptin nor Cathepsin inhibitor MDL showed protection against virus-mediated cell death. MDL did not affect ColoAd1 killing or cell proliferation; similarly Calpeptin failed to protect and even showed additional cytotoxicity in 5 days incubation (Fig5.6).

5.2.1.7 Manipulation of intracellular Ca^{2+}

Ca^{2+} channel blocker verapamil has been recently reported to enhance Ad5 killing by facilitating virus release without affecting replication (Gros, Puig et al. 2010). We also observed this synergy in killing by ColoAd1, however, the degree of enhancement was much lower than that of Ad5: for Ad5 the IC50 was decreased ten-fold whereas for ColoAd1, the reduction of IC50 is only about 3-fold (Fig5.7 A,B). Interestingly when the Ca^{2+} chelator BAPTA was applied to virus killing anticipated to antagonise cytotoxicity, we saw only slightly reduced toxicity with ColoAd1 and nothing with Ad5 (Fig 5.7 C, D).

5.2.2 Effects of inhibitors on the kinetics of virus cytotoxicity

The effects of the inhibitors on the kinetics of virus cytotoxicity were assessed with ColoAd1 at low PPC (PPC2), with viability measured after up to 7 days, As can be seen from Fig5.8, ColoAd1 (alone) started killing from day 3 even at PPC2, and the inhibitors showed protection from cytotoxicity in the order of : Necrostatin ≥ 3-ABA> Y27632 > zVAD-fmk > Ivachtin. It is notable that the inhibitors only delayed cell death and were unable to keep cells alive in the long term.

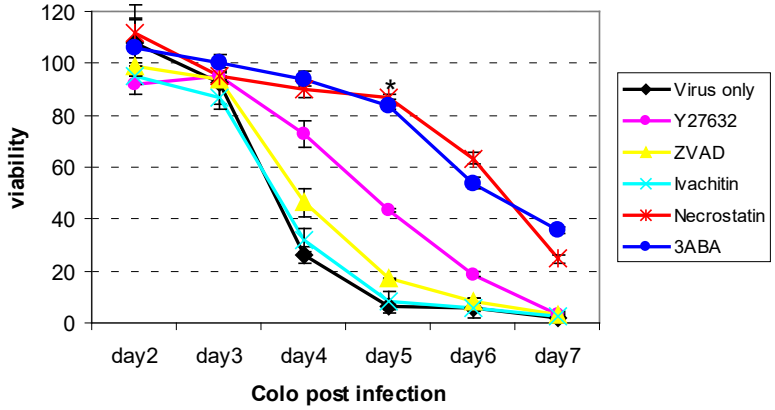


Fig 5.8 Time course study to compare the impact of the inhibitors on the timescale of ColoAd1 killing by MTS assay at PPC 2. Inhibitors concentrations were applied as: zVAD-fmk 100 μM, Ivachtin 50 μM, Necrostatin-1 50 μM, 3ABA 5mM,Y27632 50μM. Rho kinase inhibitor Y27632 was added in 2 hour after viral infection, and the other inhibitors were added 1 hour before viral infection**.** Mean data ± SD are presented, *n* =3. Statistical differences between the groups were determined using one way ANOVA. * = $p < 0.05$

The effects of the inhibitors on virus-induced changes in cell morphology were also recorded after 5 days treatment. As seen in Fig 5.9, ColoAd1 treatment caused noticeable shrinkage of the cytoplasm and cell death by this time, and VAD failed to show any protection. In contrast, Necrostatin showed good protection, with cells displaying larger morphology and slight swelling (perhaps reflecting that they were full packed with progeny virions). The Rho kinase inhibitor Y27632 had a dramatic influence on the cell cytoskeleton and the appearance of the cells was totally changed, with a portion of the cells remaining swollen and apparently viable. The PARP inhibitor-treated cells were slightly shrunken (possibly due to cells becoming rounded up as they detach from the plate) with more floating cells, so that the cells density appeared to be reduced; however the high MTS reading suggested that cell

proliferation and mitochondria activity were maintained in the presence of the inhibitor and therefore that cells remained viable.

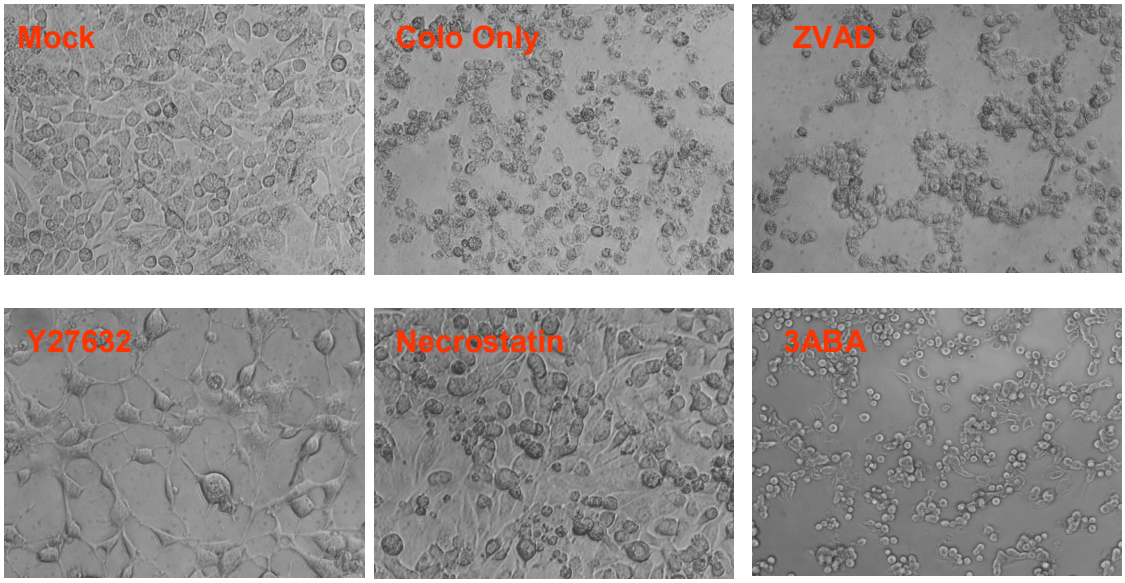


Fig 5.9 Optical microscopy images showing the effect of inhibitors on morphological changes induced by ColoAd1. A549 cells were treated as described in the legend to Fig 5.8, and photographed 5 days after addition of ColoAd1 (with a magnification of X10).

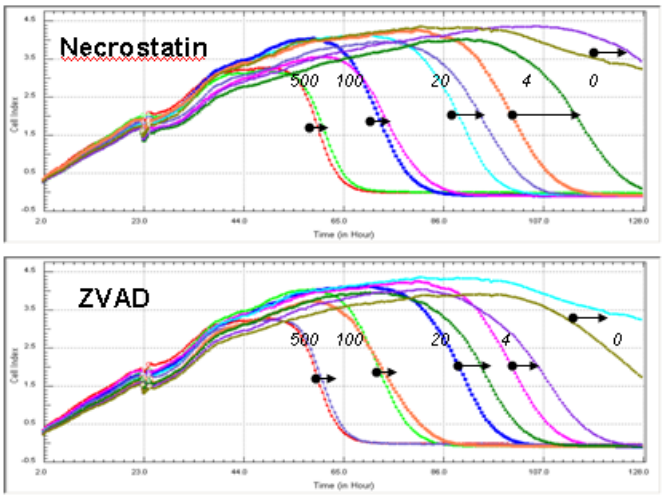


Fig 5.10 Effects of necrostatin and zVAD-fmk on the cytotoxicity of ColoAd1 on A549 cells, assessed using xCelligence. Necrostatin was used at 50 μM and zVAD-fmk was used at 100 μM. The infection doses of ColoAd1 were used at 500, 100, 20, 4 and 0 PPC respectively. The arrows indicate the changes in individual cytotoxicity curves (at set virus levels) in the presence of the inhibitors.

Additional kinetic studies were performed using the xCelligence cell monitor to assess the inhibitory effect of Necrostatin and zVAD-fmk on the cytotoxicity of ColoAd1. These studies showed that the greatest protection of Necrostatin occurs at the low viral infection dose, such as PPC 4, and no protection was observed at high doses such as PPC 100. Any protection effect from apoptosis inhibitor zVAD-fmk was weaker and also restricted to low PPC.

5.2.3 Impact of the inhibitors on replication and genome production of ColoAd1

Genomic replication of ColoAd1 genome was strongly affected by the different inhibitors (Fig 5.11.A and B). the data were coupled to the cytotoxicity study in Fig 5.8). Treatment with Necrostatin-1 slightly decreases virus replication before day 4 following infection, then the genome copy number rose steadily until reaching 3 fold of the control. This agrees with the delay in the cell death by Necrostatin-1, allowing cells to survive longer and more virions to be produced. In contrast, the Rho kinase inhibitor greatly reduced and slowed down viral replication despite keeping the cells alive. zVAD-fmk also increased virus production initially although the effect was lost after day 5. When the virion levels in the supernatant and the cells parts were analysed separately (Fig 5.11 B and C), it was found that the virus release profile was greatly modified by Necrostatin-1, which functioned to keep the virus mostly cell-associated rather than being released early into the supernatant.

5.2.4 Impact of the inhibitors on cellular uptake of ColoAd1

To assess whether the effects of the inhibitors included differential uptake of virus particles into cells, uptake of ColoAd1 was examined in short term experiments.

Here we examined the effects of Necrostatin-1, 3ABA and zVAD-fmk, all administered 1 hour before virus infection.

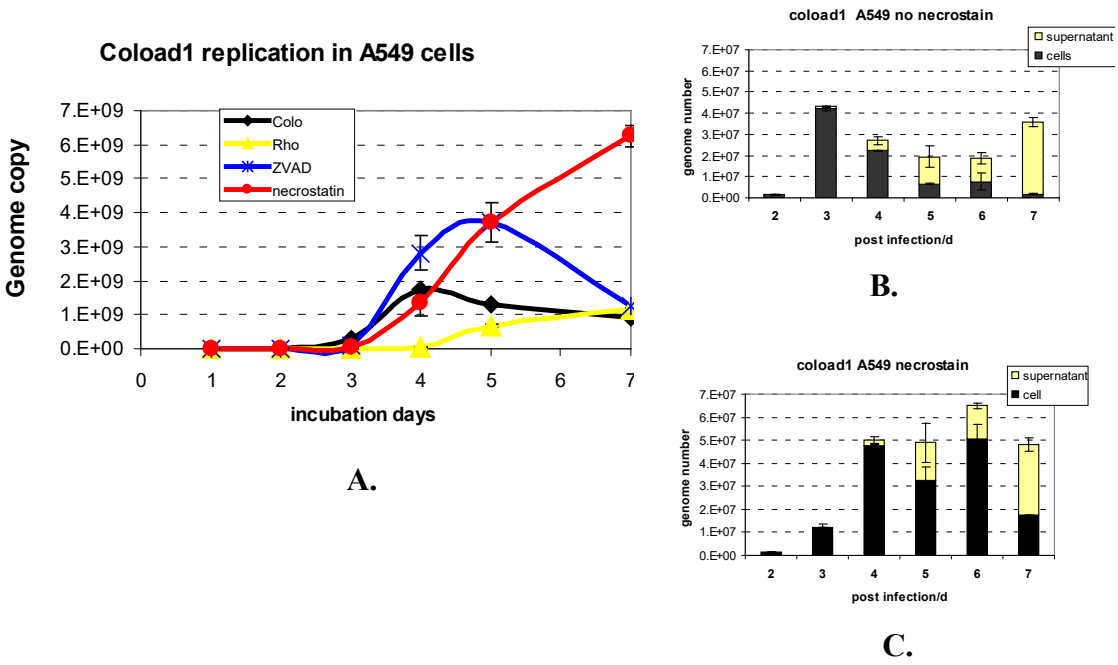


Fig 5.11 QPCR analysis to measure replication of ColoAd1 in the presence of different inhibitors (A) and genome distribution between cells and supernatant (B and C). The viral dose of infection was PPC 2 with inhibitors used at the same concentrations as described in the legend to Fig 5.8. The viability of the virus- infected cells was measured by MTS assay, then the supernatant and cells were stored separately. A. Total viral genomes produced by 10000 cells/ well in 96 well plate. The supernatant and the cells part were pooled, lysed together for DNA extraction and QPCR analysis, the data present whole genome copies for the well. B. The viral replication without Necrostatin-1. C. The viral replication with Necrostatin-1. In B and C, the supernatant and the cells part DNA were separately processed, the data presented refer to the genome in QPCR sample (5 out of 200ul). Mean data ± SD are presented, *n* =3.

As shown in Fig5.12, treatment of cells with Necrostatin-1 inhibited viral uptake by approximately 20% compared to control, whereas the PARP inhibitor and apoptosis inhibitor zVAD-fmk both did not affect the virus uptake significantly (P value >0.05).

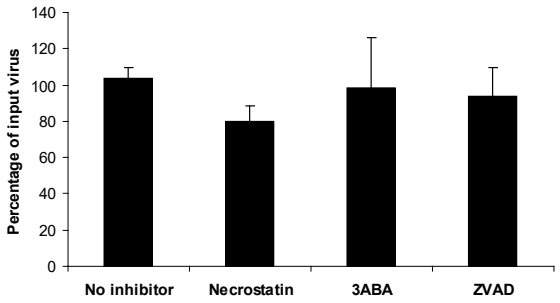


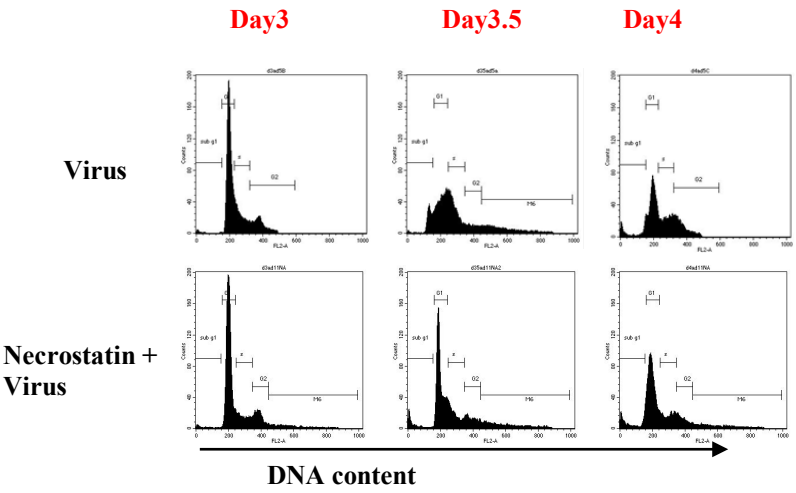
Fig5.12 The effects of the inhibitors on cellular uptake of ColoAd1 particles in A549 cells. The infection dose used is 100 PPC. The inhibitors (Necrostatin-1 50 μM, 3ABA 1mM and zVAD-fmk 100 μM) were added 2 hours before virus infection. The supernatant was removed at 6 hours post of infection, the cells washed with PBS and lysed before DNA extraction. The viral genome copies were measured by QPCR. The data presented are the percentage of input virus copies; Mean data ± SD are presented, *n* =3.

5.2.5 Effects of Necrostatin-1 on cellular features of ColoAd1 oncolysis

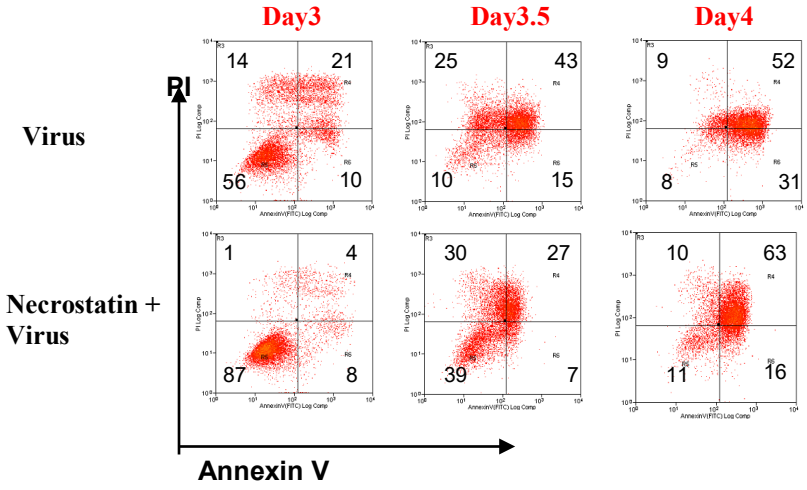
Necrostatin-1 appears to inhibit ColoAd1-mediated cytotoxicity and retains virions inside the cell for longer, allowing increased virion production. To better understand precisely how it is working its effects were studied on key features of ColoAd1 oncolysis , including cell cycle distribution, cell membrane permeability, and intracellular ATP and Ca^{2+} level.

As shown in Fig 5.13 A, Necrostatin-1 had a protective effect on ColoAd1 induced cell cycle disruption. In the presence of this inhibitor, the shape of the DNA histogram was largely conserved to normal even under conditions of complete cell death. Most notably the G1 phase peak was maintained by Necrostatin-1, whereas this peak almost disappeared in cells treated with virus only at day 3.5 post infection. A slightly increased percentage of subG1 was also observed.

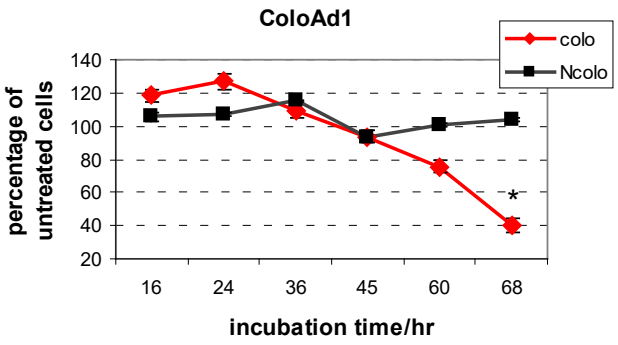
Flow cytometric analysis of Annexin V/PI staining (Fig 5.13 B) in the same cells showed that inclusion of Necrostatin-1 reduced the dying cells number and decreased leakage of the cytoplasmic membrane on day 3, with less PI staining.



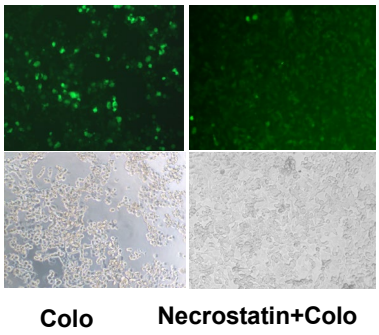
A. DNA histogram



B. Annexin V/PI stain



C. Intracellular ATP level



D. Intracellular Ca^{2+} level

Fig5.13 The impact of Necrostatin-1 on cellular features of ColoAd1 oncolysis. Necrostatin-1 at 50μM was used to treat A549 cells 1 hour before infection. ColoAd1 at PPC 10 was then used to infect the cells. The cells were harvested at the specific time for cell cycle analysis. Annexin V/ PI stain, and measurement of intracellular ATP level and Ca^{2+} level were carried out by directly staining the cells in the well. The green florescence signal in picture D refers to the increased intracellular ATP level and pictures were taken at day 3 post of infection. Statistical differences between two groups were determined using Student's t-test.

Necrostatin-1 also decreased cell death (showing as significantly reduced percentage of stained cells). The protection lasted until day 3.5. In addition, Necrostatin-1 appeared to change the mode of cell death. Instead of changing to an apoptotic pattern, the staining of cells was enriched for the secondary necrosis pattern; furthermore, the primary necrosis signals nearly disappeared in the presence of Necrostatin-1.

As shown in Fig 5.13 C and D, Necrostatin-1 inhibited viral-induced fall of cellular ATP and Ca^{2+} increase. This suggests that Necrostatin-1 probably works as a scavenger to minimize the cellular stress.

5.3 Discussion

Compared to standard chemotherapy drugs, understanding of the killing mechanisms underlying adenovirus mediated oncolysis are far more limited. Most previous research has focused on the virology aspects of these agents, whilst paying much less attention to cellular aspects that are involved in the killing and the mechanisms that are manipulated by the virus. Building on observations in chapter 4, including observations of cellular changes caused by viral oncolysis and the necrotic nature of ColoAd1 cytotoxicity, this chapter used specific inhibitors to dissect which cellular

death pathways are involved in adenovirus mediated oncolysis, specifically aiming to shed some light on the ColoAd1 killing mechanism.

5.3.1 Cytotoxic mechanisms of Cisplatin and H_2O_2

Throughout the studies in this thesis, Cisplatin and H_2O_2 treated A549 cells were used as the apoptosis and necrosis controls, respectively. Cisplatin and its derivatives are among the most active antitumor agents used in human chemotherapy, particularly in testicular, lung and ovarian cancers. Acquired resistance and toxicities associated with treatment are the major impediments inhibiting their efficacy (St Germain, Niknejad et al. 2010). The reagent is primarily considered as DNA-damaging anticancer drug, forming different types of bi-functional adducts in reaction with cellular DNA. The final cellular outcome of DNA adduct formation is generally apoptotic cell death (particularly induction of the intrinsic/mitochondria type apoptosis), which is thought to occur through halting of cellular processes such as replication and transcription, and leading to cell cycle arrest and deregulation of signal transduction pathways. Two significant cellular pathways have been demonstrated to play key roles in Cisplatin-induced apoptosis/cytotoxicity. The first is the mitogen-activated protein kinase (MAPK) cascades, and the second is through the tumour suppressor p53. Among most studies in this thesis, Cisplatin treated A549 cells showed features that fit the hallmarks of apoptosis, such as typical apoptotic morphologies (cytoplasm shrinkage, nuclear shrinkage and fragmentation, apoptotic bodies formation), cytoplasmic membrane PS externalization, caspase 3 activation and PARP cleavage; in addition, the cytotoxicity can be certain blocked by Pan caspase inhibitor zVAD-fmk (Fig5.1D), but not be protected by PARP inhibition (Fig5.3D).

The exposure to H_2O_2 with the concentration more than 1mM caused acute cytotoxicity in A549 cells. Markers of apoptosis were not seen and the cytotoxicity appeared to be based on a necrosis mechanism. The death is due to DNA damage and loss of ATP, where PARP plays an important role in the death pathway. Contrary to the normal concept that necrosis is an uncontrolled process, inhibition of PARP was found to effectively protect the cell from death (Fig5.1E), which suggested that H_2O_2-induced necrosis belongs to a type of programmed cell death, and it is similar to asbestos induced necrosis in human mesothelial cells. Interestingly, RIP1 was not involved in H_2O_2 induced necrosis because the killing was not inhibited by Necrostatin-1 (Fig5.2F).

5.3.2 Adenovirus-mediated oncolysis is not apoptotic cell death

Based on the observations in Chapter 4, cell death induced by all three oncolytic adenoviruses did not display the typical hallmarks of apoptosis, which were evident in Cisplatin treated cells. In this chapter, both the Pan caspase inhibitor zVAD-fmk and the most potent caspase 3 specific inhibitor Ivachtin were found have minimal protection against virus induced cytotoxicities (Fig5.3A, B,C, Fig5.8, Fig5.9 and Fig5.10), indicating that caspases were not the main mediator involved in the adenoviruses death pathway.

This conclusion is consistent with previous reports, for example Hassan and co-authors showed in 2004 that Ad5 mutant (dl922-947) adenovirus kills tumour cells via a basic apoptotic machinery-independent mechanism, despite the classical apoptosis mechanism for adenovirus killing that had long been presumed (Abou El Hassan, van der Meulen-Muileman et al. 2004). Their results were soon further supported by McNeish group on ovarian cancer cells (Baird, Aerts et al. 2008).

5.3.3 Autophagy is not the main mechanism for Adenovirus killing

During the adenovirus infection (particularly for ColoAd1) the granularity of the host cell cytoplasm increased substantially over time (observed by time lapse microscopy), which may be related with formation and accumulation of a large number of autophagosomes. This was consistent with western blot data (Fig4.9), which showed the upregulation of LC3 bands at day3 time point. However, the ratio of LC3II/LC3I, the hallmark of autophagy, did not show significant increases compared to mock-treated cells. Moreover, the dominance of the LC3II band was commonly seen in many cell samples, even including Cisplatin treated cells, which could mean autophagy is a general consequence of stressed cells. Furthermore, the autophagy inhibitor 3MA was unable to protect from virus mediated oncolysis, instead it accelerated cell death (Fig 5.4). Taken together, the results imply autophagy is not the main mechanism for adenovirus oncolysis, rather it is probably a mechanism for cell survival in the presence of virus infection. This agrees with McNeish group's observation and opinion (Baird, Aerts et al. 2008) who pointed out that cells are also known to instigate autophagy as a defence mechanism in response to bacterial or viral infection.

However in 2006 Ito et al reported an oncolytic adenovirus regulated by the human telomerase reverse transcriptase promoter (hTERT-Ad) that induced autophagic cell death in malignant glioma cells (Ito, Aoki et al. 2006), and subsequently other Ad5 publications support the theory that autophagy play a major role in adenovirus-induced cell lysis (Jiang, White et al. 2008). Electron microscopy showed evidence that at the late stage after adenovirus infection, numerous autophagic vacuoles accompany the disruption of cellular structure leading to cell death. On one hand, co-treatment with 5mM 3-MA rescued 8% viral cytotoxicity; on the other hand, co-treat

with rapamycin, the autophagy inducer promoted an extra 8% killing. Interestingly, the results about the impact on virus genome replication and yield were varied: some reports showed that both 3MA and rapamycin do not affect viral titres, while other reports showed 3MA represses viral protein production and decrease virus titres, In contrast, rapamycin increased virus replication (Jiang, White et al. 2011; Rodriguez-Rocha, Gomez-Gutierrez et al. 2011).

We agree that ColoAd1 oncolysis is accompanied with significant autophagy, however the results based on the above studies need to be critically assessed. First, 3MA has a limited solubility and is hard to prepare the stock solution. It dissolves in DMF at a concentration of 60 mM and in 95% ethanol or 1N hot NaOH solution at up to 200 mM, while upon cooling it will precipitate from the solution, thus in order to get 5mM final concentration in the cell culture medium a large percentage of the organic solvent has to added in. This could interfere with the results. Second, even when a high concentration of 3MA (5mM) was used the protection on cell viability achieved was only 8%, and therefore this is a very limited effect. Third, 3MA even at 1mM concentration is likely to have many non-specific effects (Baird, Aerts et al. 2008). Overall, autophagy may not be the main cause of death but simply a cellular response to virus. Furthermore, autophagy could be one effector to contribute to cell death, which will discussed in the following paragraph.

5.3.4 E4orf4 and ADP are involved in killing by Ad5 but not by group B adenoviruses

ADP (E3.11.6) and E4orf4 proteins are both important factors in Ad5 mediated oncolysis. When expressed alone, E4orf4 induces p53 independent and caspase independent apoptosis, and ADP kills cell by a non apoptosis mechanism. It is noteworthy that group B adenovirus Ad11 has no equivalent ADP sequence in its

genome, and the sequence similarity of putative E4orf4 of Ad11 is only 44.3% of that of Ad5; in ColoAd1, the E4orf4 region has been disrupted by 24bp deletion, therefore neither gene product is expected to contribute to ColoAd1-mediated oncolysis.

The Rho kinase inhibitor Y27632 was able to protect from Ad5-mediated cytotoxicity below the viral dose range of 100 PPC, on the contrary it enhanced Ad11 cytotoxicity. Interestingly, the inhibitor has a minimal protection on ColoAd1 (Fig5.5). The diverse outcomes of the inhibitions may be due to the multiple impacts of the inhibitor on the cells. Rho kinase is involved in a wide range of fundamental cellular functions, such as contraction, adhesion, migration and proliferation. The changes brought about by Y27632 to the cell morphology and proliferations are dramatic, and were evident both by microscopy (Fig5.9) and by xCelligence cell monitor (see supplementary materials S7). On the virus aspect, the inhibitor remarkably reduced the virus replication (Fig5.11A), thereby delayed the cell death.

5.3.5 Adenovirus-mediated oncolysis involves necrosis and PARP activity

As evaluated in Chapter 4, oncolysis with the three viruses showed various degrees of necrosis. Among them, ColoAd1 demonstrated the strongest impact on early plasma membrane leakage and release of intracellular content, as well as PARP activation and increased intracellular Ca^{2+} levels. More importantly, ColoAd1 caused an early fall in intracellular ATP level, and this was not evident in the case of Ad11 and Ad5; in addition, the cellular DNA fragmentation was absent with ColoAd1.

Several oncolytic adenovirus studies have stated that oncolysis resembles necrosis-like programmed cell death rather than direct use of the term “necrosis”. By excluding apoptosis characteristics, Hassan concluded that dl922-947 induced

necrosis-like death on H460 and A549 cells without much detailed evidence (Abou El Hassan, van der Meulen-Muileman et al. 2004). Based on the same virus, Baird excluded both apoptosis and autophagy, but he also argued that this adenoviral cytotoxicity did not fit a purely necrotic profile, since no wholesale disruption of cellular membrane and organelles nor a reduction of ATP concentration were observed in their study (Baird, Aerts et al. 2008). The E1/E3–deleted recombinant Adenovirus AdYB-1 which expresses the human transcription factor YB-1 under CMV promoter control is another Adenovirus to have a necrosis-like oncolysis (Glockzin, Mantwill et al. 2006). The overexpression of YB-1 facilitated viral DNA replication (even without E1) and enhanced killing as well as viral extracellular release. The dying A549 cells displayed necrosis-like morphologies under EM. Based on these examples, there appears to be a possible correlation between efficient virus replication, high viral load, enhanced killing potency, sensitive cells and subsequently necrotic cell death. Therefore, based on our observation on both on the virology aspects of ColoAd1, its rapid cell killing and the profound cellular responses of ColoAd1 oncolysis, it is not surprising that it shows as more necrotic nature than other adenoviruses.

The oncolysis of three adenoviruses were accompanied with host cell cycle disruption and cellular DNA damage. The PARP inhibitor 3ABA exhibited the protection against the three viruses-mediated oncolysis, which is similar to the protection against H_2O_2 induced necrosis (Fig5.1 A,B,C,E). This observation suggests PARP, which is involved in DNA damage repair, might plays a role in adenovirus oncolysis. The abundant nuclear enzyme PARP has also been reported to participate in the life cycle of Simian virus 40, which was inhibitable by the same inhibitor 3ABA(Gordon-Shaag, Yosef et al. 2003). 3ABA did not affect the viral

infectivity and uptake, which has been evident in our results and agrees with SV 40 study. Interestingly, at the end of the infection stage, SV40 minor capsid protein VP3 stimulates PARP activity and leads the infected cell to a necrotic pathway, which was characterized by the loss of membrane integrity thus facilitating the virion release (Daniels, Rusan et al. 2006).

As for how adenovirus interact with PARP is completely unknown so far. The fate of cells at the death crossroad is largely dependent on the degree of PARP activation and intracellular ATP levels. Adenovirus replication causes cellular DNA damage, which consequently leads to PARP activation for DNA repair. The extensity of damage determines the PARP activation degree and corresponding reduction of ATP level. All these provide a reasonable background for ColoAd1 kill by necrosis.

A recent study revealed that the inactivation of cellular DNA damage response by adenoviruses is serotype dependent (Daniels, Rusan et al. 2006; Forrester, Sedgwick et al. 2011). Group B adenovirus such as Ad11 showed significantly different behaviour to Ad5. Ad5 facilitates the degradation of Mre11, DNA ligase IV and p53, through polyubiquitination of E1B55k and Ad5 E4of6. However, group B adenoviruses cause the remarkable accumulation of p53, nevertheless, there is no evidence of p53 induces apoptosis. More importantly the p53 increases is found not be transcriptional active. At the end stage of infection, no necessity is required to inactivate DNA damage response, on the contrary, the virus more likely to use the DNA damage response to effect kill of the host cells in order to release virions. It could be imagined the consequence of PARP activation to take effect at this point, and the different serotypes of adenovirus more likely to apply specific route to take advantage of the cellular response.

5.3.6 ColoAd1 oncolysis is necroptosis and RIP1 dependent

ColoAd1 and Ad11 showed significant positive signal responding to necroptosis inhibitors in cytotoxicity study (Fig 5.2 A,B, D), which is the direct evidence to link group B adenovirus oncolysis pathway with RIP1, by the mechanism named "necroptosis". In contrast, the impact of Necrostatin-1 on Ad5-mediated killing was minimal. In addition, necrostatin-1 did not exhibit any protection against the cytotoxicity of either Cisplatin or H_2O_2. These results reflect how different the cytotoxicity mechanism of group B adenoviruses is from those of other cytotoxicity reagents.

Apart from the rescue of the virus-mediated cytotoxicity and the delayed cell killing (Fig5.2A, Fig5.10), Necrostatin-1 exhibited multiple impacts on ColoAd1 behaviours. Necrostatin-1 slightly affected the viral uptakes (Fig5.12); it reduced the virus replication rate, however as the oncolysis was postponed, the final yield was then largely improved compared with the control cells without inhibitor (5-10 times, see Fig5.11A). Moreover, it changed the distribution of progeny virions and retained a higher percentage inside cells rather than released extracellularly (Fig5.11 B and C). Furthermore, it minimized the cellular stress including maintaining the intracellular ATP level and intracellular Ca^{2+} concentration as well as normal cell cycle check points (Fig 5.13 A,C,D). All these effects are largely due to the inhibition of oncolysis. The Annexin V/PI staining data further supported this conclusion (Fig5.13B), despite without showing the inhibition completely change death mode. Interestingly, the PI signal was more intense in the presence of Necrostatin-1, which is probably due to more virus DNA retained into the cytoplasm rather being extracellular released.

In fact, this is not the first time necroptosis is reported in related with virus induced cell death. Necroptosis is a form of programmed necrosis which is dependent on two related RIP receptor-interacting protein kinase 1 and 3. The importance of RIP1 as a crucial kinase at the crossroads where the cells choose to live and die has been gradually recognized. The main inducers of RIP1 include several stress signals such as inflammatory cytokines, pathogen infections and genotoxic stress (Cho, Challa et al. 2009). In particular, the RIP1-dependent necrotic pathway has emerged as a host defence mechanism against murine cytomegalovirus, VV and HSV-1 infection. Similarly, the Necrostatin-1 inhibition to the cytotoxicity of VV and HSV-1 on A549 cancer cells also were observed in this study (see supplementary data S8). The evidence of pathogen-associated molecular patterns (PAMP) as the initiation of necroptosis via PRRs (pathogen recognition receptor) have being rapidly accumulated since the concept of necroptosis was first introduced in 2005 (Vandenabeele, Galluzzi et al. 2010). From a cellular point of view, necroptotic cell death likely serves two functions: first, it acts as a backup mechanism to kill virus-infected cells if the apoptotic pathway is blocked; second, necroptosis may promote the release of intracellular danger associated molecular patterns, which act as endogenous adjuvant that boost the innate immune response. Therefore, an oncolytic virus like ColoAd1 that elicits a necroptotic death in tumour cells may have a complicity in its therapeutic applications, which are going to be discussed in chapter 6.

5.3.6 The execution of ColoAd1 oncolysis

The adenovirus oncolysis is not caspase-dependent, for group B adenovirus ADP and E4orf4 have both also been excluded. Then the question arises, what would be the

executor for the necroptosis induced by ColoAd1? So far, no firm answer has yet been found, largely because the execution of necroptosis itself is still remaining poorly defined.

The execution pathway of necroptosis largely overlaps with that of necrosis, which may present multiple channels such as ROS (reactive oxygen species) and RNS (nitric oxide) production, lipid peroxidation**.** Among these various factors, cytosolic ATP depletion and Ca^{2+} activated proteases calpain and cathepsin are the most likely candidates contributing for ColoAd1 oncolysis. The intracellular Ca^{2+} level increase was observed in ColoAd1 oncolysis, and the manipulation Ca^{2+} concentration by verapamil and BAPTA affected the viral killing to a certain degree (Fig5.7). These facts suggest that the ColoAd1 oncolysis is Ca^{2+} related, however more evidence is needed to support this hypothesis.

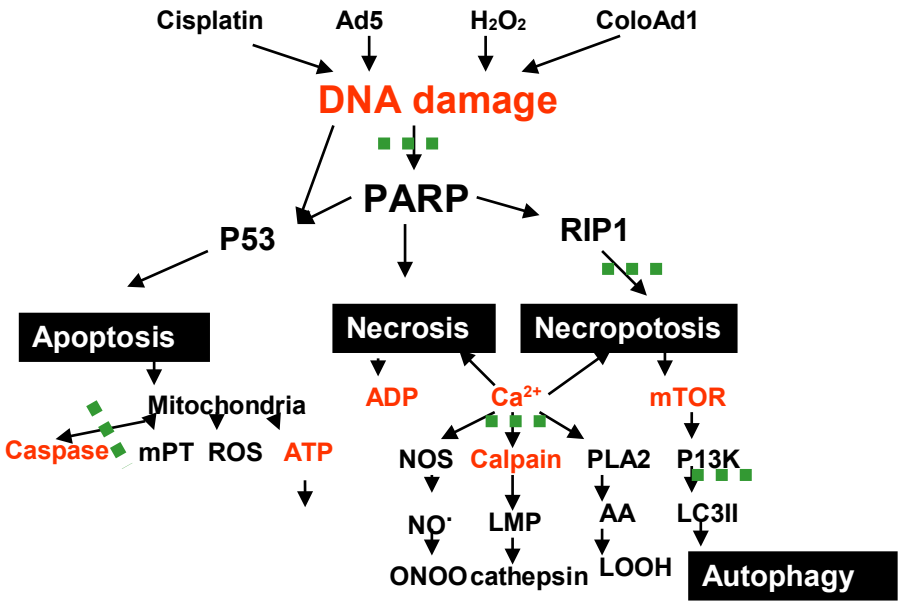


Fig5.14 The simplified cellular death pathways for different types of cytotoxic agents, including Cisplatin, H_2O_2, Ad5 and ColoAd1. The green dot line refers to blocking the pathway by the specific inhibitors.

It has been noted that autophagy may presents as an execution mechanism for ColoAd1 induced necroptosis. Similar to that seen in the cells undergoing oncolysis, autophagic vesicles are commonly observed in necroptotic cells(Xu and Zhang 2011). Necroptosis signalling may in fact activate autophagy, perhaps as a clean-up mechanism for cell death. There even is an opinion that type II autophagic cell death is actually necropotosis and induced by RIP1 activation (Christofferson and Yuan 2009).

5.3.7 The cellular pathway of ColoAd1 oncolysis

Based on the results and discussion above, we propose the possible cellular pathway of ColoAd1 induced cell death as demonstrated in Fig5.14.

As shown in Fig5.14, Cisplatin, H_2O_2, Ad5 and ColoAd1 all cause cellular DNA damages on A549 cells. However the treated cells have distinct fates depending on the degrees of PARP activation. Cisplatin induces apoptosis via p53 regulation and cell death is executed by caspases but the death pathway can be blocked by caspases inhibition. The cellular damage caused by H_2O_2, Ad5 and ColoAd1 leads to PARP over activation, which can be rescued by PARP inhibitor. However, ColoAd1 further initiates necroptosis via activating RIP1 with a declined ATP level. Ad5 probably uses ADP and E4orf4 to induce necrosis like cell death. H_2O_2 induces pure necrosis due to intracellular ATP level falling. In both cytotoxicities mediated by Ad5 and H_2O_2, RIP1 dose not play a major role. Consequently, ColoAd1 killing can be protected by Necrostatin-1 whilst Ad5 and H_2O_2 killings can not. However, the execution steps for necrosis and necroptosis are similar, Ca^{2+} may likely as one of the main effector to activate the down stream proteases; in addition the falling ATP level is able to directly cause cell disintegration for necrosis. Furthermore, autophagy

could be a main execution mechanism. Nevertheless, blocking the virus induced death pathway from the very down stream point, such as calpain and LC3II, is usually inefficient and may even enhance the cell death.

Chapter 6:

Potential Applications of ColoAd1

Oncolysis

6.1 Introduction

6.1.1 Drug resistance and Virotherapy

Drug resistance is a major obstacle to successful cancer chemotherapy, whereby resistance to a wide range of agents occurs. The patients enrolled on phase I clinical trials will likely be resistant to one or more standard of care agents. In addition, most cases of cancer, when diagnosed at an advanced stage, cannot be cured with conventional therapeutic treatment. All these challenges provide an excellent necessity and suitable clinical settings for applying oncolytic virotherapy. Since the cytotoxicity of oncolytic viruses is based on a concept that fundamentally distinct to the mechanism of chemotherapy drugs, oncolytic virotherapy has a great potential to overcome chemo-resistance and eradicate cancer stem cells (Wodarz 2009).

Cellular factors that contribute to drug resistance include: (1) drug transporter-mediated increased efflux and decreased influx of anticancer drugs; (2) activation of DNA repair machinery; (3) activation of detoxification system; and (4) blocked apoptosis pathway. However the former three factors do not have limiting a impact on oncolytic viruses and thesis viruses are therefore not susceptible to the same pathways of drug resistance. First, virus infection and transduction is mediated through specific cell receptors and dose not involve with drug transporters; second, in order to achieve productive replication, viruses have evolved to control or take advantage of the cellular DNA repair machinery and the detoxification system. For instance, the Adenovirus Ad5 express proteins from the early genes to either down regulate the damage repair enzyme O(6)-methylguanine-DNA methyltransferase, or degrade PARP or the Mre11 complex which detects DNA strand breaks (Jiang, Alonso et al. 2006); Recently Ad5 has also been reported to utilize autophagy for

effective oncolysis and progeny virus release(Jiang, White et al. 2011); moreover, there is no evidence so far shows the cross resistance of oncolytic viruses with chemotherapy drugs.

The defective apoptosis pathway is the key cellular factor for drug resistance because cancer cells are intrinsically apoptosis resistant, whereas most anticancer drugs induce apoptosis type cell death especially via mitochondrial-dependent pathway(Kaufmann and Vaux 2003; Fulda and Debatin 2006). Restoring the efficacy of the standard chemotherapy by reactivating apoptosis is theoretically possible but practically problematic However, inducing the alternative cell death pathways (such as necropotosis and autophagy) or their combinations are more likely to circumvent the drug resistance caused by apoptotic dysfunction. For instance, the cancer cells resistant to apoptotic inducers such as anthracycline antibiotics and vinca alkaloids have been demonstrated to be sensitive to the necroptotic inducer Shikonin (Han, Li et al. 2007; Hu and Xuan 2008). Similarly, certain viruses induced oncolysis may provide the possibility to bypass cancer drug resistance by activating multiple death pathways. Therefore, we speculate the ability of ColoAd1 oncolysis induces an enhanced programmed necrosis and autophagy is more likely to tackle drug resistance than other reagents.

To prove our hypothesis, we investigated the killing potency of ColoAd1, Ad5 and drugs on cell lines matched with drug sensitive and drug resistant phenotypes, including colorectal carcinoma HCT116 and pancreatic carcinoma Capan-1 cell lines. Cells resistant to Oxaliplatin, Cisplatin and 5FU were used in this study. The drug resistances either originate from passaging a cell line at a sub lethal concentration of a drug to force selection of drug resistant mutants, or it acquired from the certain gene mutations. The ability of viruses or drugs to kill the matched pairs of cells was

recorded by in vitro cytotoxicity assay. The results revealed all the cells showed resistances to the individual drug but were killed with equal efficiency by ColoAd1. This virus was shown superior potency to overcome either genetic derived or adapted drug resistance, which could be related with its necroptosis death mechanism.

6.1.2 Cancer immunotherapy and virotherapy

Most oncolytic virotherapy research has being focused on the virus direct "killing" properties on tumours, however, some preclinical and clinical data suggest that in some cases viral induced immune activation can play an important role in cancer remission. Oncolytic viruses are thought more likely to be a novel form of immunotherapy (Prestwich, Harrington et al. 2008; Prestwich, Errington et al. 2009). Systemic anticancer chemotherapy currently used is immunosuppressive and mostly induces nonimmunogenic tumour cell death (Casares, Pequignot et al. 2005). In comparison, oncolytic viruses are prime candidates to enhance the immunogenicity of tumour microenvironment (Endo, Sakai et al. 2008). Through viral oncolysis, a systemic antitumour immunity can be triggered and prolonged with multiple mechanisms: (1) virus infection directly results in pathogen-associated molecular pattern (PAMP) recognition and antigen-presenting cells (APC) activation; (2) virus infection is likely to alter the balanced tumour derived cytokine profiles. (3) endogenous danger signals are produced from stressed and/or dying cells ; (4) tumour associated antigen are released by lysed cells. All these can initiate an early influx of immune cells, including macrophages and natural killer (NK) cells in response to virus administration; and followed by dendritic cells (DC) activation and cytotoxic T cells stimulation. These changes within the tumour environment also hold the potential to alter the pre-existing immunosuppressive nature, in favour of the

generation of therapeutic immune response. Thus, oncolytic virus and its generated tumour oncolysate act as “tumour vaccine cocktail”, in which virus works as an immune “adjuvant”. Additionally, this vaccine is naturally specific to each individual patient and that could extra benefit the final therapeutic efficacy.

As proposed by Matzinger at 2001, the danger signal theory (Gallucci and Matzinger 2001) is the nucleus to explain the immunogencity of viral oncolysates. It is necessary here to briefly overview the immune outcomes brought by the different death types. As described in the introduction part, apoptotic and autophagic cell deaths are generally poorly immunogenic, or tolerogenic and even immuno suppressive; whereas necrotic cell death is highly immunogenic. This concept is currently popular but is still debatable, as it has been reported that immunogenicity of tumours is an intrinsic feature of the tumour rather than being regulated by signals associated with apoptotic or necrotic cell death(Bartholomae, Rininsland et al. 2004). The immunogencity of necrotic cells comes from the release or exposure of intrinsic cell factors, including heat-shock protein HSP, high-mobility group Box-1 HMGB-1, calreticulin, bradykinin and uric acid, which have been identified as danger signals to prime DC and then promote inflammation (Obeid, Tesniere et al. 2007; Brusa, Migliore et al. 2009; Kono, Chen et al. 2010; Yang, Rivera et al. 2010). This extracellular release of danger signal factors is considered to be a typical feature of necrosis rather than apoptosis. Some of the intrinsic cell factors like HMGB-1 only can be extracellular released by necrotic cell death. Apoptotic cells do not release HMGB1 even after undergoing secondary necrosis, and thus fail to promote inflammation even if not cleared promptly by phagocytic cells. Similarly, no HSP were detected in the supernatants of apoptotic cells even 24 h after death(Basu, Binder et al. 2000; Scaffidi, Misteli et al. 2002).

Due to the necrosis nature of ColoAd1 mediated oncolysis, we hypothesis that ColoAd1 killing of tumour cells is strongly immunogenic and able to cause stronger immune activation than Ad5. To initially explore this potential application filed, we preliminary studied the three danger signals extra-cellular release with viral oncolysis progress, including HSP70, HMGB1 and uric acid. We also used a stable macrophage NFκB reporter cell line (U937- NFκB -luc) as tool to investigate the inflammatory signal induced by viral oncolysates (dead cell debris and supernatant). The U937 cells were stably transfected with a plasmid containing three NFκB target sequences linked upstream of the luciferase reporter gene. This cell line is very sensitive to NFκB activation and can be detected through the luciferase signal under NFκB promoter. The obtained results were promising and confirmed our hypothesis to a great extent, showing that there were profound HSP70 and HMGB1 extracellular released with ColoAd1's killing although the uric acid level was not detected. Furthermore, the oncolysates of ColoAd1 demonstrated the capability to elicit an enhanced NFκB activation than that of Ad5 and other treatments.

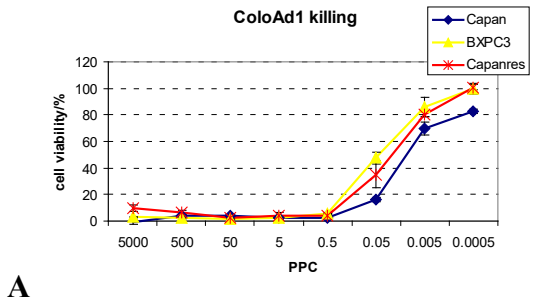
6.2 Results

6.2.1. ColoAd1's killing on Capan-1 cells

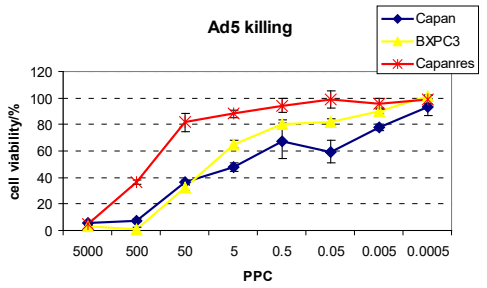
The first tested group included pancreatic carcinoma Capan-1 and the Cisplatin resistance counterpart CapanRes cell lines, as well as the control cell line BXPC3. Capan-1 has a truncated BrCA2 gene. As BrCA2 protein directly binds to and regulates RAD51, an essential protein for DNA repair through homologous recombination, BrCA2 deficient cancers are hypersensitive to DNA crosslinking agents such as Cisplatin. CapanRes has a restored BrCA2 expression level to wild

type and thus acquired Cisplatin resistance. BXPC3 has a wild type BrCA2 and is used as a normal pancreatic cancer control(Sakai, Swisher et al. 2008).

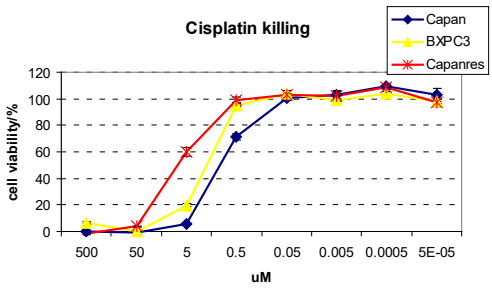
From the results demonstrated in Fig6.1, the cytotoxicity induced by Cisplatin on the three cell lines was: Capan> BXPC3> CapanRes, the Cisplatin resistance was about 10 times (IC50 left shifted from 1 μM to 10 μM) by the restored BrCA2 gene (Fig6.1 C).



A



B



C

Fig6.1 5 days end point MTS assay on Pancreatic cell lines. The top point viral doses were used at 5000 PPC, then further 1:10 serial dilutions were used; the top concentration of Cisplatin was used at 500 μM, then further 1:10 serial dilutions were used. Mean data ± SD are presented, *n* =3.

Both viruses showed killing but the potency of ColoAd1 was much stronger than that of Ad5. IC50 value of ColoAd1 on Capan was as low as 0.01 PPC while that of Ad5 had to be used as high as 8 PPC; furthermore, Ad5's killing on CapanRes was not efficient (IC50 value shifted to 500 PPC), thus the acquired the resistance for Ad5 oncolysis have increased 62.5 fold. This indicates that the BrCA2 gene possibly had some effect to interfere with Ad5's killing. As a dramatically contrast, the killing order for ColoAd1 was: Capan > CapanRes >BXPC3, in fact there is not noted difference among the three cell lines. This fact suggested that there was no correlation between ColoAd1's efficacy with BrCA2 gene expression.

6.2.2. ColoAd1's killing on HCT116 cells

The second tested drug resistance group was a colorectal carcinoma cell line HCT116, with its 5FU resistance subline HCT-5FU and oxaliplatin resistant subline HCT-OX (the p53 status unknown).

HCT116 is a highly aggressive cell line and contains mainly cancer stem cells (Yeung, Gandhi et al.; Allen, McLean et al. 2007; Prestwich, Harrington et al. 2008). The drug resistances were developed from repeated exposure to stepwise increasing concentration of 5-FU and oxaliplatin over 3 month from the first passage (to passage 19) in our lab. HCT-OX was found to have the relatively stable resistance from the beginning (compare Fig6.2 C to A); whereas the drug resistance of HCT-5FU was acquired over time (Compare Fig6.2 F to E). The oxaliplatin resistance of HCT-OX had increased by nearly 180 times compared to the parent cell line (IC 50 shifted from 5 μM to 900 μM); and 5FU resistance increased nearly 10 times (IC50 shifted from 10 μM to 100 μM) after 19 passages.

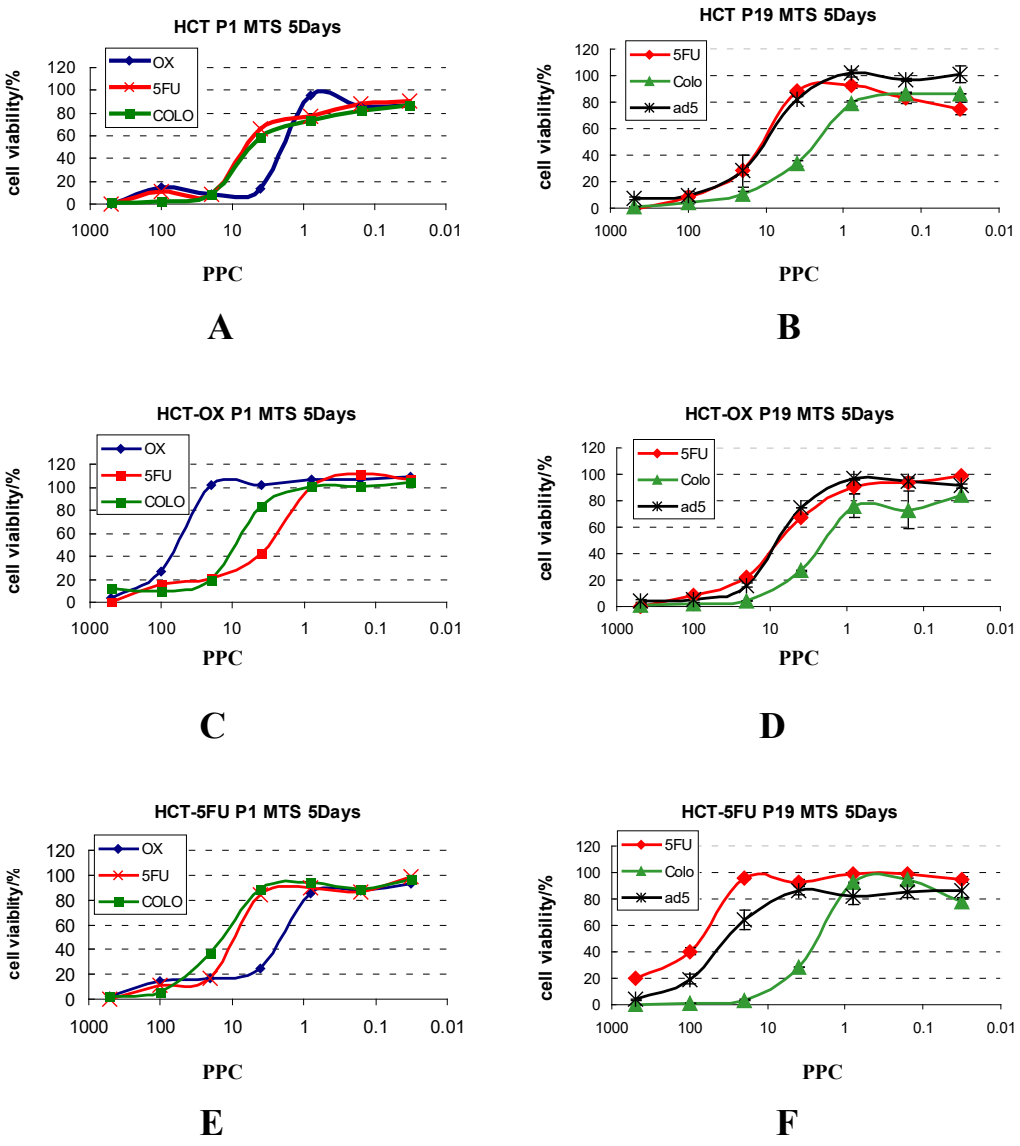


Fig 6.2 The 5 days end point MTS assay on HCT-116 cell line. The infection doses of viruses was started from 5000 PPC/cell, then 1:10 series dilution were used; Oxaliplatin started concentration from 500μM, then 1:10 dilute series dilution were used. Error bar represents SD of the three replicates**.** A. HCT 116 at passage 1; B. HCT 116 at passage 19; C.HCT-OX oxaliplatin resistance subline at passage1; D. HCT-OX oxaliplatin resistant subline at passage 19; E. HCT-5FU 5FU resistant subline at passage1; F. HCT-5FU 5 FU resistant subline at passge 10. Mean data ± SD are presented, *n* =3.

The results clearly showed that the killing by ColoAd1 was not affected by this acquired drug resistance (compare Fig6.2 A, C and E), its potency was similar on the three cell lines (tested at the same time); meanwhile, the killing even slightly

increased with the longer passage numbers and this suggested the cells did not generate resistance to virus when they acquire resistance to the chemotherapy drugs (compare Fig6.2 B to A, D to C and F to E). On the contrary, the potency of Ad5 was found to have some reduction with the cells gaining resistance to 5FU.

6.2.3 Extracellular HSP 70 release from the infected tumour cells

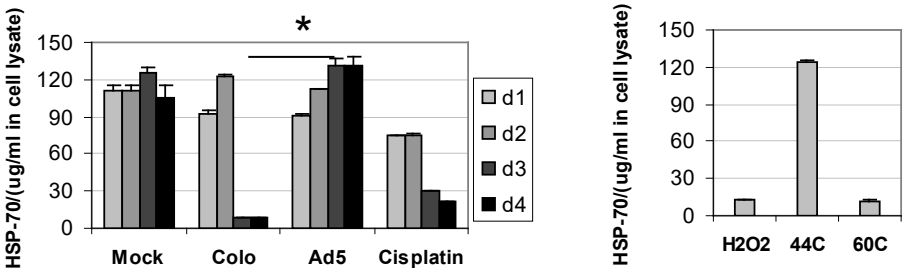
The intracellular HSP70 expression level in A549 cells and the extracellular released HSP concentration in the cell culture supernatant both have been quantified by HSP70 ELISA, with the oncolysis progress of ColoAd1 and Ad5. Cisplatin and H_2O_2 treated samples were used as apoptotic and necrotic cell controls respectively. In addition the samples from cells heated of 44ºC and 60ºC, 1 hour for HSP70 induction, were also as used HSP70 positive control. Cells heated at 44ºC mainly underwent apoptotic cell death, while those heated at 60ºC experienced necrotic cell death due to hyperthermia causes membrane leakage(Brusa, Migliore et al. 2009). The results are shown in Fig6.3.

The majority of A549 cells were still alive after 44ºC heat treatment for 1 hour. There were about 10% intracellular increase compared to the untreated cells. Extracellular HSP70 two fold increased than the control was observed partially owing to some lytic cells. After 60ºC treatment the A549 cells showed a necrotic morphology and the HSP70 protein was almost entirely released into the supernatant. H_2O_2 treated cells demonstrated a similar pattern. The final extracellular HSP70 level of H_2O_2 treated cells were 30% higher than those of 60ºC, this could be related with the protein stability being impaired by high temperature. .

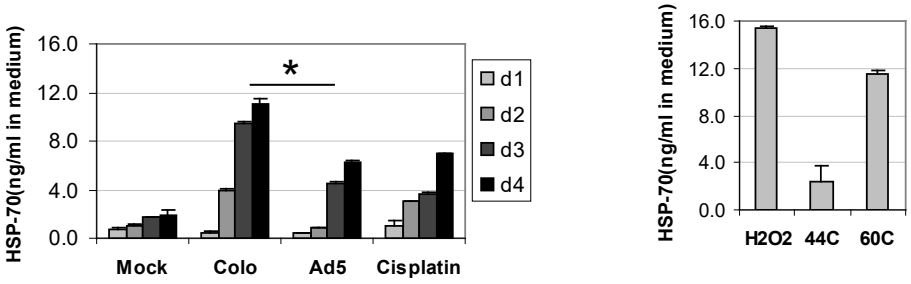
Compared to the mocked cells, Cisplatin treated cells showed notable intracellular HSP reduction starting from day1 post of treatment in comparison with the control; however the extracellular HSP level was not significantly high. With longer

incubation, more HSP was gradually released into the supernatant and this may due to secondary necrosis.

For both adenovirus infected cells, the HSP70 expression level in the cells slightly dropped at the early infection stage (post infection day 1); however, the levels were



A. Intracellular HSP70 level



B. Extracellular HSP70 level

Fig6.3 HSP70 concentration quantified by ELISA. A549cells were seeded in 24 well plate by the density of 50,000cell/ well in full growth medium. Next day, the cells were treated with ColoAd1, Ad5 and Cisplatin and H_2O_2 (with the concentration of 10 PPC, 100 PPC, 50 μM and 1mM, respectively). H_2O_2 treated cells were incubated with H_2O_2 containing medium for 6 hours before harvest. Two other cell groups were incubated at 44ºC and 60ºC for 1hours then moved to incubation at 37ºC for another 4 hours before harvest. The supernatants were then collected and stored at -80ºC. The cells were lysed using 200μl RIPA buffer containing of cocktail protease inhibitors and collected for -80ºC storage. All the samples were assayed together using ELISA. The cell lysates were used for measuring the intracellular HSP 70 level while supernatant was used to measure extracellular HSP level. Mean data ± SD are presented, *n* =3. Statistical differences between two groups were determined using Student's t-test.

raised again from post infection day 2 and reached 10% increasing (particularly for ColoAd1). At post infection of day 3 a distinguishable difference between the patterns of two viruses treated cells could be seen. Because of high efficient oncolysis, ColoAd1 induced cellular membrane leakage and caused a robust HSP70 releasing into extracellular environment. In contrast, Ad5 caused further intracellular HSP rise and mediated a much slower release.

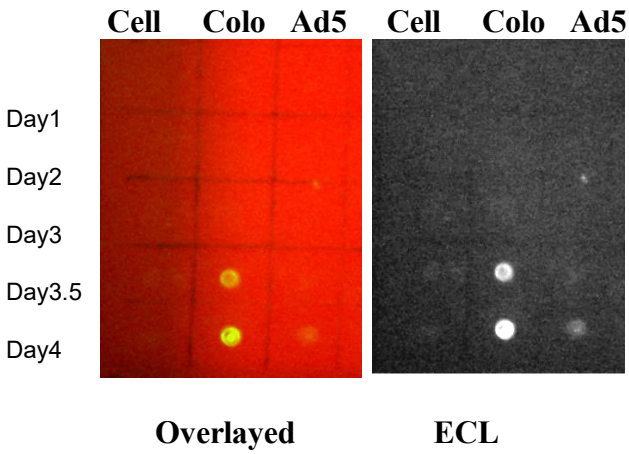


Fig 6.4 Dot blot method to detect extracellular HMGB1 release. 1µl of supernatant samples was loaded on NC membrane. The blotting procedure is according to the Chapter 2 Materials and Methods part. A primary anti human HSP70 was used at the dilution of 1:1000 and the secondary anti human IgG-HRP was used at the dilution of 1:5000. The ECL signal (on right)was detected by the gel imager after 3 mins exposure, then overlayed with the normal light images (left) to locate the individual samples.

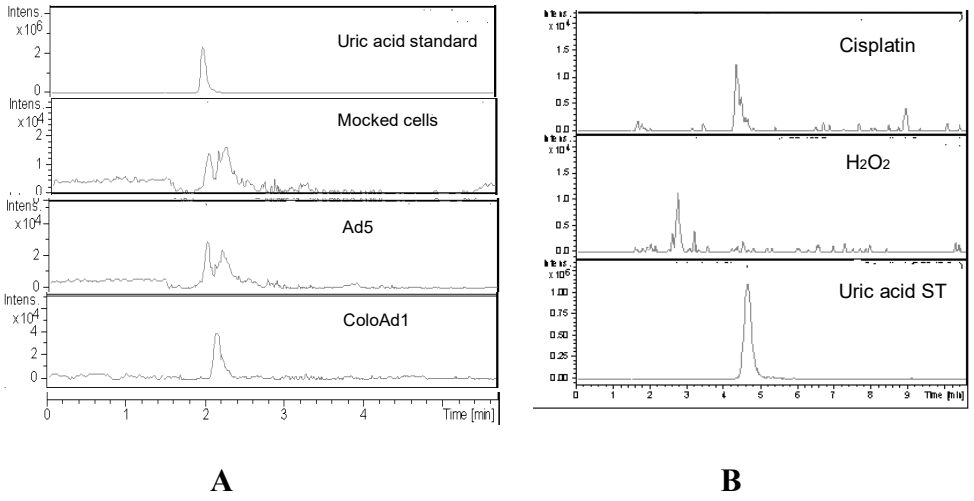
6.2.4 HMGB1 extracellular release from the infected tumour cells

The extracellular release profiles of HMGB1 by ColoAd1 and Ad5 infected cells are demonstrated by dot blot. As shown in Fig6.4, HMGB1 signal started to be detected in ColoAd1 treated cells supernatant from post infection day3 (the beginning of oncolysis), the signal significantly rose at day3.5. In contrast, HMGB1 signal for Ad5 treated cells only started to appear at day4 post infection time point (at this time

the majority of the cells have been dead verified by MTS and Annexin V/PI staining assay)

6.2.5 Extracellular uric acid level from the infected tumour cells

The extracellular uric acid levels were detected by LC-MS. The elution time of the standard uric acid (concentration) is at 2min. However, when using the same conditions, uric acid only from the mocked cells and Ad5 sampled was detected (the samples from Cisplatin treated cells was detected in another run, shown in Fig 6.5B), no signal was detected for ColoAd1 and H_2O_2 treated samples (see Fig6.5 A).

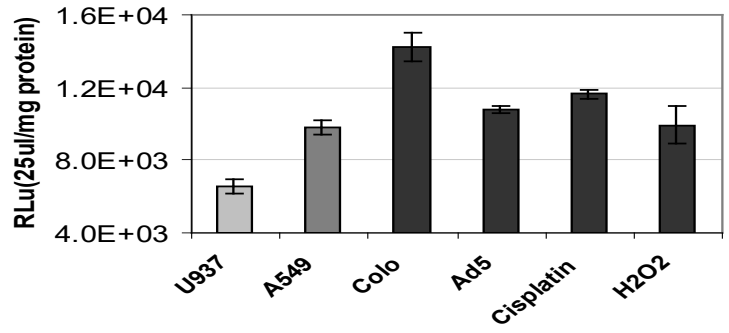


A **B**

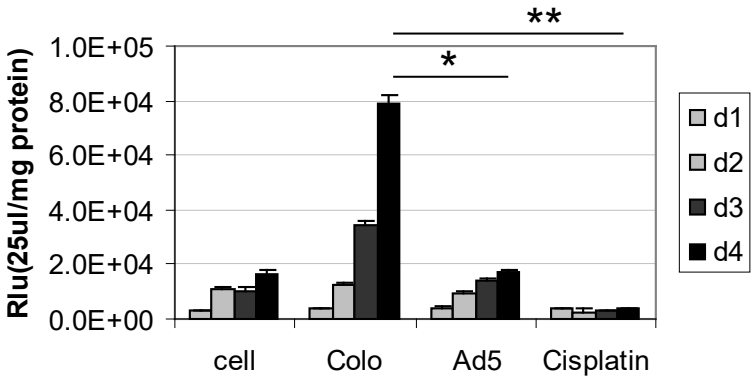
Fig6.5 **Extracted ion chromatograms (m/z 167) from LC-MS analysis of cell culture supernatants** (cells treated with Ad5, ColoAd1 (panel A), Cisplatin and H_2O_2 (panel B)) comparing with uric acid standard.

6.2.6 ColoAd1 oncolysates induce NF-κB activation

Both cellular part and the supernatant parts from the different treatments were tested on the U937- NF-κB -LUC cells for immunogenicity and inflammatory signal. For this reporter cells, the NF-κB activity is correlated with the luciferase activity, which was measured as luciferin light units (RLu). As can be seen from Fig6.6, ColoAd1



A. NF-κB **activation induced by cell debris**



B. NF-κB **activation induced by supernatants**

Fig6.6 The immunogenic properties of viral oncolysates and cell lysates from other treatments, measured by NF-κB **activation.** The A549 cells were treated the same conditions as previous. The cells part was washed by PBS and collected by gently trypsinization. The obtained cell pellet was frozen and thawed in -80ºC and RT for three times to get the cell debris. The protein concentration was quantified before the concentration. The supernatant part was collected and stored at -80ºC before the assay. 20 µg protein or 50 µl of the supernatant was used to stimulate 1 million reporter cells for 8 hours. Mean data ± SD are presented, *n* =3. . Statistical differences between two groups were determined using Student's t-test.

elicited a stronger NF-κB activation than other treatments, either by dead cell debris or by the cell supernatants. Moreover, the major activation response came from the supernatant part, and the intensity of signal correlated with ColoAd1 mediated oncolysis progress. There are slightly increase for Ad5 with time, nevertheless, it is

nearly the same as the background (the mocked cells). The supernatant from Cisplatin treated cells produced a weaker signal than the mocked cells, which suggested its immune suppressive characters.

However, after we used 300kD spin filter to remove virus in the supernatant, we found the NF-κB activation signals were removed by the filtration. In order to know the virus direct impact on the U937 reporter cells, we used the virus lonely in the assay. Both viruses did not show activation (Colo≈Ad5≈blank cells, data is shown in the supplementary materials S9), therefore should not be the major factor responsible for the immunogenicity of viral oncolysates.

6.3 Discussion

Overcoming drug resistance and induce immune activation tumour killing both are the advanced targets in cancer therapy. Oncolytic biotherapy holds much promise in these two fields, largely because viral mediated killing on tumour cells is distinctive from that of conventional treatments. We have demonstrated that ColoAd1 is a much more potent oncolytic virus than Ad5, and it capable to successfully circumvent drug resistance and revoke tumour immune response. These advantages are closely related to the viral induced programmed necrosis.

6.3.1 Circumstances drug resistance by ColoAd1 oncolysis

Oncolytic virus is a selectively replicating virus that kills tumour cells by direct lysis. This represents a gain of function killing mechanism imposed on the cell by the virus. In contrast, most of small molecule chemotherapeutic agents rely entirely on the cells own death mechanisms (apoptosis) following DNA damage. Therefore, cells can mutate pathways to become resistant to some specific drugs, or more

generally, resistant to apoptosis. Since the viruses were not been subjected to the mutation pressure of the tumour cells, we hypothesized that cell lines resistant to standard chemotherapy agents would be killed with equal efficiency by oncolytic virus. Our results for ColoAd1 on the two group drug resistance cells (HCT116 and Capan-1) supported this hypothesis. The drug resistance gained either from genetic mutation or epigenetic pressure, both was eradiated by ColoAd1, whereby the viral cytotoxicity was the same on the resistant sublines with their parental cell lines. As a contrast, the killing potency of Ad5 was somewhat affected by the resistances.

This data indicated that ColoAd1 does not utilize the same pathways of resistance that have emerged for existing clinical drugs. In addition, there could be a correlation between the overcoming drug resistance and the special killing mechanism of ColoAd1. The direct lysis or necrosis mechanism, rather than reactivating apoptosis, allowed it more effectively circumvent drug resistance, and the risk of cross-resistance was therefore largely reduced.

Ad5 was reported recently by different groups to mediate autophagy cell death in oncolysis and use it as the strategy for progeny virions release. However, the study suggests that the autophagy also activate the capsase-8 signaling (Jiang, White et al. 2011), thus the Ad5 induced cell death pathway may still be apoptosis –related. Compared to Ad5, ColoAd1 induced cell death is more necrotic, therefore it possibly gained more potency to bypass the drug resistance.

Before coming to a complete conclusion, it is important to test the viruses on more drug resistant cell lines and assess other types of oncolytic viruses as well. As discussed in the Chapter 1: Introduction, a various oncolytic viruses especially RNA

viruses, induce oncolysis based on the apoptosis mechanism. It is unknown that whether they still hold the ability to overcome drug resistance; the concern is more serious particularly for those resistances come from a defective apoptotic pathway or due to apoptosis inhibiting tumour microenvironment. If the viruses use the receptor dependent apoptotic pathway (extrinsic pathway), it would have more opportunity to tackle this target; moreover, DNA oncolytic viruses could be more successful candidates than RNA oncolytic viruses as they have more chance to induce cell death by multiple pathways.

Targeting cancer-initiating cells or so called cancer stem cells (CSC) is the next step for testing ColoAd1's potential, as it would be important to prove that cancer stem cells are susceptible to ColoAd1's killing. CSCs have been shown to be relatively more resistant to conventional anticancer therapies and are thus thought to be responsible for disease relapse, and they could be a major factor responsible for tumour drug resistance. Both HSV and adenovirus have been reported to show the ability to kill certain types of CSCs (Cripe, Wang et al. 2009). It is noteworthy that one of the target cells used in this study, HCT116 contains a high percentage of CSC and ColoAd1 still demonstrated a killing with 0.5-1 log higher potency than Ad5, even on the drug-resistant sublines. It will be important to test ColoAd1 on CSCs from different tissue resources, but extra attention needs to be paid on viral infectivity on the specific CSCs. We also have tested ColoAd1 on high grade primary glioblastoma CSC cultured from brain cancer patient biopsies, ColoAd1 did not show strong cytotoxicity, similar to Ad11 and Ad5; however a parallel study was carried out on the glioblastoma cell line U87MG and the same weak cytoxicities from the three adenoviruses were found (data not shown). This suggests that the viruses may not transducer well into CSCs rather than not being able to kill them.

6.3.2 Induction of antitumour immunity by ColoAd1 oncolysis

By detection of some endogenous danger signals (HSP 70 and HMGB1) extracellular release and NF-κB activation, ColoAd1 was demonstrated its oncolysis potentially is able to induce an enhanced anti-tumour immunity in comparison to Ad5. The oncolysate induced by ColoAd1 displayed an immunogenicity level similar to the cell lysate from H_2O_2 necrosis, and much stronger than those induced by Cisplatin apoptosis. Our results are consistent with the following scenario: viral oncolysis particularly ColoAd1 oncolysis causes tumour cells necrotic cell death and the release of HSP70 and HMGB1, this in turn promotes an inflammatory response via activating NF-κB pathway in macrophages. The results based on the two models used have excluded the immunogenicity from progeny virions, although in vivo it is one of the major factors contributing to the total immunity.

The induced expression of HSP 70 and release of both HSP 70 and HMBG1 by some Ad5 based conditional replication oncolytic viruses oncolysis has been reported very recently (Schierer, Hesse et al. 2011). According to this report, the oncolysis also correlated with a necrotic death mode in melanoma cells. The remarkable elevation of uric acid concentration in the tumour cells undergoing oncolysis was observed by Endo and the group, and was considered as a general effect of adenovirus infection(Endo, Sakai et al. 2008). Nevertheless, in both samples either from ColoAd1 oncolysis or from H_2O_2 induced necrosis, higher level uric acid was not detected in the extracellular environment, our results about Ad5 oncolysis also were contradictory to the report.

Apart from the endogenous danger signals released from necrotic dying cells, there may be other mechanism potentially linking the immnostimulation effect of the oncolysate with ColoAd1 oncolysis. According to the study in Chapter 5, we found

the ColoAd1 oncolysis has necroptosis nature with necrosis features, this is particularly noticed by the involvement of kinase RIP1 in ColoAd1 but not in Ad5 oncolysis. It is noteworthy that RIP1 is crucial for necroptosis, but also mediates activation of NF-κB. During some virus (such as Vaccinia) infection, and TNF induced programmed necrosis, the phosphorylation of RIP1 and RIP3 to form a complex which activates the pronecrotic kinase activity, and triggers down stream reactive oxygen species production that causes inflammation (Cho, Challa et al. 2009). From the host cells aspects, the proinflammatoy effects of necrosis are important for successful antiviral immune response; while the virus aspect, certain viruses use inhibition of programmed necrosis as an important immune evasion strategy. Compared to Ad5, the short term forced Evolution and E3 region deletion more likely cause ColoAd1 to lose this immune regulation ability with the host cells.

More clinical evidence has been showing that the oncolytic viruses with immunomodulatory activity are able to lead tumour regression. Very recently, a recombinant Vaccinia virus overexpressing the inflammatory cytokine human GM-CSF (granulocyte-macrophage colony-stimulating factor), JX-594, has finished a phase I trial by systemic administration route to treat metastasized tumours (Breitbach, Burke et al. 2011). The results reported are very promising, 50% from 23 cancer patients, all with advanced solid tumour that were resistant to other treatments showed positive response. Two out of five patients received high dose of virus had antitumor activity by FDG-PED (>25% decrease in standard of uptake value). Similarly, an attenuated strain of Herpes simplex viruse-1 HSV-1 encoding GM-CSF is also at phase III trial stage. The Ad5 based oncolytic adenovirus constructed with GM-CSF has been found to stimulate antitumour immunity and break tumour

associate immunotolerance to treat advanced chemotherapy refractory solid tumours (Pesonen, Diaconu et al. 2011). Therefore, an oncolytical virus with an intrinsic immunomodulatory activity like ColoAd1 would be desirable, and further genetic modification based on this prototype to overexpress the inflammatory cytokines would greatly enhance its potential.

Beside inserting immunostimulatory genes into oncolytic viral genome, the intrinsic immunomodulatory activity of oncolytic viral oncolysate also gains the interest of virotherapists and immunotherapiests. The killing mechanism and efficacy of oncolytic viruses is not only due to a direct cytotoxic effect of oncolysis, but can also be a consequence of the immunostimulatory character of the oncolysates, which induce specific CTL for the remaining antigen-bearing tumour cells. Studies with some oncolytic viruses including HSV-1 and VSV, in immunocompetent animal models indicate antitumor immune activation can contribute to tumour control. On the other hand, the data either from clinical trial or from in-vivo studies have shown oncolytic adenoviruses (based on Ad5) are well tolerated after local or systemic application, but also that their antitumour activity needs improvement. The relatively shortage of immunomodulatory character may provide one of the main reasons to explain the poor performance of Ad5. Therefore, it is particularly encouraging that in our in vitro results ColoAd1 demonstrated an enhanced immunostimulation capacity than Ad5, the virus can be expected to elicit a more potent anti-tumour in vivo.

The data reported in this study is preliminary and the study needs further exploration. Firstly, the cytokine release profiles of both the lysed tumour cells and loaded dendritic cells DC (particularly proinflammatory cytokines TNFα, IFNγ, IL6, IL12)

need to be characterized. Those cytokines work in combination with extracellular released HSP70 and HMBG1 to achieve stimulations; secondly, since the antitumour immune activation largely depend on antigen presentation and T cell activation by DC, investigation about the interaction between vial oncolysates and DC will be essential, although this can be complicated. The study published by Stephan and co-authors have revealed that human DC can efficiently phagocytose adenoviral (Ad5 based) oncolysate, when the cell die and showing preferentially features of necrotic cell death. However, the DC requires additional stimulation to mature. The oncolytic adenoviruses and adenoviral oncolysate do not stimulate DC maturation, which is in contrast to reports for other oncolytic viruses. Trigger and shape DC-induced antitumour immunity only can be achieved through arming the virus with some immunostimulatory genes. Thereby, the similar experiment observation upon ColoAd1 oncolysis is completely necessary, and the results will be certainly important to design next generation virus based on the ColoAd1 prototype.

Reference:

Allen, W. L., E. G. McLean, et al. (2007). "The role of spermidine/spermine N1-acetyltransferase in determining response to chemotherapeutic agents in colorectal cancer cells." Mol Cancer Ther **6**(1): 128-37.

Bartholomae, W. C., F. H. Rininsland, et al. (2004). "T cell immunity induced by live, necrotic, and apoptotic tumor cells." J Immunol **173**(2): 1012-22.

Basu, S., R. J. Binder, et al. (2000). "Necrotic but not apoptotic cell death releases heat shock proteins, which deliver a partial maturation signal to dendritic cells and activate the NF-kappa B pathway." Int Immunol **12**(11): 1539-46.

Breitbach, C. J., J. Burke, et al. (2011). "Intravenous delivery of a multi-mechanistic cancer-targeted oncolytic poxvirus in humans." Nature **477**(7362): 99-102.

Brusa, D., E. Migliore, et al. (2009). "Immunogenicity of 56 degrees C and UVC-treated prostate cancer is associated with release of HSP70 and HMGB1 from necrotic cells." Prostate **69**(12): 1343-52.

Casares, N., M. O. Pequignot, et al. (2005). "Caspase-dependent immunogenicity of doxorubicin-induced tumor cell death." J Exp Med **202**(12): 1691-701.

Cho, Y. S., S. Challa, et al. (2009). "Phosphorylation-driven assembly of the RIP1-RIP3 complex regulates programmed necrosis and virus-induced inflammation." Cell **137**(6): 1112-23.

Cripe, T. P., P. Y. Wang, et al. (2009). "Targeting cancer-initiating cells with oncolytic viruses." Mol Ther **17**(10): 1677-82.

Endo, Y., R. Sakai, et al. (2008). "Virus-mediated oncolysis induces danger signal and stimulates cytotoxic T-lymphocyte activity via proteasome activator upregulation." Oncogene **27**(17): 2375-81.

Fulda, S. and K. M. Debatin (2006). "Extrinsic versus intrinsic apoptosis pathways in anticancer chemotherapy." Oncogene **25**(34): 4798-811.

Gallucci, S. and P. Matzinger (2001). "Danger signals: SOS to the immune system." Curr Opin Immunol **13**(1): 114-9.

Gatti, L. and F. Zunino (2005). "Overview of tumor cell chemoresistance mechanisms." Methods Mol Med **111**: 127-48.

Han, W., L. Li, et al. (2007). "Shikonin circumvents cancer drug resistance by induction of a necroptotic death." Mol Cancer Ther **6**(5): 1641-9.

Hu, X. and Y. Xuan (2008). "Bypassing cancer drug resistance by activating multiple death pathways--a proposal from the study of circumventing cancer drug resistance by induction of necroptosis." Cancer Lett **259**(2): 127-37.

Jiang, H., M. M. Alonso, et al. (2006). "Oncolytic viruses and DNA-repair machinery: overcoming chemoresistance of gliomas." Expert Rev Anticancer Ther **6**(11): 1585-92.

Jiang, H., E. J. White, et al. (2011). "Human adenovirus type 5 induces cell lysis through autophagy and autophagy-triggered caspase activity." J Virol **85**(10): 4720-9.

Kaufmann, S. H. and D. L. Vaux (2003). "Alterations in the apoptotic machinery and their potential role in anticancer drug resistance." Oncogene **22**(47): 7414-30.

Kono, H., C. J. Chen, et al. (2010). "Uric acid promotes an acute inflammatory response to sterile cell death in mice." J Clin Invest **120**(6): 1939-49.

Obeid, M., A. Tesniere, et al. (2007). "Calreticulin exposure dictates the immunogenicity of cancer cell death." Nat Med **13**(1): 54-61.

Pesonen, S., I. Diaconu, et al. (2011). "Integrin targeted oncolytic adenoviruses Ad5-D24-RGD and Ad5-RGD-D24-GMCSF for treatment of patients with advanced chemotherapy refractory solid tumors." Int J Cancer.

Prestwich, R. J., F. Errington, et al. (2009). "The case of oncolytic viruses versus the immune system: waiting on the judgment of Solomon." Hum Gene Ther **20**(10): 1119-32.

Prestwich, R. J., K. J. Harrington, et al. (2008). "Oncolytic viruses: a novel form of immunotherapy." Expert Rev Anticancer Ther **8**(10): 1581-8.

Sakai, W., E. M. Swisher, et al. (2008). "Secondary mutations as a mechanism of cisplatin resistance in BRCA2-mutated cancers." Nature **451**(7182): 1116-20.

Scaffidi, P., T. Misteli, et al. (2002). "Release of chromatin protein HMGB1 by necrotic cells triggers inflammation." Nature **418**(6894): 191-5.

Schierer, S., A. Hesse, et al. (2011). "Human dendritic cells efficiently phagocytose adenoviral oncolysate but require additional stimulation to mature." Int J Cancer.

Wodarz, D. (2009). "Use of oncolytic viruses for the eradication of drug-resistant cancer cells." J R Soc Interface **6**(31): 179-86.

Yang, H., Z. Rivera, et al. (2010). "Programmed necrosis induced by asbestos in human mesothelial cells causes high-mobility group box 1 protein release and resultant inflammation." Proc Natl Acad Sci U S A **107**(28): 12611-6.

Yeung, T. M., S. C. Gandhi, et al. (2010)."Cancer stem cells from colorectal cancer-derived cell lines." Proc Natl Acad Sci U S A **107**(8): 3722-7.

Abou El Hassan, M. A., I. van der Meulen-Muileman, et al. (2004). "Conditionally replicating adenoviruses kill tumor cells via a basic apoptotic machinery-independent mechanism that resembles necrosis-like programmed cell death." J Virol **78**(22): 12243-51.

Arnoult, D., M. Karbowski, et al. (2003). "Caspase inhibition prevents the mitochondrial release of apoptosis-inducing factor." Cell Death Differ **10**(7): 845-9.

Baird, S. K., J. L. Aerts, et al. (2008). "Oncolytic adenoviral mutants induce a novel mode of programmed cell death in ovarian cancer." Oncogene **27**(22): 3081-90.

Cho, Y. S., S. Challa, et al. (2009). "Phosphorylation-driven assembly of the RIP1-RIP3 complex regulates programmed necrosis and virus-induced inflammation." Cell **137**(6): 1112-23.

Christofferson, D. E. and J. Yuan (2009). "Necroptosis as an alternative form of programmed cell death." Curr Opin Cell Biol **22**(2): 263-8.

Daniels, R., N. M. Rusan, et al. (2006). "Simian virus 40 late proteins possess lytic properties that render them capable of permeabilizing cellular membranes." J Virol **80**(13): 6575-87.

Degterev, A., J. Hitomi, et al. (2008). "Identification of RIP1 kinase as a specific cellular target of necrostatins." Nat Chem Biol **4**(5): 313-21.

Forrester, N. A., G. G. Sedgwick, et al. (2011). "Serotype-specific inactivation of the cellular DNA damage response during adenovirus infection." J Virol **85**(5): 2201-11.

Glockzin, G., K. Mantwill, et al. (2006). "Characterization of the recombinant adenovirus vector AdYB-1: implications for oncolytic vector development." J Virol **80**(8): 3904-11.

Gordon-Shaag, A., Y. Yosef, et al. (2003). "The abundant nuclear enzyme PARP participates in the life cycle of simian virus 40 and is stimulated by minor capsid protein VP3." J Virol **77**(7): 4273-82.

Gros, A., C. Puig, et al. (2010). "Verapamil enhances the antitumoral efficacy of oncolytic adenoviruses." Mol Ther **18**(5): 903-11.

Ishizaki, T., M. Uehata, et al. (2000). "Pharmacological properties of Y-27632, a specific inhibitor of rho-associated kinases." Mol Pharmacol **57**(5): 976-83.

Ito, H., H. Aoki, et al. (2006). "Autophagic cell death of malignant glioma cells induced by a conditionally replicating adenovirus." J Natl Cancer Inst **98**(9): 625-36.

Ito, S., N. Koshikawa, et al. (2007). "3-Methyladenine suppresses cell migration and invasion of HT1080 fibrosarcoma cells through inhibiting phosphoinositide 3-kinases independently of autophagy inhibition." Int J Oncol **31**(2): 261-8.

Jiang, H., E. J. White, et al. (2008). "Adenovirus's last trick: you say lysis, we say autophagy." Autophagy **4**(1): 118-20.

Jiang, H., E. J. White, et al. (2011). "Human adenovirus type 5 induces cell lysis through autophagy and autophagy-triggered caspase activity." J Virol **85**(10): 4720-9.

Kravchenko, D. V., Y. A. Kuzovkova, et al. (2005). "Synthesis and structure-activity relationship of 4-substituted 2-(2-acetyloxyethyl)-8-(morpholine-4-sulfonyl)pyrrolo[3,4-c]quinoline-1,3- diones as potent caspase-3 inhibitors." J Med Chem **48**(11): 3680-3.

Nanavaty, U. B., R. Pawliczak, et al. (2002). "Oxidant-induced cell death in respiratory epithelial cells is due to DNA damage and loss of ATP." Exp Lung Res **28**(8): 591-607.

Robert, A., N. Smadja-Lamere, et al. (2006). "Adenovirus E4orf4 hijacks rho GTPase-dependent actin dynamics to kill cells: a role for endosome-associated actin assembly." Mol Biol Cell **17**(7): 3329-44.

Rodriguez-Rocha, H., J. G. Gomez-Gutierrez, et al. (2011). "Adenoviruses induce autophagy to promote virus replication and oncolysis." Virology **416**(1-2): 9-15.

St Germain, C., N. Niknejad, et al. (2010). "Cisplatin induces cytotoxicity through the mitogen-activated protein kinase pathways and activating transcription factor 3." Neoplasia **12**(7): 527-38.

Vandenabeele, P., L. Galluzzi, et al. (2010). "Molecular mechanisms of necroptosis: an ordered cellular explosion." Nat Rev Mol Cell Biol **11**(10): 700-14.

Waters, R., F. Ramsay, et al. (1982). "3-Aminobenzamide, an inhibitor of poly ADP-ribose polymerase, decreases the frequency of alkaline labile lesions and increases growth in human fibroblasts exposed to 3-methyl 4-nitroquinoline 1-oxide." Carcinogenesis **3**(12): 1463-7.

Xu, M. and H. L. Zhang (2011). "Death and survival of neuronal and astrocytic cells in ischemic brain injury: a role of autophagy." Acta Pharmacol Sin **32**(9): 1089-99.

Yamashima, T. (2004). "Ca2+-dependent proteases in ischemic neuronal death: a conserved 'calpain-cathepsin cascade' from nematodes to primates." Cell Calcium **36**(3-4): 285-93.

Yang, H., Z. Rivera, et al. (2010). "Programmed necrosis induced by asbestos in human mesothelial cells causes high-mobility group box 1 protein release and resultant inflammation." Proc Natl Acad Sci U S A **107**(28): 12611-6.

Abou El Hassan, M. A., I. van der Meulen-Muileman, et al. (2004). "Conditionally replicating adenoviruses kill tumor cells via a basic apoptotic machinery-independent mechanism that resembles necrosis-like programmed cell death." J Virol **78**(22): 12243-51.

Almeida, G. M., T. L. Duarte, et al. (2008). "Multiple end-point analysis reveals cisplatin damage tolerance to be a chemoresistance mechanism in a NSCLC model: implications for predictive testing." Int J Cancer **122**(8): 1810-9.

Artal-Sanz, M. and N. Tavernarakis (2005). "Proteolytic mechanisms in necrotic cell death and neurodegeneration." FEBS Lett **579**(15): 3287-96.

Connell, C. M., A. Shibata, et al. (2011). "Genomic DNA damage and ATR-Chk1 signaling determine oncolytic adenoviral efficacy in human ovarian cancer cells." J Clin Invest **121**(4): 1283-97.

Criddle, D. N., J. V. Gerasimenko, et al. (2007). "Calcium signalling and pancreatic cell death: apoptosis or necrosis?" Cell Death Differ **14**(7): 1285-94.

Darzynkiewicz, Z., S. Bruno, et al. (1992). "Features of apoptotic cells measured by flow cytometry." Cytometry **13**(8): 795-808.

Forrester, N. A., G. G. Sedgwick, et al. (2011). "Serotype-specific inactivation of the cellular DNA damage response during adenovirus infection." J Virol **85**(5): 2201-11.

Glockzin, G., K. Mantwill, et al. (2006). "Characterization of the recombinant adenovirus vector AdYB-1: implications for oncolytic vector development." J Virol **80**(8): 3904-11.

Gros, A., J. Martinez-Quintanilla, et al. (2008). "Bioselection of a gain of function mutation that enhances adenovirus 5 release and improves its antitumoral potency." Cancer Res **68**(21): 8928-37.

Ha, H. C. and S. H. Snyder (1999). "Poly(ADP-ribose) polymerase is a mediator of necrotic cell death by ATP depletion." Proc Natl Acad Sci U S A **96**(24): 13978-82.

Ju, J. S., S. E. Miller, et al. (2009). "Quantitation of selective autophagic protein aggregate degradation in vitro and in vivo using luciferase reporters." Autophagy **5**(4): 511-9.

Leist, M., Kühnle, S, Single, B, Nicotera, P (1998). "Differentiation Between Apoptotic and Necrotic Cell Death by Means of the BM Cell Death Detection ELISA or Annexin V Staining " Biochemica **2**: 4.

Lemasters, J. J., T. Qian, et al. (2002). "Role of mitochondrial inner membrane permeabilization in necrotic cell death, apoptosis, and autophagy." Antioxid Redox Signal **4**(5): 769-81.

Maddocks, O. D. and K. H. Vousden (2011). "Metabolic regulation by p53." J Mol Med (Berl) **89**(3): 237-45.

Mullen, J. T. and K. K. Tanabe (2002). "Viral oncolysis." Oncologist **7**(2): 106-19.

Naito, M., K. Nagashima, et al. (1997). "Phosphatidylserine externalization is a downstream event of interleukin-1 beta-converting enzyme family protease activation during apoptosis." Blood **89**(6): 2060-6.

Pagano, A., C. Pitteloud, et al. (2005). "Poly(ADP-ribose)polymerase activation mediates lung epithelial cell death in vitro but is not essential in hyperoxia-induced lung injury." Am J Respir Cell Mol Biol **33**(6): 555-64.

Porter, A. G. and R. U. Janicke (1999). "Emerging roles of caspase-3 in apoptosis." Cell Death Differ **6**(2): 99-104.

Roulston, A., R. C. Marcellus, et al. (1999). "Viruses and apoptosis." Annu Rev Microbiol **53**: 577-628.

Szczepanski, M. A., A. Grzanka, et al. (2010). "Cytoskeletal changes during cellular response of the A549 lung cancer cells to continuous cisplatin treatment." Cell Biol Int **34**(2): 197-211.
van Kuppeveld, F. J., J. G. Hoenderop, et al. (1997). "Coxsackievirus protein 2B modifies endoplasmic reticulum membrane and plasma membrane permeability and facilitates virus release." Embo J **16**(12): 3519-32.
Wei, N., J. K. Fan, et al. (2010). "Double-regulated oncolytic adenovirus-mediated interleukin-24 overexpression exhibits potent antitumor activity on gastric adenocarcinoma." Hum Gene Ther **21**(7): 855-64.
Yun, C. O., E. Kim, et al. (2005). "ADP-overexpressing adenovirus elicits enhanced cytopathic effect by induction of apoptosis." Cancer Gene Ther **12**(1): 61-71.
Zhao, Y., H. L. Wieman, et al. (2008). "Mechanisms and methods in glucose metabolism and cell death." Methods Enzymol **442**: 439-57.
Bremer, E., G. M. van Dam, et al. (2008). "Potent systemic anticancer activity of adenovirally expressed EGFR-selective TRAIL fusion protein." Mol Ther **16**(12): 1919-26.
Carlisle, R. C., Y. Di, et al. (2009). "Human erythrocytes bind and inactivate type 5 adenovirus by presenting Coxsackie virus-adenovirus receptor and complement receptor 1." Blood **113**(9): 1909-18.
Chang, C. J., Y. H. Chen, et al. (2007). "Combined GM-CSF and IL-12 gene therapy synergistically suppresses the growth of orthotopic liver tumors." Hepatology **45**(3): 746-54.
Greig, J. A., S. M. Buckley, et al. (2009). "Influence of coagulation factor x on in vitro and in vivo gene delivery by adenovirus (Ad) 5, Ad35, and chimeric Ad5/Ad35 vectors." Mol Ther **17**(10): 1683-91.
Hall, K., M. E. Blair Zajdel, et al. (2010). "Unity and diversity in the human adenoviruses: exploiting alternative entry pathways for gene therapy." Biochem J **431**(3): 321-36.
Holterman, L., R. Vogels, et al. (2004). "Novel replication-incompetent vector derived from adenovirus type 11 (Ad11) for vaccination and gene therapy: low seroprevalence and non-cross-reactivity with Ad5." J Virol **78**(23): 13207-15.
Hu, X. and Y. Xuan (2008). "Bypassing cancer drug resistance by activating multiple death pathways--a proposal from the study of circumventing cancer drug resistance by induction of necroptosis." Cancer Lett **259**(2): 127-37.
Kuhn, I., P. Harden, et al. (2008). "Directed evolution generates a novel oncolytic virus for the treatment of colon cancer." PLoS One **3**(6): e2409.
Leopold, P. L. and R. G. Crystal (2007). "Intracellular trafficking of adenovirus: many means to many ends." Adv Drug Deliv Rev **59**(8): 810-21.
Mei, Y. F., J. Skog, et al. (2003). "Comparative analysis of the genome organization of human adenovirus 11, a member of the human adenovirus species B, and the commonly used human adenovirus 5 vector, a member of species C." J Gen Virol **84**(Pt 8): 2061-71.
Senac, J. S., K. Doronin, et al. (2010). "Infection and killing of multiple myeloma by adenoviruses." Hum Gene Ther **21**(2): 179-90.
Yamamoto, M. and D. T. Curiel (2010). "Current issues and future directions of oncolytic adenoviruses." Mol Ther **18**(2): 243-50.
Zhang, L. Q., Y. F. Mei, et al. (2003). "Human adenovirus serotypes 4 and 11 show higher binding affinity and infectivity for endothelial and carcinoma cell lines than serotype 5." J Gen Virol **84**(Pt 3): 687-95.

Karber, G. (1931). "50% end-point calculation." Archives of Experimental Pathology and Pharmacology **162**: 480-483.

Sauthoff, H., T. Pipiya, et al. (2002). "Late expression of p53 from a replicating adenovirus improves tumor cell killing and is more tumor cell specific than expression of the adenoviral death protein." Hum Gene Ther **13**(15): 1859-71.

Toth, K., H. Djeha, et al. (2004). "An oncolytic adenovirus vector combining enhanced cell-to-cell spreading, mediated by the ADP cytolytic protein, with selective replication in cancer cells with deregulated wnt signaling." Cancer Res **64**(10): 3638-44.

Abou El Hassan, M. A., I. van der Meulen-Muileman, et al. (2004). "Conditionally replicating adenoviruses kill tumor cells via a basic apoptotic machinery-independent mechanism that resembles necrosis-like programmed cell death." J Virol **78**(22): 12243-51.

Bachtarzi, H., M. Stevenson, et al. (2011). "E-selectin is a viable route of infection for polymer-coated adenovirus retargeting in TNF-?-activated human umbilical vein endothelial cells." J Drug Target.

Baird, S. K., J. L. Aerts, et al. (2008). "Oncolytic adenoviral mutants induce a novel mode of programmed cell death in ovarian cancer." Oncogene **27**(22): 3081-90.

Bardell, D. and T. G. Metcalf (1972). "Differential release of cellular lactate dehydrogenase during replication of adenovirus types 5 and 12." J Gen Virol **14**(2): 219-22.

Bazan-Peregrino, M., R. C. Carlisle, et al. (2008). "Factors influencing retention of adenovirus within tumours following direct intratumoural injection." Gene Ther **15**(9): 688-94.

Berghe, T. V., N. Vanlangenakker, et al. (2010). "Necroptosis, necrosis and secondary necrosis converge on similar cellular disintegration features." Cell Death Differ **17**(6): 922-30.

Braithwaite, A. W. and I. A. Russell (2001). "Induction of cell death by adenoviruses." Apoptosis **6**(5): 359-70.

Cary, Z. D., M. C. Willingham, et al. (2011). "Oncolytic vesicular stomatitis virus induces apoptosis in U87 glioblastoma cells by a type II death receptor mechanism and induces cell death and tumor clearance in vivo." J Virol **85**(12): 5708-17.

Chen, W., Y. Wu, et al. (2011). "Enhanced antitumor efficacy of a novel fiber chimeric oncolytic adenovirus expressing p53 on hepatocellular carcinoma." Cancer Lett.

Christofferson, D. E. and J. Yuan (2009). "Necroptosis as an alternative form of programmed cell death." Curr Opin Cell Biol **22**(2): 263-8.

Colunga, A. G., J. M. Laing, et al. (2010). "The HSV-2 mutant DeltaPK induces melanoma oncolysis through nonredundant death programs and associated with autophagy and pyroptosis proteins." Gene Ther **17**(3): 315-27.

Connell, C. M., S. P. Wheatley, et al. (2008). "Nuclear survivin abrogates multiple cell cycle checkpoints and enhances viral oncolysis." Cancer Res **68**(19): 7923-31.

Davison, A. J., M. Benko, et al. (2003). "Genetic content and evolution of adenoviruses." J Gen Virol **84**(Pt 11): 2895-908.

Degterev, A., J. Hitomi, et al. (2008). "Identification of RIP1 kinase as a specific cellular target of necrostatins." Nat Chem Biol **4**(5): 313-21.

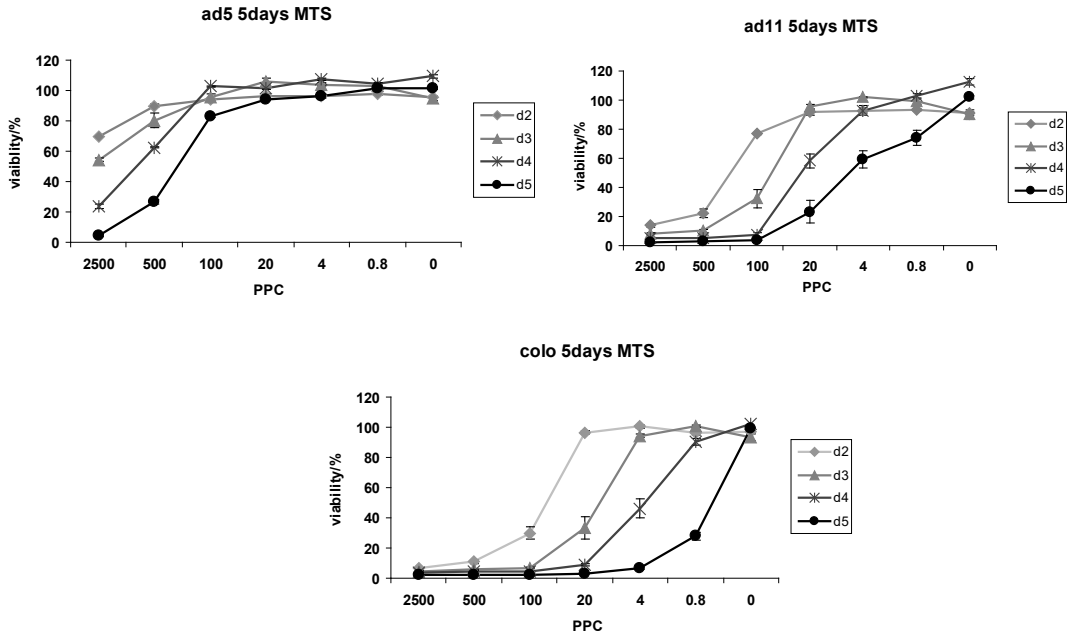
Doronin, K., K. Toth, et al. (2003). "Overexpression of the ADP (E3-11.6K) protein increases cell lysis and spread of adenovirus." Virology **305**(2): 378-87.
Echchgadda, I., S. Kota, et al. (2009). "Anticancer oncolytic activity of respiratory syncytial virus." Cancer Gene Ther **16**(12): 923-35.
Elankumaran, S., D. Rockemann, et al. (2006). "Newcastle disease virus exerts oncolysis by both intrinsic and extrinsic caspase-dependent pathways of cell death." J Virol **80**(15): 7522-34.
Errington, F., C. L. White, et al. (2008). "Inflammatory tumour cell killing by oncolytic reovirus for the treatment of melanoma." Gene Ther **15**(18): 1257-70.
Fink, S. L. and B. T. Cookson (2005). "Apoptosis, pyroptosis, and necrosis: mechanistic description of dead and dying eukaryotic cells." Infect Immun **73**(4): 1907-16.
Flak, M. B., C. M. Connell, et al. (2010.). "p21 Promotes oncolytic adenoviral activity in ovarian cancer and is a potential biomarker." Mol Cancer **9**: 175.
Glockzin, G., K. Mantwill, et al. (2006). "Characterization of the recombinant adenovirus vector AdYB-1: implications for oncolytic vector development." J Virol **80**(8): 3904-11.
Hall, A. R., B. R. Dix, et al. (1998). "p53-dependent cell death/apoptosis is required for a productive adenovirus infection." Nat Med **4**(9): 1068-72.
Harrison, S. C. (2010). "Virology. Looking inside adenovirus." Science **329**(5995): 1026-7.
Holterman, L., R. Vogels, et al. (2004). "Novel replication-incompetent vector derived from adenovirus type 11 (Ad11) for vaccination and gene therapy: low seroprevalence and non-cross-reactivity with Ad5." J Virol **78**(23): 13207-15.
Ito, H., H. Aoki, et al. (2006). "Autophagic cell death of malignant glioma cells induced by a conditionally replicating adenovirus." J Natl Cancer Inst **98**(9): 625-36.
Jiang, H., E. J. White, et al. (2008). "Adenovirus's last trick: you say lysis, we say autophagy." Autophagy **4**(1): 118-20.
Jiang, H., E. J. White, et al. (2011). "Human adenovirus type 5 induces cell lysis through autophagy and autophagy-triggered caspase activity." J Virol **85**(10): 4720-9.
Jones, M. S., 2nd, B. Harrach, et al. (2007). "New adenovirus species found in a patient presenting with gastroenteritis." J Virol **81**(11): 5978-84.
Knipe, D. M., Howley, P.M. (2007). "Fields Virology." **II**(the 5th edition): 63-64.
Krumschnabel, G., H. L. Ebner, et al. (2010). "Apoptosis and necroptosis are induced in rainbow trout cell lines exposed to cadmium." Aquat Toxicol **99**(1): 73-85.
Kuhn, I., P. Harden, et al. (2008). "Directed evolution generates a novel oncolytic virus for the treatment of colon cancer." PLoS One **3**(6): e2409.
Liang, M. (2011). "Clinical Development of Oncolytic viruses in China." Curr Pharm Biotechnol.
Liskova, J., J. Knitlova, et al. (2011). "Apoptosis and necrosis in vaccinia virus-infected HeLa G and BSC-40 cells." Virus Res **160**(1-2): 40-50.
Majno, G. and I. Joris (1995). "Apoptosis, oncosis, and necrosis. An overview of cell death." Am J Pathol **146**(1): 3-15.
Mei, Y. F., J. Skog, et al. (2003). "Comparative analysis of the genome organization of human adenovirus 11, a member of the human adenovirus species B, and

the commonly used human adenovirus 5 vector, a member of species C." J Gen Virol **84**(Pt 8): 2061-71.
Miao, B. and A. Degterev (2009). "Methods to analyze cellular necroptosis." Methods Mol Biol **559**: 79-93.
Nanavaty, U. B., R. Pawliczak, et al. (2002). "Oxidant-induced cell death in respiratory epithelial cells is due to DNA damage and loss of ATP." Exp Lung Res **28**(8): 591-607.
Nandi, S., I. V. Ulasov, et al. (2009). "A chimeric adenovirus with an Ad 3 fiber knob modification augments glioma virotherapy." J Gene Med **11**(11): 1005-11.
Peri, P., K. Nuutila, et al. (2011). "Cathepsins are involved in virus-induced cell death in ICP4 and Us3 deletion mutant herpes simplex virus type 1-infected monocytic cells." J Gen Virol **92**(Pt 1): 173-80.
Pesonen, S., L. Kangasniemi, et al. (2010). "Oncolytic adenoviruses for the treatment of human cancer: focus on translational and clinical data." Mol Pharm **8**(1): 12-28.
Robert, A., N. Smadja-Lamere, et al. (2006). "Adenovirus E4orf4 hijacks rho GTPase-dependent actin dynamics to kill cells: a role for endosome-associated actin assembly." Mol Biol Cell **17**(7): 3329-44.
Rodriguez-Rocha, H., J. G. Gomez-Gutierrez, et al. (2011). "Adenoviruses induce autophagy to promote virus replication and oncolysis." Virology **416**(1-2): 9-15.
Saito, K., K. Uzawa, et al. (2009). "Oncolytic activity of Sindbis virus in human oral squamous carcinoma cells." Br J Cancer **101**(4): 684-90.
Sir, D. and J. H. Ou (2010). "Autophagy in viral replication and pathogenesis." Mol Cells **29**(1): 1-7.
Stanziale, S. F., H. Petrowsky, et al. (2004). "Infection with oncolytic herpes simplex virus-1 induces apoptosis in neighboring human cancer cells: a potential target to increase anticancer activity." Clin Cancer Res **10**(9): 3225-32.
Tollefson, A. E., A. Scaria, et al. (1996). "The adenovirus death protein (E3-11.6K) is required at very late stages of infection for efficient cell lysis and release of adenovirus from infected cells." J Virol **70**(4): 2296-306.
Toth, K., M. Kuppuswamy, et al. (2011). "A fully replication-competent adenovirus vector with enhanced oncolytic properties." Cancer Gene Ther **17**(11): 761-70.
Tsujimoto, Y. and S. Shimizu (2005). "Another way to die: autophagic programmed cell death." Cell Death Differ **12 Suppl 2**: 1528-34.
Ulasov, I. V., M. A. Tyler, et al. (2009). "Oncolytic adenoviral vectors which employ the survivin promoter induce glioma oncolysis via a process of beclin-dependent autophagy." Int J Oncol **34**(3): 729-42.
Vandenabeele, P., L. Galluzzi, et al. (2010). "Molecular mechanisms of necroptosis: an ordered cellular explosion." Nat Rev Mol Cell Biol **11**(10): 700-14.
Wigand, R. and G. Kumel (1977). "The kinetics of adenovirus infection and spread in cell cultures infected with low multiplicity." Arch Virol **54**(3): 177-87.
Yamamoto, M. and D. T. Curiel (2010). "Current issues and future directions of oncolytic adenoviruses." Mol Ther **18**(2): 243-50.
Yang, H., Z. Rivera, et al. (2010). "Programmed necrosis induced by asbestos in human mesothelial cells causes high-mobility group box 1 protein release and resultant inflammation." Proc Natl Acad Sci U S A **107**(28): 12611-6.

Yun, C. O., E. Kim, et al. (2005). "ADP-overexpressing adenovirus elicits enhanced cytopathic effect by induction of apoptosis." Cancer Gene Ther **12**(1): 61-71.
Zhang, L. Q., Y. F. Mei, et al. (2003). "Human adenovirus serotypes 4 and 11 show higher binding affinity and infectivity for endothelial and carcinoma cell lines than serotype 5." J Gen Virol **84**(Pt 3): 687-95.
Zhivotovsky, B. and S. Orrenius (2010). "Cell death mechanisms: cross-talk and role in disease." Exp Cell Res **316**(8): 1374-83.
Zong, W. X. and C. B. Thompson (2006). "Necrotic death as a cell fate." Genes Dev **20**(1): 1-15.

Supplementary material

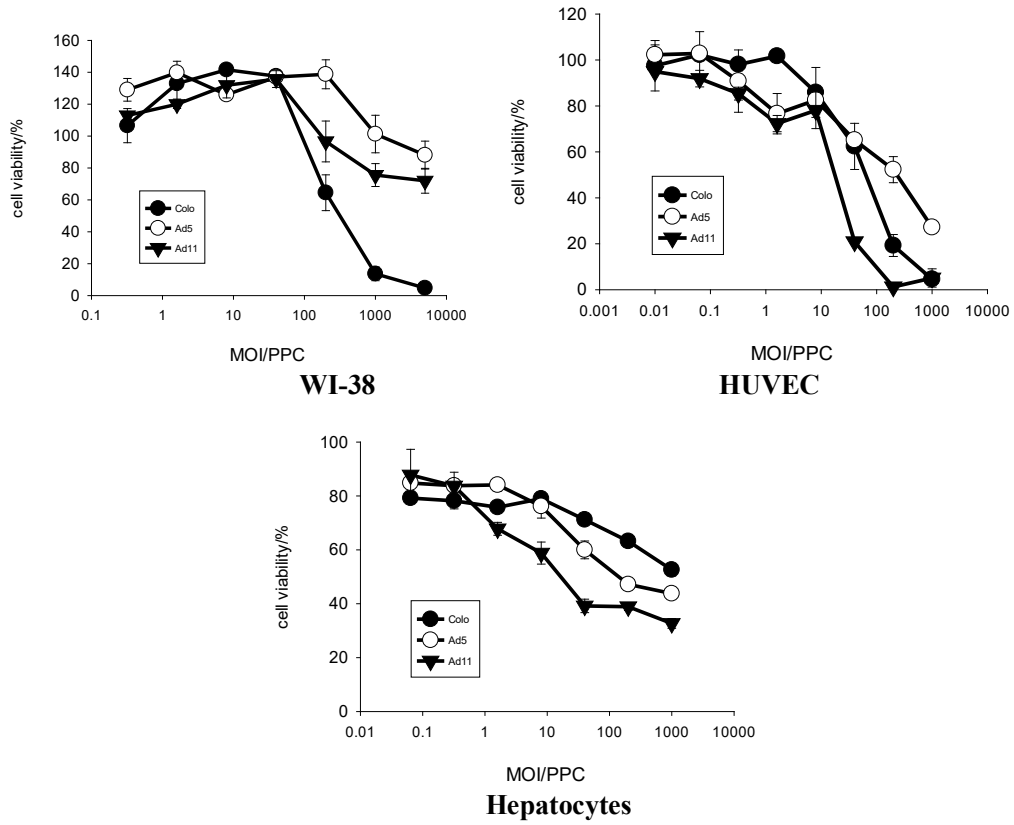
S1



F.S1 Effect of time on cytotoxicity of oncolytic adenoviruses on A549 cells. The experimental procedures employed are as described above for studies performed using HepG2 cells, and cell viability was assessed using the MTS assay on A549 cells.. Four identical plates were set up for infection with each virus allowing time points to be taken on days 2,3,4 and 5. Mean data ± SD are presented, *n* =3.

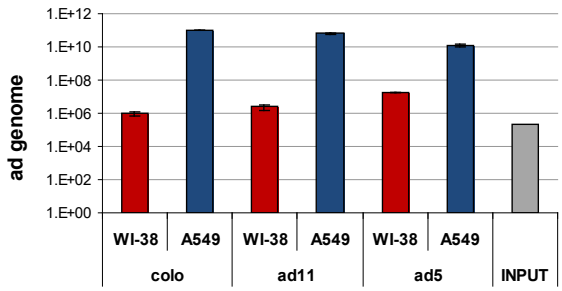
For each cell line tested, critical factors determining the efficiency of viral oncolysis are the MOI used and the duration of infection. Figure S1 shows IC50 values for each virus at the final time point as well as provides kinetic information about the relationship between time and dose. At a high dose of ColoAd1, cytotoxicity was seen beginning day 2 (IC50 100PPC), and the potency increased with the time (by the rate of 1 in 5th decrease of IC50 per day; Ad11 mediated cytotoxicity was observed on day2 with an IC50 of 200PPC, and 1 in 3rd decrease of IC50 per day; in comparison, the lytic activity of Ad5 is less effective, with cytotoxicity only evident on day 4 with IC50 decrease with the rate of 1 in 2nd per day.

S2



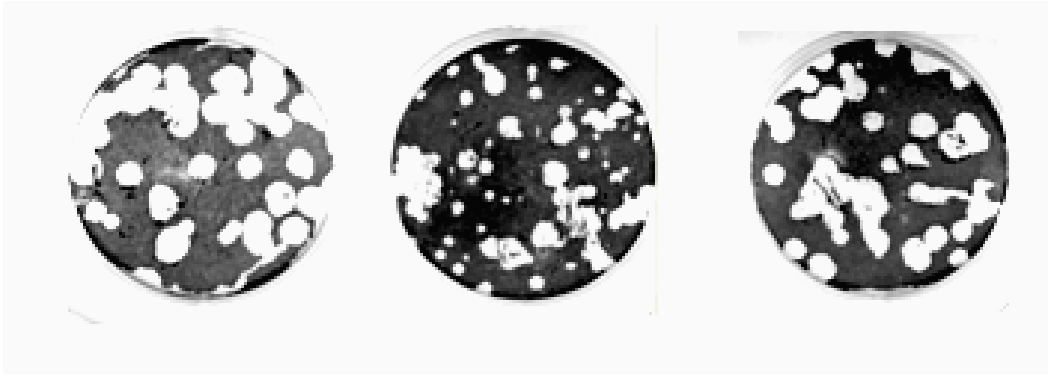
F S2. **Cytotoxicities of oncolytic adenoviruses in normal human cells as measured by the MTS assay.** Cell viability was measured by MTS assay according to the manufacture's instructions. HUVECs and WI-38 cells were measured at 5 days post-infection, while human hepatocytes were measured at day 3 post-infection. - The highest virus dose used was 1000 PPC for human hepatocytes and HUVECs, while for WI-38 cells the highest dose was 10,000 PPC. Three-fold dilutions were then carried out. Mean data ± SD are presented, *n* =3.

S3



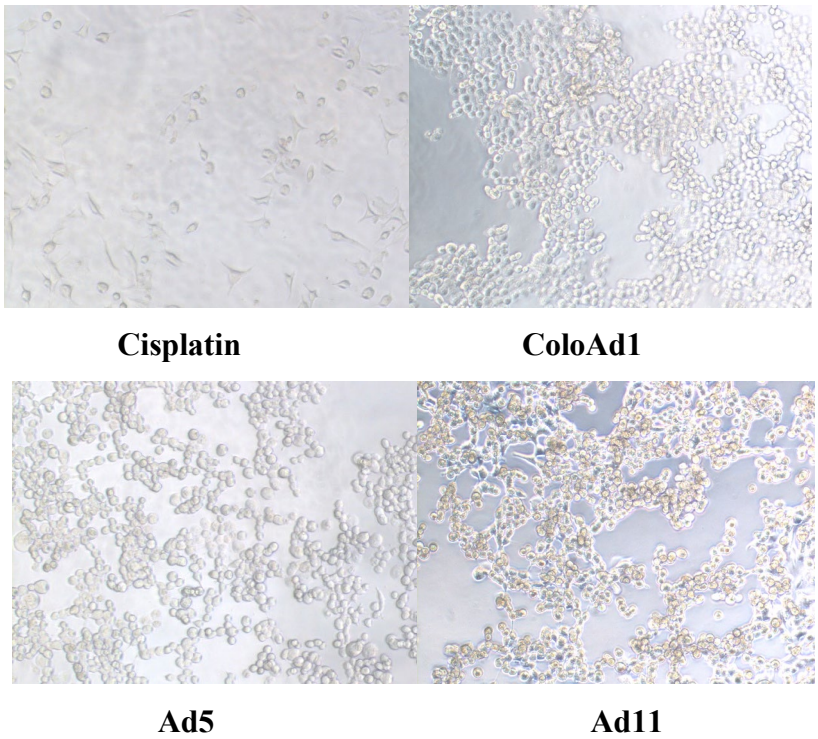
F S3 3 days viral genome replication of ColoAd1, Ad11, Ad5 in WI-38 and A549 cells at the PPC 20 input. Cells were seeded at 10000 cells per well in 96 well plates.

S4



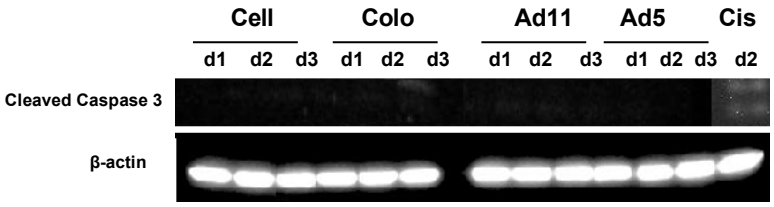
F S4. **Agar plaque forming assay**. A monolayer culture of A549 cells was infected by Ad5, Ad11 or ColoAd1 at 10 folds series dilution from the stock virus (the number above the wells are the specific dilution.. After 2 hours infection and PBS wash, the wells were incubated with a 1% agarose overlay on A549 cell monolayer. After 10days incubation the agar was removed, and plate was fixed with 4% formaldehyde and stained with 1% crystal violet to visualize plaques. The diameters of the plaques were measured.

S5



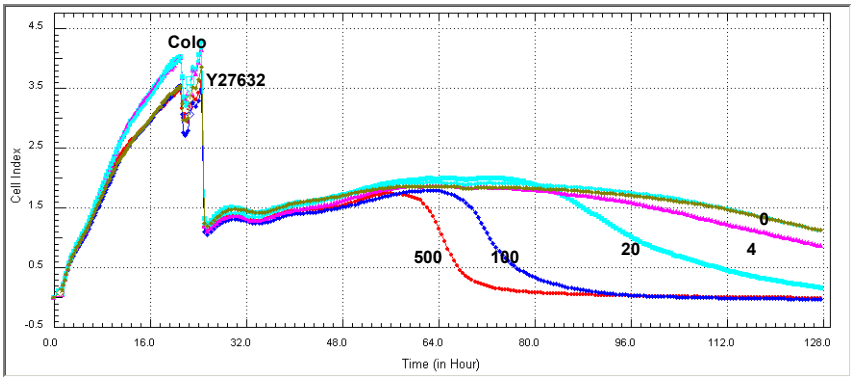
F S5 The corresponding optical microscopy images for Fig 4.4. The cells conditions and the treatments were the same as used in Fig 4.4

S6



S F6 The western blots for cell lysates, detected by cleaved caspase 3 antibody and β-actin antibody. β-actin was used as SDS-PAGE loading control. The experiment conditions were the same as in Fig4.9. There was a very weak cleaved caspase 3 signal detected at Coload1 d3 cell lysate, however it was able to see for cisplatin treated cell lysate.

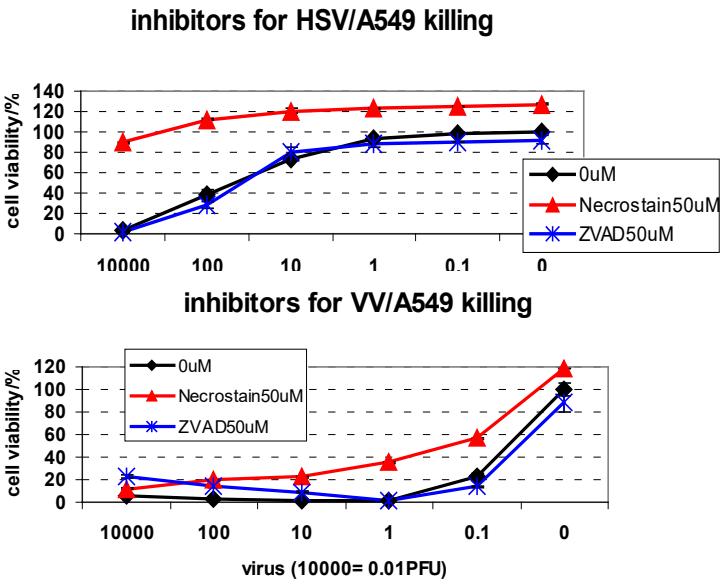
S 7



FS7 The cell proliferation with Coload1 virus infection with the presence of Rho kinase inhibitor Y27632, recorded by xCelligency cell monitor. The numbers on the curves referred to the infection viral dosed used. The A549 cells wwere seeded at time 0 hr, the virus infection was then started at 24hours latter. 50μM inhibitor was added in 2 hour after the infection. The virus only cell proliferation curves can be seen from Fig 5.10

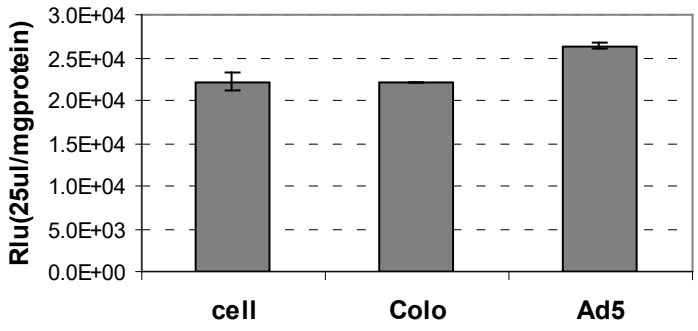
S8

.



F S8: **The inhibitors impact to HSV and VV oncolysis on A549 cells, measured by 5 days MTS cell proliferation assay.** Necrostatin 50 μM or zVAD-fmk 50 μM was used to treat the cells 1hour before viruses infection. The virus infection doses were started from 0.006 PFU (HSV) and 0.01PFU (VV), followed 1:10 serial dilutions were used. Mean data ± SD are presented, *n* =3.

S9



F S9 The NFKB activation by the viruses, tested by U937-NFBK-Luc cells luciferase assay. The viruses were used at $1E^{10}$ PPC /1ml concentration. The U937 cells (1million/ml) were incubated at 37˚C at 8hours after the stimulation, followed harvested for luciferase assay. Mean data ± SD are presented, *n* =3.